

**BUKTI KORESPONDENSI ARTIKEL
PADA JURNAL INTERNASIONAL BEREPUTASI**



PENGUSUL

Rusiyanto, S.Pd., M.T / NIDN 0021037407

UNIVERSITAS NEGERI SEMARANG

Yth. Bapak/Ibu Penilai Angka Kredit (PAK)

Bersama dengan surat ini, saya bermaksud menyertakan bukti bukti korespondensi proses review artikel pada Jurnal Internasional dengan judul Effect of Sintering Temperature on the Physical Properties of $\text{Ba}_{0.6}\text{Sr}_{0.4}\text{TiO}_3$ Prepared by Solid-State Reaction, yang dimuat pada International Journal of Automotive and Mechanical Engineering (IJAME), Edisi Vol. 18 No. 2, 17 Juni 2021, ISSN (p) : 2229-8649, ISSN (e) : 2180-1606, hal : 8752 - 8759. Adapun susunan kronologi bukti korespondensi publikasi artikel terdiri dari beberapa poin, pada tabel di bawah ini:

No	Tanggal	Aktivitas
1	30 Juli 2020	Submission Files untuk publikasi di Jurnal IJAME
2	30 Juli 2020	Pemberian nomor ID manuscript dari editor (C-4962-Article Text-17744-1-4-20200730)
3	18 Agustus 2020	Pre-Review discussion (editor mengkonfirmasi diperlukan penambahan reviewer)
4	18 Agustus 2020	Membalas email editor dengan menyertakan daftar usulan reviewer baru
5	17 Maret 2021	Editor Decisions yang pertama : Revisions Required
6	22 Maret 2021	Melakukan submit naskah publikasi yang telah di revisi berdasarkan saran dan masukan dari reviewer
7	22 Maret 2021	Melakukan submit draft Response to reviewers yang berisikan jawaban penulis terhadap setiap saran dan masukan dari reviewer
8	18 Mei 2021	Editor Decisions yang kedua : Accept submission
9	18 Mei 2021	Permintaan pengisian form author agreement
10	27 Mei 2021	Editor meminta perbaikan pada referensi yang digunakan. Hal ini terjadi karena hanya 15% dari referensi yang digunakan yang memiliki umur ≤ 5 tahun (2015-2020). Persyaratan dari editor jurnal IJAME adalah 60% referensi yang digunakan memiliki umur ≤ 5 tahun.
11	6 Juni 2021	Submit naskah yang sudah direvisi
12	11 Juni 2021	Permintaan proofreading sebelum publication
13	11 Juni 2021	Mengirimkan naskah yang telah dilakukan final proofread
14	14 Juni 2021	Editor Decisions yang ketiga : Manuscript sent to production

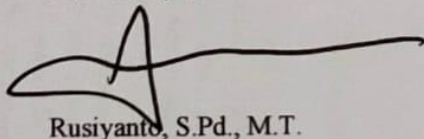
No	Tanggal	Aktivitas
15	17 Juni 2021	Artikel telah publish : https://journal.ump.edu.my/ijame/article/view/4962

Demikian, agar dapat menjadi periksa.

Terimakasih

Semarang, 8 Februari 2023

Hormat saya,



Rusiyanto, S.Pd., M.T.

NIP: 197403211999031002

**KRONOLOGI KORESPONDENSI PUBLIKASI ARTIKEL PADA JURNAL
INTERNASIONAL BEREPUTASI DAN BERFAKTOR DAMPAK.**

Judul : Effect of Sintering Temperature on the Physical Properties of
Ba_{0.6}Sr_{0.4}TiO₃ Prepared by Solid-State Reaction

Jurnal : International Journal of Automotive and Mechanical Engineering
(IJAME)

Volume : 18

Nomor : 2

Tanggal publikasi : 17 Juni 2021

ISSN (p) : 2229-8649

ISSN (e) : 2180-1606

Hal : 8752 - 8759.

Penerbit : The Automotive Engineering Centre (AEC), Universiti Malaysia
Pahang 26600
Pekan, Pahang, MALAYSIA



SJR jurnal : **0.29 (2021)**

Quartile : Q3 (Scopus)

Cite Score : 2.27


Penulis : Rusiyanto, Rahmat Doni Widodo, Dony Hidayat Al-Janan,
Kholifatur Rohmah, Januar Parlaungan Siregar, Agus Nugroho,
Deni Fajar Fitriyana.

Bukti indexing jurnal :

   resurchify.com/find/?query=International+Journal+of+Automotive+and+Mechanical+Engineering#search_results

1. International Journal of Automotive and Mechanical Engineering

International Journal of Automotive and Mechanical Engineering is a **journal** covering the categories related to **Automotive Engineering (Q3); Mechanical Engineering (Q3)**. It is published by **The Automotive Engineering Centre (AEC), Universiti Malaysia Pahang**. The overall rank of International Journal of Automotive and Mechanical Engineering is **15192**. ISSN of this journal is/are **22298649, 21801606**.

 **Impact Score: 1.19**  **h-Index: 27**  **SJR: 0.287**  **Overall Ranking: 15192**

More Details

← → ↻ scimagojr.com/journalsearch.php?q=21100235622&tip=sid&clean=0

SJR Scimago Journal & Country Rank Enter Journal Title, ISSN or Publisher Name

Home Journal Rankings Country Rankings Viz Tools Help About Us

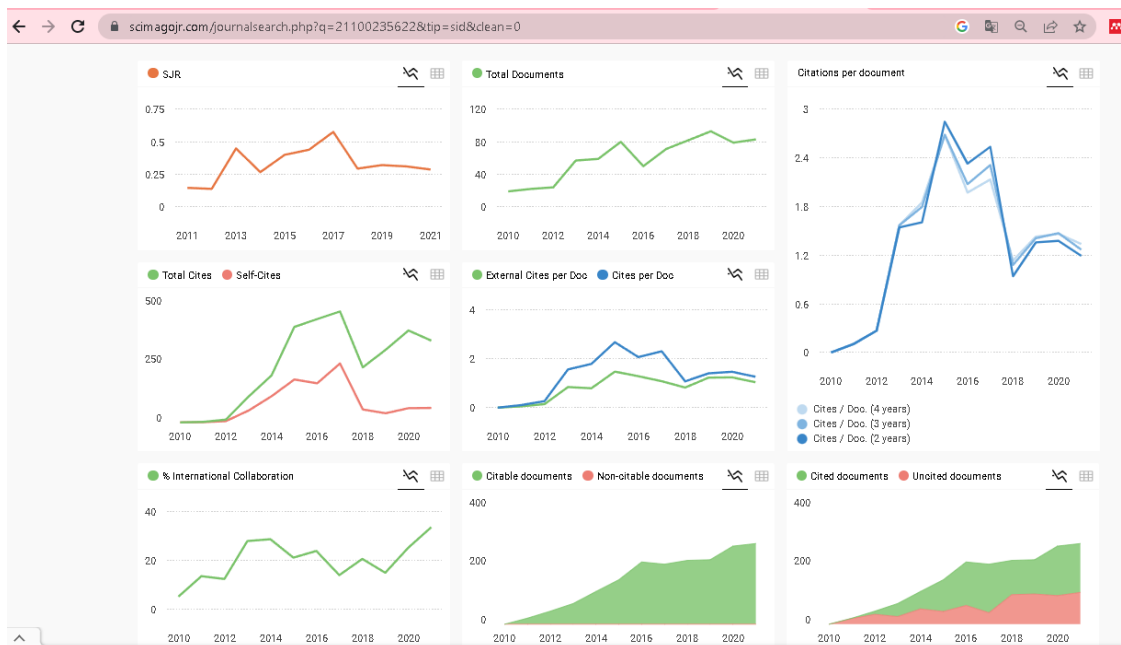
←

Ads by Google

Stop seeing this ad Why this ad?

International Journal of Automotive and Mechanical Engineering 8

COUNTRY	SUBJECT AREA AND CATEGORY	PUBLISHER	H-INDEX
Malaysia	Engineering Automotive Engineering Mechanical Engineering	The Automotive Engineering Centre (AEC), Universiti Malaysia Pahang	27
Universities and research institutions in Malaysia		University of Malaysia, Pahang in Scimago Institutions Rankings	
Media Ranking in Malaysia			



International Journal of Automotive and Mechanical Engineering

Q3 Automotive Engineering best quartile

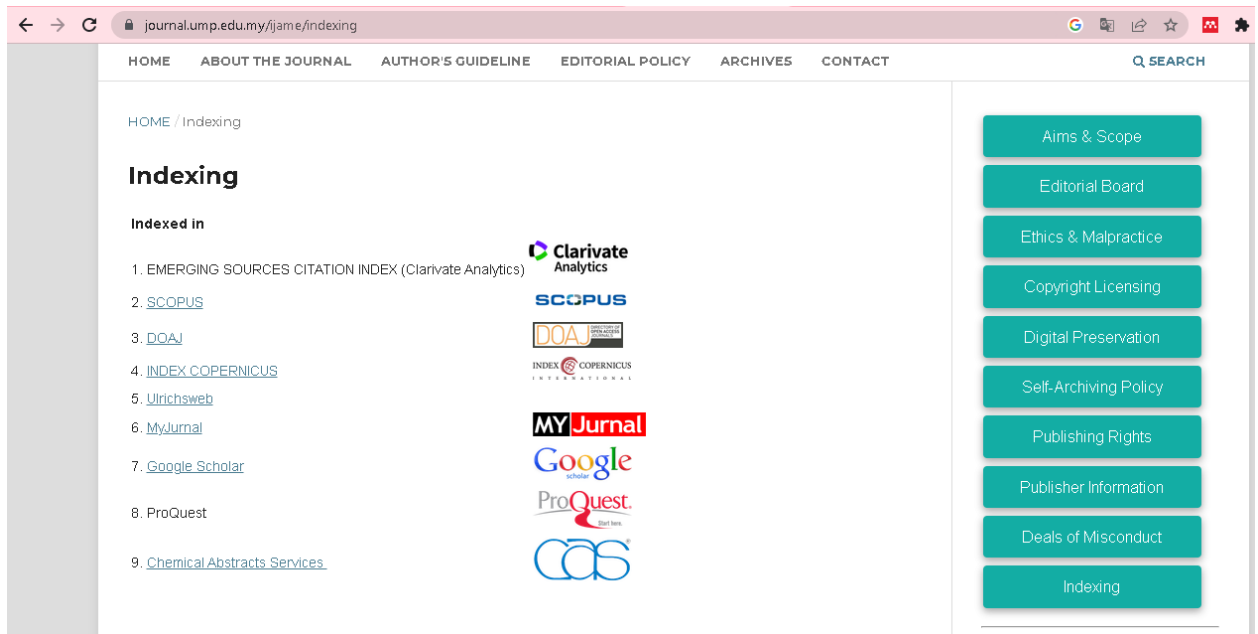
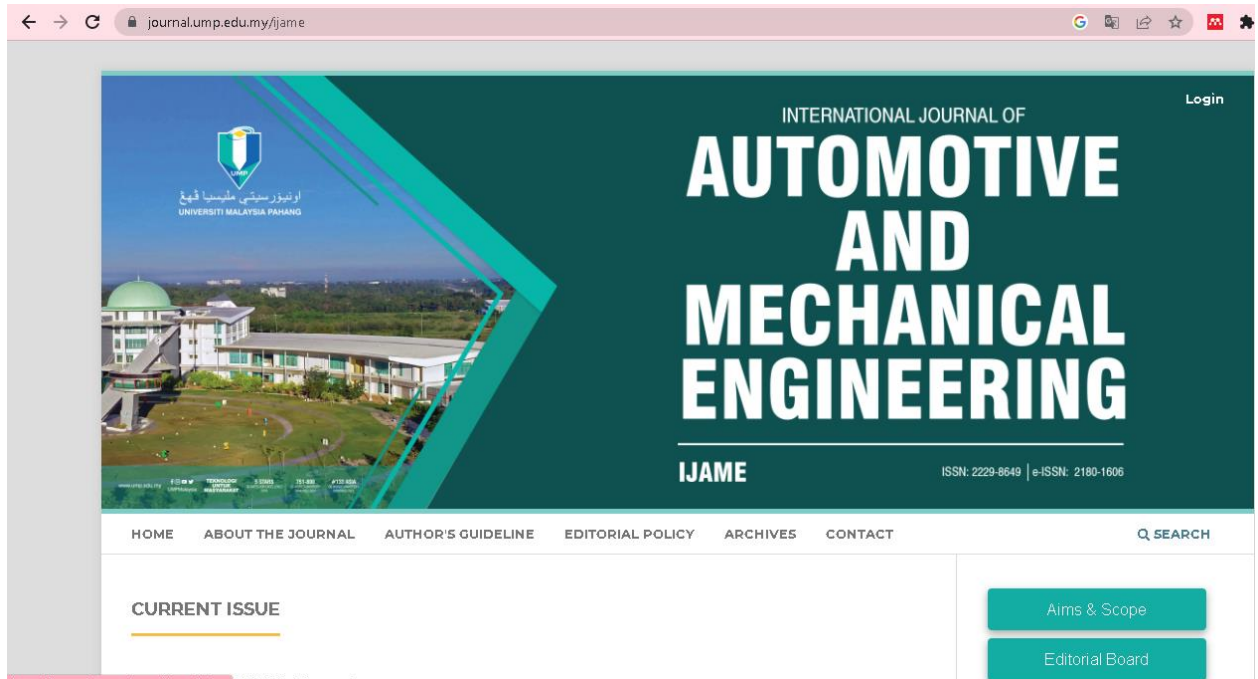
SJR 2021 0.29

powered by scimagojr.com

← Show this widget in your own website

Just copy the code below and paste within your html code:

```
<a href="https://www.scimagojr.com/journalsearch.php?q=21100235622&tip=sid&clean=0">
```





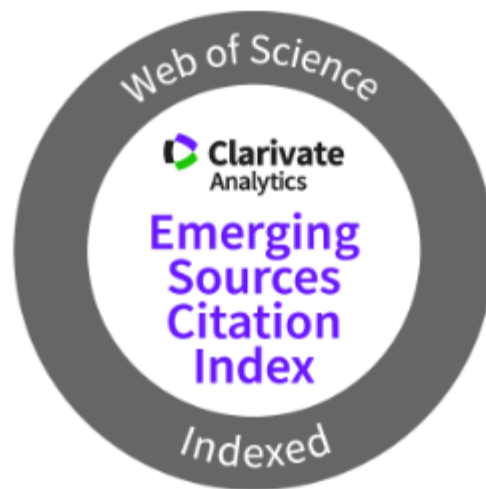
Indexed by:

2.27 2017
CiteScore

82nd percentile - Automotive Engineering
Powered by Scopus

2.27 2017
CiteScore

80th percentile - Mechanical Engineering
Powered by Scopus



ESCI, Clarivate Analytics

International Journal of
Automotive and Mechanical...

Q3

Automotive
Engineering

best quartile

SJR 2021

0.29





powered by scimagojr.com

I SUBMISSION PROCESS

[← Back to Submissions](#)4962 / **Rusiyanto et al.** / Effect of Sintering Temperature on the Physical Properties of Ba...[Library](#)[Workflow](#)[Publication](#)[Submission](#)[Review](#)[Copyediting](#)[Production](#)

Submission Files

[Q Search](#)

- | | | | | |
|---|---|---|---------------|--------------|
| ▶ |  17039 | januar, Manuscript - JPS.doc | July 30, 2020 | Article Text |
| ▶ |  17040 | januar, LIST OF REVIEWER.docx | July 30, 2020 | Article Text |

[Download All Files](#)

Pre-Review Discussions

[Add discussion](#)

Name	From	Last Reply	Replies	Closed
▶ Comments for the Editor	januar 2020-07-30 10:15 AM	-	0	<input type="checkbox"/>
List of reviewer required	aqida 2020-08-18 10:20 AM	januar 2020-08-18 09:24 PM	1	<input type="checkbox"/>

Effect of Milling Times and Annealing on The Physical Properties of $\text{Ba}_{0.6}\text{Sr}_{0.4}\text{TiO}_3$ Prepared by Conventional Solid-State Reaction Process

Rusiyanto¹, R.D. Widodo¹, D.H. Al-Janani¹, K. Rohmah¹, J.P. Siregar^{2*} and A. Nugroho¹

¹Department of Mechanical Engineering, Universitas Negeri Semarang, Kampus Sekaran, Gunungpati, 50229 Semarang, Indonesia

²Department of Mechanical Engineering, Faculty of Engineering, Universiti Malaysia Pahang, 26300 Gambang, Kuantan, Malaysia

*Email: januar@ump.edu.my

Phone: +6094246282; Fax: +609424222

ABSTRACT

Synthesis of $\text{Ba}_{0.6}\text{Sr}_{0.4}\text{TiO}_3$ was prepared via a conventional solid-state reaction process of BaCO_3 , SrCO_3 and TiO_2 precursors. The effect of milling times on the physical properties (particle and crystallite size) of $\text{Ba}_{0.6}\text{Sr}_{0.4}\text{TiO}_3$ powder is investigated. The size of the powder particle is determined using the particle-size analyzer (PSA). The X-ray diffraction method is used for qualitative and quantitative phases analyzation as well as crystallite-size determination. The average particle size of the powder initially increased due to the laminated layers formation which then decreased to an asymptotic value of 0.4 μm at 58 h. The crystallite-size of $\text{Ba}_{0.6}\text{Sr}_{0.4}\text{TiO}_3$ was sintered at 1100°C for 1 h the holding time is 43 nm. The crystallite-size of barium-strontium titanate phase is dependent on the temperature and time of their sintering.

Keywords: Particle-size; crystallite-size; barium-strontium titanate; solid-state reaction.

INTRODUCTION

Barium Strontium Titanate (BST) with the formula $\text{Ba}_x\text{Sr}_{(1-x)}\text{TiO}_3$, $0 < x < 1$, is a ferroelectric material which has a perovskite-structure, is a solid solution composed of barium titanate and strontium titanate. The BST ceramic material is widely known to be used as a material in electronic devices such as dynamic random access memories (DRAM), dielectric capacitors, microwave phase shifters, varactor, tunable filter, transducers, positive temperature coefficient resistor (PTC), piezoelectric sensors, uncooled infrared detectors, antennas, high-Q resonators for radar and communication applications [1–3]. The vast usage of BST ceramic material, both in the forms of bulk ceramics and thin films, is caused by its unique combination of large dielectric constant, stable operation at high temperature, high tunability, low loss tangent, low dc leakage and alterable Curie temperature [4–6].

The uniqueness of BST is caused by several factors such as chemical formula or x composition known as the Ba/Sr ratio, method to synthesize, as well as particle and crystallite size [7]. Ceramics $\text{Ba}_{(1-x)}\text{Sr}_x\text{TiO}_3$ with various x composition (Ba/Sr ratio) consists of the following x compositions given by: $x = 0.05, 0.10, 0.15$ and 0.20 [8]; $x = 0$ to 0.5 [9]; $x = 0.25, 0.35, 0.40, 0.5, 0.6, 0.75, 0.90$ [10]; $x = 0.35$ and 0.6 [11]; $x = 0.25, 0.50, 0.75$ and 0.90 [12]; $x = 0.1$ [13]; $x = 0.5$ [14]; $x = 0.1$ and 0.6 [15]; $x = 0$ – to 0.2 [16]; $x = 0.4$ [17–21]. In addition, synthesized $\text{Ba}_x\text{Sr}_{(1-x)}\text{TiO}_3$ ceramics with the composition $x = 0.4$ [22]. High dielectric and pyroelectric properties of $\text{Ba}_{(1-x)}\text{Sr}_x\text{TiO}_3$ composition with $0.3 \leq x \leq 0.5$ results in a decrease in the ferroelectric-paraelectric phase transformation temperature or Curie temperature (T_C) down to temperatures close to room temperature (RT, 25°C). For example, for $\text{Ba}_{0.6}\text{Sr}_{0.4}\text{TiO}_3$, the bulk T_C is just below RT (5°C). Ceramics $\text{Ba}_{(1-x)}\text{Sr}_x\text{TiO}_3$ has attracted significant interest as material systems of choice for such application [2, 9, 13, 17].

The following methods are generally used to synthesize $\text{Ba}_{(1-x)}\text{Sr}_x\text{TiO}_3$: hydrothermal method [20, 23], sol-gel method [24], and conventional solid-state reaction method [8, 11, 12, 15, 18, 21,

22, 25–27]. The BST nanoparticles which are synthesized by hydrothermal and sol-gel methods are smaller than 100 nm, but they contain residual hydroxide ions, which results in the formation of inter-granular pores [25]. BST nanoparticle with large-scale production, mechanochemical or solid-state reaction processing route is considered to be the most method (Clark et al., 1999). The conventional solid-state method has several advantages such as low-cost raw materials, a simplified process and the ability to obtain fine particles [29]. The conventional solid-state method such as high-energy ball milling is characterized by the repeated welding, deformation and fracture of the constituent powder materials [26]. The mechanical activation during solid-state reaction via mechanical milling leads to an increase in specific surface area of the particles powder, as a consequence of the destruction of agglomerates and particles of the initial precursors [30]. Microstructure of the particle and crystallite size is caused by the initial state or the characteristics of the powder used, the duration of the mechanical milling and the heating temperature. During the mechanical milling process, particle size can be reduced $> 1 \mu\text{m}$, and crystallite size can increase along with the temperature and holding time of sintering process [31].

The objective of this paper is, therefore, to investigate the effects of milling times on the physical properties (particle and crystallite size) during the synthesis of $\text{Ba}_{0.6}\text{Sr}_{0.4}\text{TiO}_3$ powder and the subsequent annealing process. The discussion includes results of mean particle size characterization by a Laser Particle Size Analyzer and mean crystallite size determination by using the line broadening analysis employing a step scanning counting in the x-ray diffraction (XRD) apparatus.

METHODS AND MATERIALS

$\text{Ba}_{0.6}\text{Sr}_{0.4}\text{TiO}_3$ powders are composed of basic compounds of BaCO_3 , SrCO_3 and TiO_2 which have purity percentage of more than 98% where the stoichiometry was utilized to calculate the amount of basic compound in the mixture. The mechanical alloying process to mix the basic compound powder was performed for 58 hours using the vibratory ball milling. The weight ratio of the steel balls to the compounds was 10:1. The characterization of the particle size weight was conducted using Particle Size Analyser (PSA) Malvern ZS Nanoseries. Furthermore, the Philips X-ray diffractometer was used to perform phase analysis and crystallite size of milled powders. The “step-scan” method was performed to record the X-ray diffraction patterns. The annealing process of the powders was completed in the electric chamber furnace (Nabertherm N31/H) at 500°C , 600°C , 700°C , 800°C , 900°C , 1000°C and 1100°C in the air under atmospheric pressure up to 1 hour. The Rietveld analysis was performed applying the High Score Plus program which is an updated version of Rietveld refinement with PC and mainframe computers. The description of the diffraction line profiles at Rietveld refinement was achieved using the pseudo-Voigt function. The Williamson-Hall method was then used to estimate the crystallite sizes for BaCO_3 , SrCO_3 and TiO_2 as well as $\text{Ba}_{(1-x)}\text{Sr}_x\text{TiO}_3$ phases [32]. Intensity data during the scanning was taken every 2 seconds for each step of the diffraction angle of 0.005° . The diffraction peak width (B) and the mean crystallite size (D) is given in Equation 1 and Equation 2 as follows.

$$B = \frac{0.9\lambda}{D\cos\theta} + \eta\tan\theta \quad (1)$$

$$B\cos\theta = \frac{0.9\lambda}{D} + \eta\sin\theta \quad (2)$$

where λ denotes the X-ray wavelength, η represents the strain in the materials and θ denotes the Bragg angle. Furthermore, the peak width B obtained after the correction due to instrument broadening is given by Equation 3 as follows

$$B = \sqrt{B_0^2 - B_s^2} \quad (3)$$

where B_o is the Full Width at Half Maximum (FWHM) of the test sample while B_s is the FWHM standard samples that used Silicon (Si).

RESULTS AND DISCUSSION

The results of PSA testing on the particle size of the BaCO_3 , SrCO_3 and TiO_2 powder showed that the mean of the initial particle size was $1.979\ \mu\text{m}$, $3.182\ \mu\text{m}$ and $0.795\ \mu\text{m}$, respectively. The diffraction patterns of TiO_2 , SrCO_3 and BaCO_3 precursors are shown in Fig. 1. The diffraction patterns of TiO_2 and PbCO_3 precursors were matched with the diffraction patterns of TiO_2 , SrCO_3 and BaCO_3 in the *Inorganic Crystal Structure Database* (ICSD) number 98-009-6946, 98-016-6088 and 98-016-6090, respectively. Based on the Rietveld analysis performed by applying the High Score Plus program revealed that the crystal system of TiO_2 , SrCO_3 and BaCO_3 is tetragonal, orthorhombic and orthorhombic, respectively.

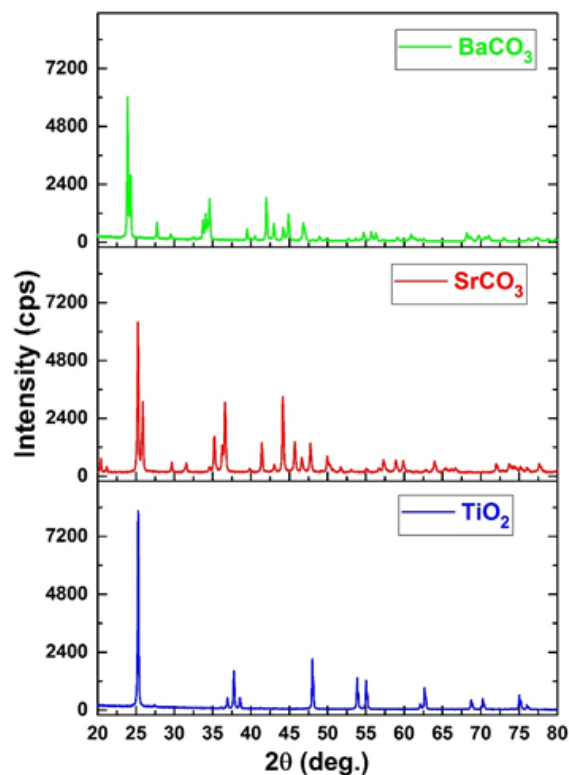


Figure 1. X-ray diffraction patterns of TiO_2 , SrCO_3 and BaCO_3 precursors.

Figure 2 shows the mean particle size of TiO_2 , SrCO_3 and BaCO_3 powder mixture which are the chemical components of the BST milled up to 58 hours. These results indicate that at the initial stage of the mechanical alloying process, all particles from the components of the BST were mixed and alloyed into one cold weld. As a consequence, the mean particle size increased in which the maximum particle size was approximately $22.6\ \mu\text{m}$ obtained during 10 hours of the milling process. The particles yield from the mechanical milling process had a lamellar structure with relatively high crystallite defects due to the deformation [33]. The internal lamellar structure of the particles occurred due to the process of alloying the particles which initially had a relatively high level of elasticity. If the duration of the mechanical alloying process was increased, then the particles with lamellar structure experienced an increase in the internal stress so that the level of particle brittleness was also increased [34]. Subsequent treatment of this mechanical alloying stage causes the particles to experience brittleness due to internal stress and deformation which then caused the particle size to disintegrate into finer particles with a mean size of approximately $0.4\ \mu\text{m}$. The mean size then had a tendency to be constant even though the deformation continued after a 58-hour milling duration.

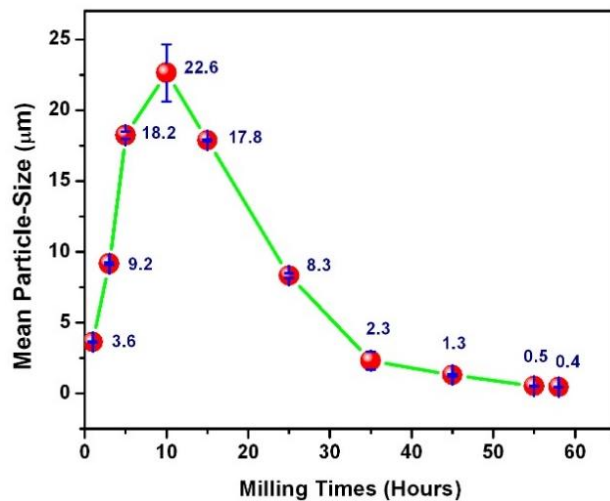


Figure 2. The mean particle sizes of TiO_2 , SrCO_3 and BaCO_3 mixture as a function of milling time.

Figure 3 illustrates the calculation of the mean size of crystallite in TiO_2 , SrCO_3 and BaCO_3 powder mixtures based on x-ray diffraction patterns. It can be seen that the mechanical alloying process for 55 hours did not change the diffraction pattern of the mixture of TiO_2 , SrCO_3 and BaCO_3 where the identification of diffraction peak of TiO_2 , SrCO_3 and BaCO_3 can still be identified. However, it can be seen that there is a widening of the diffraction peak which shows a reduction in the mean size of the crystallite along with the increase in milling duration, as shown in Figure 4. The diffraction peak of the level (111) shows that the increase in milling duration results in the increase of the diffraction peak along with the decrease in the intensity of the diffraction peak. This indicates that there has been deformation and milling of crystallite size [35].

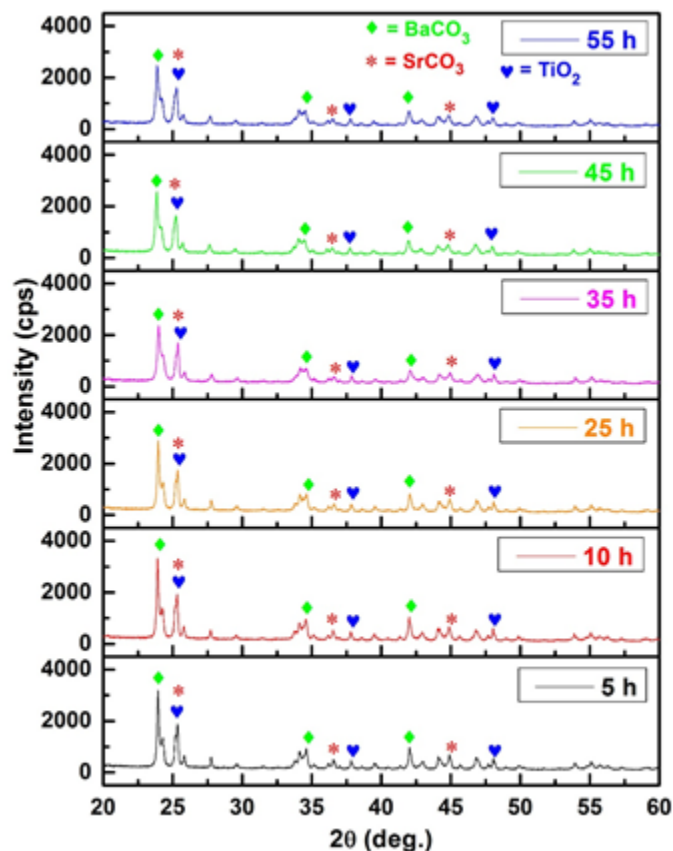


Figure 3. X-ray diffraction patterns of TiO_2 , SrCO_3 and BaCO_3 mixture.

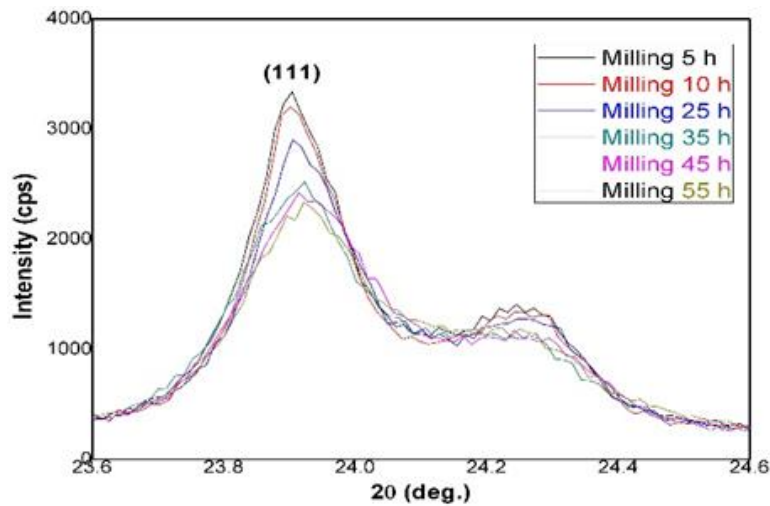


Figure 4.X-ray diffraction peak on the hkl area (111).

The mean size of TiO_2 , SrCO_3 and BaCO_3 crystallite mixture powder obtained from the calculation using the Williamson-Hall method can be seen in Figure 5. The results show that the crystallite size milling process occurred along with the increasing duration of the milling process. The results of the crystallite size calculation as a function of the milling process duration is also illustrated in Figure 5.

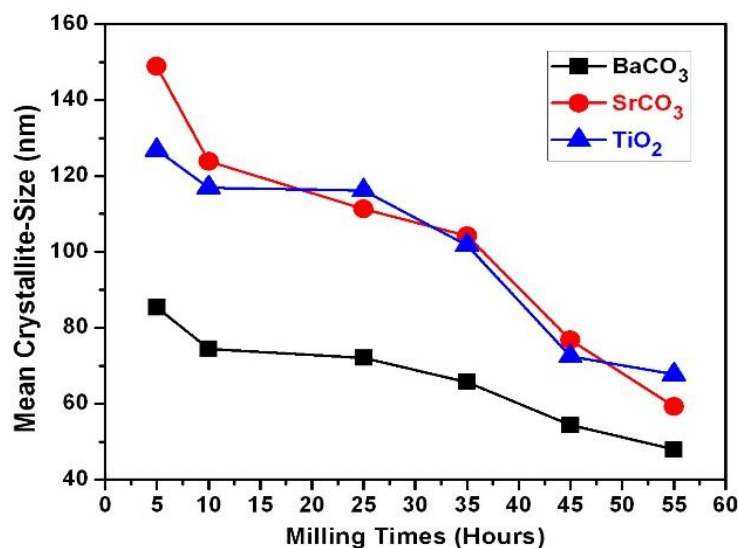


Figure 5.The mean crystallite size of TiO_2 , SrCO_3 and BaCO_3 mixture.

Figure 3 and 5 show that the continuous collision force between the mixture of TiO_2 , SrCO_3 and BaCO_3 powder with a steel ball in the alloying process for 55 hours causes deformation of the crystal structure. The deformation process of the powder mixture leads to the longer milling duration than 55 hours which resulted in a greater reduction rate of the crystallite mean size. The crystallite sizes of TiO_2 , SrCO_3 and BaCO_3 which were milled up to 55 hours were 68, 59 and 48 nm, respectively.

The annealing process for the TiO_2 , SrCO_3 and BaCO_3 powder mixtures at temperatures of 500°C, 600°C, 700°C, 800°C, 900°C, 1000°C and 1100°C was performed for 1 hour and the x-ray diffraction pattern is shown in Figure 6. This process was conducted to determine the phases present in the material after the annealing process.

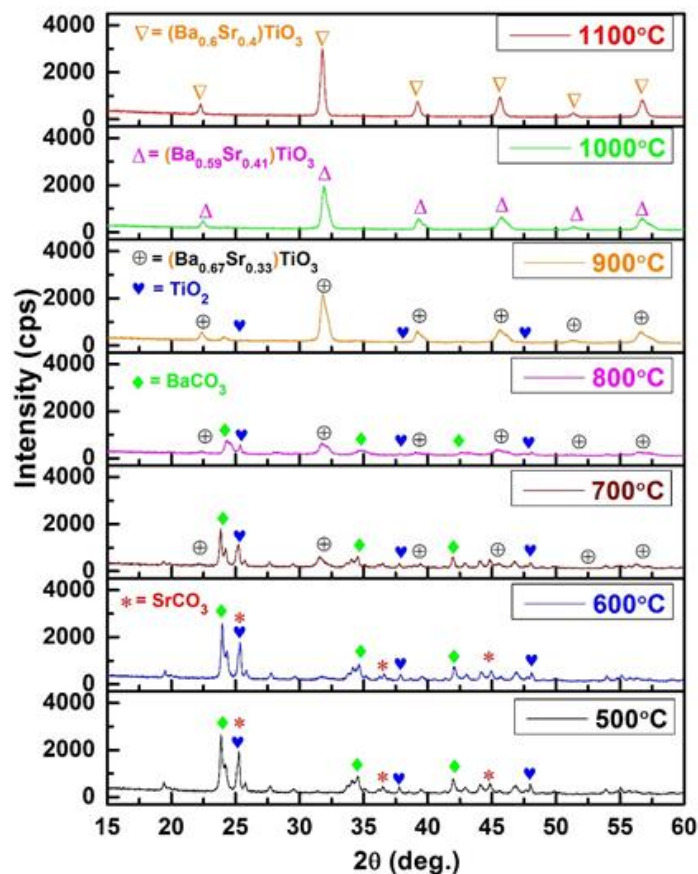


Figure 6.X-ray diffraction patter on the TiO_2 , SrCO_3 and BaCO_3 during annealing proses for 1 hour.

The Rietveld analysis result was performed by applying the High Score Plus program based on the x-ray diffraction pattern in Figure 6. The sample which was annealed at 500°C produced the most dominant phase which was BaCO_3 (witherite) = 47%, TiO_2 (anatase) = 27% and SrCO_3 (strontianite) = 26%. On the other hand, the annealing process at 600°C produced BaCO_3 (witherite) phase = 49.7%, SrCO_3 (strontianite) = 25.5% and TiO_2 (anatase) = 24.7%. Apart from that, the 700°C annealing process produced BaCO_3 phase (witherite) = 39.7%, TiO_2 phase (anatase) = 23.4% and a new phase of $(\text{Ba}_{0.67}\text{Sr}_{0.33})\text{TiO}_3$ with a percentage of 36.9%. The $(\text{Ba}_{0.67}\text{Sr}_{0.33})\text{TiO}_3$ phase was formed from the phase of SrCO_3 and BaCO_3 and TiO_2 phases, in which the Sr element substituted the Ba element which was unstable due to the existence of Sr element in the SrCO_3 phase which has not fully substituted. Furthermore, in the annealing process at 800°C , phase $(\text{Ba}_{0.67}\text{Sr}_{0.33})\text{TiO}_3$ experienced a percentage increase to 43.1% caused by the growth phase due to the increasing heat. The increased percentage then lead to a decrease in the SrCO_3 and TiO_2 phase percentages. In addition, the 900°C annealing process yield an increase in the percentage phase of $(\text{Ba}_{0.67}\text{Sr}_{0.33})\text{TiO}_3$ to 93.4% which was caused by the growth phase due to the increasing heat and the SrCO_3 phase transformation. $(\text{Ba}_{0.67}\text{Sr}_{0.33})\text{TiO}_3$ phase was almost formed into a single phase of $(\text{Ba}_{0.6}\text{Sr}_{0.4})\text{TiO}_3$ and only left 6.6% of TiO_2 phase. On the other hand, the 1000°C annealing process caused TiO_2 phase transformation into a single phase of $(\text{Ba}_{0.59}\text{Sr}_{0.41})\text{TiO}_3$. The percentage of Ba changed from 0.67% to 0.6% and the percentage of Sr atoms changes to 0.41% from the original percentage of 0.33% when transformed into a single phase of $(\text{Ba}_{0.6}\text{Sr}_{0.4})\text{TiO}_3$. Finally, the annealing process at 1100°C showed that the single phase of $(\text{Ba}_{0.6}\text{Sr}_{0.4})\text{TiO}_3$ formed became stable and there was an increase in the size of the crystallite. Table 1 shows the effect of the annealing process on the physical properties of the formation process $(\text{Ba}_{0.6}\text{Sr}_{0.4})\text{TiO}_3$.

Table 1. The physical properties in the formation of (Ba_{0.6}Sr_{0.4})TiO₃.

Annealing Temperature (°C)	Phase	Composition Phase (%)	Crystal system	Crystallite Size (nm)
500	BaCO ₃	47	orthorhombic	52
	TiO ₂	27	terragonal	111
	SrCO ₃	26	orthorhombic	78
600	BaCO ₃	49.7	orthorhombic	57
	TiO ₂	24.7	terragonal	95
	SrCO ₃	25.5	orthorhombic	101
700	BaCO ₃	39.7	orthorhombic	55
	TiO ₂	23.4	terragonal	37
	(Ba _{0.67} Sr _{0.33})TiO ₃	36.9	terragonal	17
800	BaCO ₃	39.6	orthorhombic	15
	TiO ₂	17.3	terragonal	59
	(Ba _{0.67} Sr _{0.33})TiO ₃	43.1	terragonal	20
900	TiO ₂	6.6	terragonal	68
	(Ba _{0.67} Sr _{0.33})TiO ₃	93.4	terragonal	27
1000	(Ba _{0.59} Sr _{0.41})TiO ₃	100	cubic	30
1100	(Ba _{0.6} Sr _{0.4})TiO ₃	100	cubic	43

CONCLUSIONS

The effect of milling time and an annealing process in the production of ceramic material (Ba_{0.6}Sr_{0.4})TiO₃ on its physical properties such as particle size and crystallite and the process of phase formation through conventional solid-state reaction routes has been investigated. Particle size in TiO₂, SrCO₃ and BaCO₃ powder mixtures which was milled in the high-energy vibratory milling up to 58 hours was 0.4 μm, while the crystallite sizes of TiO₂, SrCO₃ and BaCO₃ were 68 nm, 59 nm and 48 nm, respectively. The deformation process that occurred in the TiO₂, SrCO₃ and BaCO₃ powder mixture caused an increase in the milling time to 55 hours which led to the reduction of the particles and crystallites mean size. The annealing process was conducted to a mixture of TiO₂, SrCO₃ and BaCO₃ at a temperature of 500°C to 1100°C resulting in a phase transformation, and at an annealing temperature of 1100°C, a single and stable phase of (Ba_{0.6}Sr_{0.4})TiO₃ was formed. The increase in annealing temperature also affected the increase in crystallite size.

ACKNOWLEDGEMENTS

We would like to express our gratitude to the Ministry of Research and Higher Education for funding this research through Competitive Research Grant with No. 042.06.1.401516/2016.

REFERENCES

[1] T. Rimmel, R. Gregory, and B. Baumert, “Characterization of barium strontium titanate films using XRD,” *Int. Cent. Diffr. Data*, 1999.

[2] G. Akcay, I. B. Misirlioglu, and S. P. Alpay, “Dielectric and pyroelectric properties of barium strontium titanate films on orthorhombic substrates with (110)/(100) epitaxy,” *J. Appl. Phys.*, vol. 101, no. 10, p. 104110, 2007.

[3] M. Enhessari, A. Parviz, K. Ozaee, and H. Habibi Abyaneh, “Synthesis and characterization of barium strontium titanate (BST) micro/nanostructures prepared by improved methods,” *Int. J. Nano Dimens.*, vol. 2, no. 2, pp. 85–103, 2011.

[4] L. Zhou, P. M. Vilarinho, and J. L. Baptista, “Dependence of the structural and dielectric properties of Ba1-xSrxTiO3 ceramic solid solutions on raw material processing,” *J. Eur. Ceram. Soc.*, vol. 19, no. 11, pp. 2015–2020, 1999.

[5] B. Su, J. E. Holmes, B. L. Cheng, and T. W. Button, “Processing effects on the microstructure and dielectric properties of barium strontium titanate (BST) ceramics,” *J. electroceramics*, vol. 9, no. 2, pp. 111–116, 2002.

[6] S. Maensiri, W. Nuansing, J. Klinkaewnarong, P. Laokul, and J. Khemprasit, “Nanofibers

- of barium strontium titanate (BST) by sol–gel processing and electrospinning,” *J. Colloid Interface Sci.*, vol. 297, no. 2, pp. 578–583, 2006.
- [7] W. ZHU, D. PENG, J. CHENG, and Z. MENG, “Effect of (Ba+ Sr)/Ti ratio on dielectric and tunable properties of Ba_{0.6}Sr_{0.4}TiO₃ thin film prepared by sol-gel method,” *Trans. Nonferrous Met. Soc. China*, vol. 16, pp. s261–s265, 2006.
 - [8] M. H. Badr, L. M. S. El-Deen, A. H. Khafagy, and D. U. Nassar, “Structural and mechanical properties characterization of barium strontium titanate (BST) ceramics,” *J. electroceramics*, vol. 27, no. 3–4, pp. 189–196, 2011.
 - [9] D. Y. Lee, K.-H. Lee, M.-H. Lee, N.-I. Cho, and B.-Y. Kim, “Synthesis of electrospun BaSrTiO₃/PVP nanofibers,” *J. sol-gel Sci. Technol.*, vol. 53, no. 1, pp. 43–49, 2010.
 - [10] C. Berbecaru *et al.*, “Ceramic materials Ba (1– x) Sr_xTiO₃ for electronics—Synthesis and characterization,” *Thin Solid Films*, vol. 516, no. 22, pp. 8210–8214, 2008.
 - [11] A. Ioachim *et al.*, “Transitions of barium strontium titanate ferroelectric ceramics for different strontium content,” *Thin Solid Films*, vol. 515, no. 16, pp. 6289–6293, 2007.
 - [12] A. Ioachim *et al.*, “Barium strontium titanate-based perovskite materials for microwave applications,” *Prog. Solid State Chem.*, vol. 35, no. 2–4, pp. 513–520, 2007.
 - [13] J. Q. Qi, Y. Wang, W. Ping Chen, L. Tu Li, and H. Lai Wah Chan, “Direct large-scale synthesis of perovskite barium strontium titanate nano-particles from solutions,” *J. Solid State Chem.*, vol. 178, no. 1, pp. 279–284, Jan. 2005, doi: 10.1016/J.JSSC.2004.12.003.
 - [14] H. Yu, M. Li, C. Hui, A. Xu, and W. Shao, “Effect of bottom electrodes on the dielectric properties of barium strontium titanate thin films,” *Thin Solid Films*, vol. 493, no. 1, pp. 20–23, 2005, doi: <https://doi.org/10.1016/j.tsf.2005.06.018>.
 - [15] Y. Yu, X. Wang, and X. Yao, “Dielectric properties of Ba_{1–x}Sr_xTiO₃ ceramics prepared by microwave sintering,” *Ceram. Int.*, vol. 39, pp. S335–S339, 2013, doi: <https://doi.org/10.1016/j.ceramint.2012.10.089>.
 - [16] W. Jiang, X. Gong, Z. Chen, Y. Hu, X. Zhang, and X. Gong, “Preparation of barium strontium titanate Ba_{1–x}Sr_xTiO₃ (0≤x≤0.2) single-crystal nanorods by a novel combined method,” *Ultrason. Sonochem.*, vol. 14, no. 2, pp. 208–212, 2007, doi: <https://doi.org/10.1016/j.ultsonch.2006.02.002>.
 - [17] D. S. Paik, A. V. P. Rao, and S. Komarneni, “Ba Titanate and Barium/Strontium Titanate Thin Films from Hydroxide Precursors: Preparation and Ferroelectric Behavior,” *J. Sol-Gel Sci. Technol.*, vol. 10, no. 2, pp. 213–220, 1997, doi: 10.1023/A:1018312032470.
 - [18] S. Tusseau-Nenez, J.-P. Ganne, M. Maglione, A. Morell, J.-C. Niepce, and M. Paté, “BST ceramics: Effect of attrition milling on dielectric properties,” *J. Eur. Ceram. Soc.*, vol. 24, no. 10, pp. 3003–3011, 2004, doi: <https://doi.org/10.1016/j.jeurceramsoc.2003.11.019>.
 - [19] Y. Xing, H. Liang, X. Li, and L. Si, “High-frequency dielectric properties of BSTO ceramic prepared with hydrothermal synthesized SrTiO₃ and BaTiO₃ powders,” *Particuology*, vol. 7, no. 5, pp. 414–418, 2009, doi: <https://doi.org/10.1016/j.partic.2009.03.011>.
 - [20] X. H. Zuo *et al.*, “A novel method for preparation of barium strontium titanate nanopowders,” *Mater. Lett.*, vol. 64, no. 10, pp. 1150–1153, 2010, doi: <https://doi.org/10.1016/j.matlet.2010.02.034>.
 - [21] C. Liu, P. Liu, X. Lu, C. Gao, G. Zhu, and X. Chen, “A simple method to synthesize Ba_{0.6}Sr_{0.4}TiO₃ nano-powders through high-energy ball-milling,” *Powder Technol.*, vol. 212, no. 1, pp. 299–302, 2011, doi: <https://doi.org/10.1016/j.powtec.2011.05.010>.
 - [22] Q. Zhang, J. Zhai, B. Shen, H. Zhang, and X. Yao, “Grain size effects on dielectric properties of barium strontium titanate composite ceramics,” *Mater. Res. Bull.*, vol. 48, no. 3, pp. 973–977, 2013, doi: <https://doi.org/10.1016/j.materresbull.2012.11.085>.
 - [23] L. Yang, Y. Wang, Y. Wang, X. Wang, X. Guo, and G. Han, “Synthesis of single-crystal Ba_{1–x}Sr_xTiO₃ (x=0–1) dendrites via a simple hydrothermal method,” *J. Alloys Compd.*, vol. 500, no. 1, pp. L1–L5, 2010, doi: <https://doi.org/10.1016/j.jallcom.2010.03.196>.
 - [24] H. Zhang, L. Zhang, and X. Yao, “Fabrication and electrical properties of barium strontium titanate thick films by modified sol–gel method,” *J. Electroceramics*, vol. 21, no. 1, pp. 503–507, 2008, doi: 10.1007/s10832-007-9229-9.
 - [25] J. Li, D. Jin, L. Zhou, and J. Cheng, “Dielectric properties of Barium Strontium Titanate (BST) ceramics synthesized by using mixed-phase powders calcined at varied temperatures,” *Mater. Lett.*, vol. 76, pp. 100–102, 2012, doi:

- <https://doi.org/10.1016/j.matlet.2012.02.045>.
- [26] T. Sundararajan, S. B. Prabu, and S. M. Vidyavathy, "Combined effects of milling and calcination methods on the characteristics of nanocrystalline barium titanate," *Mater. Res. Bull.*, vol. 47, no. 6, pp. 1448–1454, 2012, doi: <https://doi.org/10.1016/j.materresbull.2012.02.044>.
 - [27] S. Chowdhury, T. Mathan Kr., S. Sen, A. K. Mukhopadhyay, and J. Ghosh, "Influence of crystal structure on dielectric properties of Barium Strontium Titanate during high energy ball milling," *Mater. Today Proc.*, vol. 4, no. 4, Part E, pp. 5631–5639, 2017, doi: <https://doi.org/10.1016/j.matpr.2017.06.022>.
 - [28] I. J. Clark, T. Takeuchi, N. Ohtori, and D. C. Sinclair, "Hydrothermal synthesis and characterisation of BaTiO₃ fine powders: precursors, polymorphism and properties," *J. Mater. Chem.*, vol. 9, no. 1, pp. 83–91, 1999, doi: 10.1039/A805756G.
 - [29] B. D. Stojanovic, "Mechanochemical synthesis of ceramic powders with perovskite structure," *J. Mater. Process. Technol.*, vol. 143–144, pp. 78–81, 2003, doi: [https://doi.org/10.1016/S0924-0136\(03\)00323-6](https://doi.org/10.1016/S0924-0136(03)00323-6).
 - [30] T. Tsuzuki and P. G. McCormick, "Mechanochemical synthesis of nanoparticles," *J. Mater. Sci.*, vol. 39, no. 16–17, pp. 5143–5146, 2004.
 - [31] M. A. Elqudsy, R. D. Widodo, Rusiyanto, and W. Sumbodo, "The particle and crystallite size analysis of BaTiO₃ produced by conventional solid-state reaction process," *AIP Conf. Proc.*, vol. 1818, no. 1, p. 20012, Mar. 2017, doi: 10.1063/1.4976876.
 - [32] G. K. Williamson and W. H. Hall, "X-ray line broadening from filed aluminium and wolfram," *Acta Metall.*, vol. 1, no. 1, pp. 22–31, 1953, doi: [https://doi.org/10.1016/0001-6160\(53\)90006-6](https://doi.org/10.1016/0001-6160(53)90006-6).
 - [33] T. J. Chen, H. J. Zhao, Y. Ma, and Y. Hao, "Microstructure Observation of Naturally Aged Thixoforming ZA27 Alloy," *Mater. Res.*, vol. 18, no. 6, pp. 1322–1330, 2015.
 - [34] C. Suryanarayana, "Mechanical alloying and milling," *Prog. Mater. Sci.*, vol. 46, no. 1, pp. 1–184, 2001, doi: [https://doi.org/10.1016/S0079-6425\(99\)00010-9](https://doi.org/10.1016/S0079-6425(99)00010-9).
 - [35] X. Z. Liao, J. Y. Huang, Y. T. Zhu, F. Zhou, and E. J. Lavernia, "Nanostructures and deformation mechanisms in a cryogenically ball-milled Al-Mg alloy," *Philos. Mag.*, vol. 83, no. 26, pp. 3065–3075, 2003.

II

REVIEW PROCESS



← Back to Submissions

4962 / Rusiyanto et al. / Effect of Sintering Temperature on the Physical Properties of Ba...

Library

Workflow

Publication

Submission

Review

Copyediting

Production

Round 1

Round 1 Status

Submission accepted.

Notifications

[\[IJAME\] Editor Decision](#)

2021-03-17 03:34 PM

[\[IJAME\] Editor Decision](#)

2021-05-18 02:07 PM

[\[IJAME\] Editor Decision](#)

2021-06-14 01:07 AM

Reviewer's Attachments

Q Search



18012

, 4962-Article Text-17744-1-4-20200730.doc

September
21, 2020

Revisions

Q Search

Upload File



21911

Article Text, 4962-Article Text-21412-1-18-

March

Article Text

20210304_REV01.docx

22,
2021

►  21912 Article Text, Response to Reviewers.docx

March Article Text
22,
2021

Review Discussions

[Add discussion](#)

Name	From	Last Reply	Replies	Closed
Request for extension	salwani 2020-09-27 09:59 AM	januar 2020-09-27 10:15 AM	1	<input type="checkbox"/>
Soft reminder: Request for extension	salwani 2020-12-15 10:51 AM	-	0	<input type="checkbox"/>
► Revision of the manuscript	januar 2021-03-04 01:35 AM	-	0	<input type="checkbox"/>

[IJAME] Editor Decision

2021-03-17 03:34 PM

Dear Dr. R. Rusiyanto, R.D. Widodo, D.H. Al-Janan, K. Rohmah, Januar Parlaungan Siregar, A. Nugroho,

I am pleased to inform you that we have received reviewer comments for your manuscript "Effect of Milling Times and Annealing on The Physical Properties of Ba_{0.6}Sr_{0.4}TiO₃ Prepared by Conventional Solid-State Reaction Process".

The reviewers have indicated that the manuscript needs to be improved according to the recommendations. Please carefully address the issues raised in the comments and submit your revised version within two (2) weeks after receiving this email.

Please, also provide a separate "response to the reviews" letter, in which you outline each change made (point by point, in red colour) as raised in the reviewer comments. Provide a suitable rebuttal to each reviewer comment, which is not addressed in the revised version of your manuscript. Please find the attached for the manuscript and reviewer comments for your reference.

Kind regards,
Salwani Mohd Salleh
ijame2@ump.edu.my

Reviewer A:

Recommendation: Revisions Required

Originality and Significance

Acceptable

Methodology well discussed

Good

Conclusion supported by results of work

Excellent

References

Good

Overall Rating

Good

Is this work technically correct?

Yes

Are you aware of prior publication of this manuscript?

Yes

Is the manuscript's length appropriate?

Yes

Comments to author

To assist the author in revising the manuscript, please provide your comments on the technical aspects. Please comment as much as possible to assist author to improve the manuscript.

Perhaps it could be considered surface morphology to support the claim that there is a change in crystal size with milling time

Reviewer C:

Recommendation: Revisions Required

Originality and Significance

Acceptable

Methodology well discussed

Poor

Conclusion supported by results of work

Good

References

Acceptable

Overall Rating

Poor

Is this work technically correct?

Yes

Are you aware of prior publication of this manuscript?

Yes

Is the manuscript's length appropriate?

Yes

Comments to author

To assist the author in revising the manuscript, please provide your comments on the technical aspects. Please comment as much as possible to assist author to improve the manuscript.

This work is interesting, however, authors may clarify and revise the result and discussion (as attached)

Reviewer D:

Recommendation: Revisions Required

Originality and Significance

Acceptable

Methodology well discussed

Acceptable

Conclusion supported by results of work

Acceptable

References

Acceptable

Overall Rating

Acceptable

Is this work technically correct?

Yes

Are you aware of prior publication of this manuscript?

Yes

Is the manuscript's length appropriate?

Yes

Comments to author

To assist the author in revising the manuscript, please provide your comments on the technical aspects. Please comment as much as possible to assist author to improve the manuscript.

The tenses This paper is about Synthesis of $\text{Ba}_{0.6}\text{Sr}_{0.4}\text{TiO}_3$ that was prepared via a conventional solid-state reaction process of BaCO_3 , SrCO_3 and TiO_2 precursors. The effect of milling times on the physical properties (particle and crystallite size) of $\text{Ba}_{0.6}\text{Sr}_{0.4}\text{TiO}_3$ powder is investigated.

It should be considered consistently use present tenses in the result and discussion. The past tenses are only for past process and past event.

It will be better for reader by adding an implication statement in the end of abstract and conclusion.

I suggest the paper is accepted with some revision

Reviewer E:

Recommendation: Accept Submission

Originality and Significance

Good

Methodology well discussed

Good

Conclusion supported by results of work

Good

References

Good

Overall Rating

Good

Is this work technically correct?

Yes

Are you aware of prior publication of this manuscript?

Yes

Is the manuscript's length appropriate?

Yes

Comments to author

To assist the author in revising the manuscript, please provide your comments on the technical aspects. Please comment as much as possible to assist author to improve the manuscript.

To improve:

1. The BaCO₃ size reading is increasing from 52 nm (500 celcius) to 57 then deceasing to 55 to 15 nm and then disappeared at 900 celcius. The same happen with the phase composition %. Please explain. A graph would be a nice addition.
2. Do we have any micrograph to support our XRD discovery?

International Journal of Automotive and Mechanical Engineering (IJAME)

<http://journal.ump.edu.my/ijame>

Response to Reviewers

Reviewer A:

Perhaps it could be considered surface morphology to support the claim that there is a change in crystal size with milling time

- Thank you for the suggested improvements to our article. For us these suggestions are very constructive to improve the quality of our articles. All changes have been shown in a marked version of the article (in 'red font'), which is attached with this submission. In our revised article, we deleted the discussion on the effect of milling duration on crystal size change. Because the sintering process is *only carried out* on precursors that have been milled for 58 hours, so that the discussion focuses on the effect of sintering on the resulting BST.

Reviewer C:

This work is interesting; however, authors may clarify and revise the result and discussion (as attached).

1. What did you mean with "conventional" reaction process? You may not use "conventional" term

- Thank you for the suggested improvements to our article, already fixed.

Before: Conventional Solid-State Reaction Process

After: Solid State Reaction

2. Ceramics $\text{Ba}(1-x)\text{Sr}(x)\text{TiO}_3$ has attracted significant interest as material systems of choice for such application. ➔ You may mention its applications.

- The manuscript has been revised.

3. You are sure very much so you choose this "conventional" method, while there is sol gel methods that may more simple and economics. What is its specialty?

- The manuscript has been revised.

The BST material synthesized by the hydrothermal and sol-gel method produces crystals less than 100 nm. Subsequently, it produces residual hydroxide ions, which resulted in the formation of intergranular pores [25]. The mechanochemical or solid-state method is the most

used method for BST nanoparticles large-scale production [28]. The solid-state method has several advantages; it uses low-cost raw materials, simple synthesis processes, and the ability to produce fine particles [29].

For number 4-8: In our revised article, we deleted the discussion on the effect of milling duration on crystal size change. Because the sintering process is *only carried out* on precursors that have been milled for 58 hours, so that the discussion focuses on the effect of sintering on the resulting BST.

4. The larger duration of alloying affects to decreasing of mean size particle. How to explain that with smaller particle size, the level particle brittleness increase?

- Discussion part has been revised

5. The duration of 58 hours obtains the constant mean size. What the mean size of the duration smaller than 58 hours? It may correspond to smaller duration, i.e. 55 h that does not change the diffraction pattern.

- Discussion part has been improved

6. The diffraction peak of the level (111) shows that the increase in milling duration results in the increase of the diffraction peak along with the decrease in the intensity → Are you sure to argue this statement? Increase of diffraction peaks vs decrease the diffraction peak intensity?

- Discussion part has been changed and improved.

7. It is relation between crystalline mean size with the diffraction peak due to milling duration. Could you explain further with the 55 hrs so that the mean crystallite size of TiO₂, SrCO₃ and BaCO₃ mixture tends to be constant? Are you sure that the SrCO₃ (red line) tends to be constant too. It is likely still to be reduce.

- Discussion part has been changed and improved.

8. Figure 3 and 5 show that the continuous collision force → This argument must be strengthen clearly and you have to explain where is the continuous collision force cause the deformation of crystal structure for 55 h duration.

- Discussion part has been improved

9. You may elaborate this result to the (for example) the heat properties of each material, so it can be explain further why with 1100 annealing temperature, the single phase was formed and it is more stable.
 - The higher temperature makes it easier for the atoms to interact and bond with each other, causing the impurity phase to disappear [36], [38]. Besides, increasing the sintering temperature causes the atomic bonds to become stronger. Thus, sintering carried out at 1000°C and 1100°C resulted in forming a single phase of $\text{Ba}_{0.6}\text{Sr}_{0.4}\text{TiO}_3$ which is more stable. Increasing the sintering temperature will result in a recrystallization process in the raw materials (BaCO_3 , SrCO_3 , and TiO_2) so that a more stable $\text{Ba}_{0.6}\text{Sr}_{0.4}\text{TiO}_3$ phase is formed. An increase in sintering temperature will produce $\text{Ba}_{0.6}\text{Sr}_{0.4}\text{TiO}_3$ with a higher phase composition (%). The crystallite sizes also increased, as reported in previous studies [43], [45]–[47].
10. With this result, you get various $(\text{Ba}_{0.6}\text{Sr}_{0.4}) \text{TiO}_3$. You may show the best properties relating in crystalline size (for example).
 - At temperatures of 700°C, 800°C, and 900°C, the crystal system in the material $\text{Ba}_{0.6}\text{Sr}_{0.4}\text{TiO}_3$ is tetragonal. Whereas at temperatures of 1000°C and 1100°C, the crystal system in the $\text{Ba}_{0.6}\text{Sr}_{0.4}\text{TiO}_3$ is cubic with a higher peak intensity with increasing sintering temperature. The $\text{Ba}_{0.6}\text{Sr}_{0.4}\text{TiO}_3$ with cubic structure will increase the dielectric properties of the material $\text{Ba}_{0.6}\text{Sr}_{0.4}\text{TiO}_3$ produced [36], [38], [52]. Besides the crystal structure, the dielectric properties of the $\text{Ba}_{0.6}\text{Sr}_{0.4}\text{TiO}_3$ material are also influenced by the crystal size. The dielectric property increase with the crystallite size increasing [36]. In this study, the sintering temperature of 1100°C produces $\text{Ba}_{0.6}\text{Sr}_{0.4}\text{TiO}_3$ material with the best physical properties because it has a cubic-shaped crystal structure and the largest crystal size.

Reviewer D

The tenses This paper is about Synthesis of $\text{Ba}_{0.6}\text{Sr}_{0.4}\text{TiO}_3$ that was prepared via a conventional solid-state reaction process of BaCO_3 , SrCO_3 and TiO_2 precursors. The effect of milling times on the physical properties (particle and crystallite size) of $\text{Ba}_{0.6}\text{Sr}_{0.4}\text{TiO}_3$ powder is investigated. It should be consider consistently use present tenses in the result and discussion. The past tenses are only for past process and past event. It will be better for reader by adding an implication statement in the end of abstract and conclusion.

- Thank you for the suggested improvements to our article. The manuscript has been fixed.

Reviewer E

1. The BaCO₃ size reading is increasing from 52 nm (500 celcius) to 57 then deceasing to 55 to 15 nm and then disappeared at 900 celcius. The same happen with the phase composition %. Please explain. A graph would be a nice addition.
- Thank you for the suggested improvements to our article, already fixed. In the revised article, an explanation is added to why this phenomenon occurs.

The results of this study indicate that the Ba_{0.6}Sr_{0.4}TiO₃ material has begun to form at a sintering temperature of 700°C. However, a secondary phase is still formed and completely into single-phase Ba_{0.6}Sr_{0.4}TiO₃ at 1000°C and 1100°C. The effect of sintering temperature on the phase composition (%) and crystallite sizes of Ba_{0.6}Sr_{0.4}TiO₃ formed is shown in Figure 12. The impurity phase disappears proportionately with the increase in sintering temperature. The kinetic energy in atoms increases due to higher sintering temperatures. The higher temperature makes it easier for the atoms to interact and bond with each other, causing the impurity phase to disappear [36], [38]. Besides, increasing the sintering temperature causes the atomic bonds to become stronger. Thus, sintering carried out at 1000°C and 1100°C resulted in forming a single phase of Ba_{0.6}Sr_{0.4}TiO₃ which is more stable. So that an increase in sintering temperature will produce Ba_{0.6}Sr_{0.4}TiO₃ with a higher phase composition (%). The crystallite sizes also increased, as reported in previous studies [43], [45]–[47].

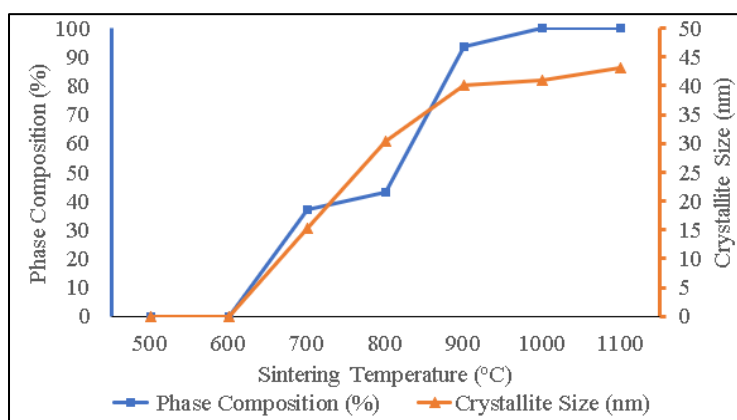


Figure 12. The effect of sintering temperature on the physical properties of Ba_{0.6}Sr_{0.4}TiO₃

2. Do we have any micrograph to support our XRD discovery?
- Sorry, we don't have the micrograph testing.

ORIGINAL ARTICLE

The Effect of Sintering Temperature on The Physical Properties of $\text{Ba}_{0.6}\text{Sr}_{0.4}\text{TiO}_3$ Prepared by Solid State Reaction

Rusiyanto¹, R.D. Widodo¹, D.H. Al-Janani¹, K. Rohmah¹, J.P. Siregar^{2*}, A. Nugroho¹ and D.F. Fitriyana¹

¹Department of Mechanical Engineering, Universitas Negeri Semarang, Kampus Sekaran, Gunungpati, 50229 Semarang, Indonesia

²College of Engineering, Universiti Malaysia Pahang, 26300 Gambang, Kuantan, Malaysia

ABSTRACT – Barium Strontium Titanate (BST) ceramic materials are widely used in electronic devices due to their stable operation at high temperatures, high tunability, low tangent loss, low DC leakage, and alterable curie temperatures. While pure BST materials are usually produced at high sintering temperatures (1250°C), there are limited studies on the temperature and duration of the sintering process to produce pure BST, synthesized from micro or even nano-sized raw materials. This study aims to determine the effective sintering temperature for producing pure BST material using a mixture of raw materials with a mean particle size of 0.4 μm after milled for 58 hours. The BaCO_3 , SrCO_3 , and TiO_2 materials as raw materials for $\text{Ba}_{0.6}\text{Sr}_{0.4}\text{TiO}_3$ synthesis were milled for 58 hours to produce a homogeneous mixture with a mean particle size of 0.4 μm . Sintering was carried out in a temperature range of 500°C – 1100°C for 1 hour. This study investigates the impact of sintering temperature on the physical properties and the purity of $\text{Ba}_{0.6}\text{Sr}_{0.4}\text{TiO}_3$ powder using the X-ray diffraction method. The results showed that the $\text{Ba}_{0.6}\text{Sr}_{0.4}\text{TiO}_3$ phase was formed at a sintering temperature of 700°C. Pure BST material was formed at the sintering temperature of 1000°C with a crystallite size of 41 nm. Whereas at a higher sintering temperature (1100°C), the pure BST material formed produced a larger crystallite, sized at 43 nm with cubic structure. The synthesis temperature and duration recorded in this research are lower than recorded in the BST material preparation using the solid-state method. The results of this study indicate that the sintering temperature greatly affects the purity, crystal system and crystallite size of the $\text{Ba}_{0.6}\text{Sr}_{0.4}\text{TiO}_3$ material produced. The sintering temperature of 1100°C produces $\text{Ba}_{0.6}\text{Sr}_{0.4}\text{TiO}_3$ material with the best physical properties because it has a cubic-shaped crystal system and the largest crystal size.

ARTICLE HISTORY

Received: xxxx

Revised: xxxx

Accepted: xxxx

KEYWORDS

Particle-size

crystallite-size

barium-strontium titanate

solid-state reaction

INTRODUCTION

Barium Strontium Titanate (BST), $\text{Ba}_x\text{Sr}_{(1-x)}\text{TiO}_3$, $0 < x < 1$, is a ferroelectric material with a perovskite structure. This material composes of barium titanate (BaTiO_3) and strontium titanate (SrTiO_3). When SrTiO_3 is added to BaTiO_3 , Sr ion will replace Ba ion to form the BST material structure. Barium Strontium Titanate (BST) ceramic material is widely used in electronic devices [1]–[3]. As bulk ceramics and thin films, this material has a unique combination of large dielectric constant. It demonstrates a stable operation at high temperature, high tunability, low loss tangent, low DC leakage, and alterable curie temperature [4]–[6].

The uniqueness of the BST material is attributed by several factors, such as the Ba / Sr ratio, the synthesis method, and the particle and crystal size [7]. $\text{Ba}_x\text{Sr}_{(1-x)}\text{TiO}_3$ ceramics with various compositions of x (Ba / Sr ratio) has been widely studied.; for example $x = 0.05, 0.10, 0.15$ and 0.20 [8]; $x = 0$ to 0.5 [9]; $x = 0.25, 0.35, 0.40, 0.5, 0.6, 0.75, 0.90$ [10]; $x = 0.35$ and 0.6 [11]; $x = 0.25, 0.50, 0.75$ and 0.90 [12]; $x = 0.1$ [13]; $x = 0.5$ [14]; $x = 0.1$ and 0.6 [15]; $x = 0$ - to 0.2 [16]; and $x = 0.4$ [17]–[22]. Furthermore, the high dielectric and pyroelectric properties of the composition $\text{Ba}_x\text{Sr}_{(1-x)}\text{TiO}_3$ with $0.3 \leq x \leq 0.5$ resulted in the Curie temperature (TC) or ferroelectric-paraelectric phase transformation temperature decrease to near room temperature (25°).

$\text{Ba}_x\text{Sr}_{(1-x)}\text{TiO}_3$ materials are generally synthesized by hydrothermal method [20], [23], sol-gel method [24], and conventional solid-state reaction method [21], [25]–[27]. The BST material synthesized by the hydrothermal and sol-gel method produces crystals less than 100 nm. Subsequently, it produces residual hydroxide ions, which resulted in the formation of intergranular pores [25]. The mechanochemical or solid-state method is the most used method for BST nanoparticles large-scale production [28]. The solid-state method has several advantages; it uses low-cost raw materials, simple synthesis processes, and the ability to produce fine particles [29]. During solid-state processes such as high-energy ball milling, the steps that occur during solid-state processes, specifically, welding, deformation, and fracture of powder raw materials, are repeated [26]. The mechanical activation during solid-state reaction with mechanical milling increases the raw material's specific surface area due to the destruction of agglomerates and particles of the initial precursors [30]. In this regard, the mechanical milling process can produce particles sized $> 1 \mu\text{m}$. In general, the microstructure of the particle and crystallite size of mechanical milling products are influenced by the characteristics of the raw materials used, the duration, and the heating temperature during the mechanical milling process [31].

In recent years, several studies have focused on the effect of sintering temperature on the synthesis of Barium Strontium Titanate (BST). In general, the increase of the temperature and duration time of the sintering process will affect the BST material's purity and increase the crystallite size [31-43]. Pure BST materials are usually produced at high sintering temperatures [32]. Zhang et al. performed sintering at temperatures between 1350 - 1600°C to produce BST-MgO ceramics using a conventional solid-state process [33]. In the meantime, Berbecaru et al. carried out a sintering process at temperatures between 1200-1260°C for 2 hours to produce pure BST material by the solid-state reaction method [34]. Yustanti et al. reported that the sintering raw materials measuring an average size of 2.4 µm at a temperature of 1200°C produced pure BST material without the presence of impurities [35]. Barium strontium titanate ceramic material was synthesized from fine constituent powders produced from high energy ball milling processes at sintering temperatures 1200-1350°C, as reported by Mudinepalli et al., [36]. Meanwhile, Zhu et al. synthesized barium strontium titanate glass and ceramics using the sol-gel method and was sintered at temperatures between 1000 and 1150°C [37]. Lastly, Gate et al. conducted a sintering process at a temperature of 1100°C for 3 hours to produce a pure $\text{Ba}_{0.6}\text{Sr}_{0.4}\text{TiO}_3$ material using the sol-gel method [38].

The high sintering temperature to produce pure BST material has prompted various studies to produce pure BST materials at lower sintering temperatures. One way to produce BST material at low sintering temperatures is to add B_2O_3 material, as reported by Rhim et al. [39] and Hu et al. [40]. Rhim et al. investigated the effect of adding B_2O_3 on the sintering temperature of commercial BST. It was found that by adding 0.5 wt%, B_2O_3 could reduce the sintering temperature to 1150°C [39]. The sintering of BST powder synthesized using the sol-gel method was studied by Hu et al. The study demonstrated that the addition of B_2O_3 to the fine BST powder could reduce the sintering temperature to 900°C. However, the XRD test showed two secondary phases as impurities caused by the addition of boron. Besides, this research method has many limitations when applied to commercial production because it requires a very high cost [40].

However, the BST material's sintering ability decreased along with the broader particle size distribution [41]. Accordingly, reducing the particle size is another way that can be used to speed up or shorten the sintering time. The sintering temperature is reduced with smaller raw material particles. The smaller the raw material particle size, the faster the grain becomes coarse due to the high particle surface energy compared to the large grain size distribution in the batch under the same sintering conditions [42]. In another reference, the raw material with smaller dimensions causes a larger contact surface so that the sinterability increases due to the maximal diffusion process [43]. Therefore, this study uses a vibratory ball milling for 58 hours to mix BaCO_3 , SrCO_3 , and TiO_2 to obtain a homogeneous mixture with a mean particle size of 0.4 µm. This research aims to determine the effective sintering temperature to produce pure BST material using a mixture of BaCO_3 , SrCO_3 , and TiO_2 ball-milled for 58 hours.

METHODS AND MATERIALS

$\text{Ba}_{0.6}\text{Sr}_{0.4}\text{TiO}_3$ was synthesized from BaCO_3 , SrCO_3 , and TiO_2 powders using the mechanical alloying method with a purity level of 99%. The powers were obtained from Sigma-Aldrich, as shown in Figure 1.

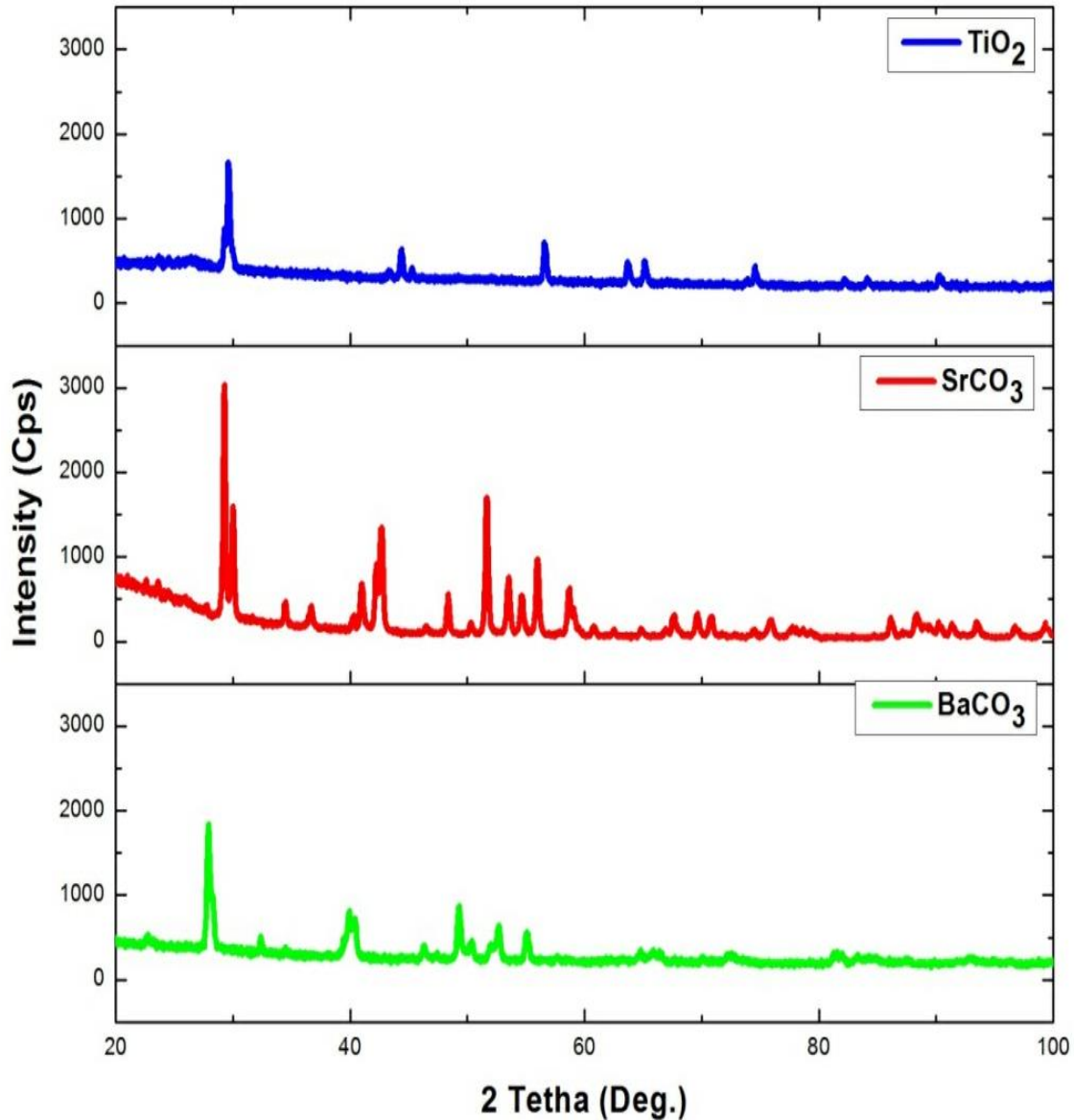


Figure 1. Powder of BaCO_3 , SrCO_3 and TiO_2 as The Raw Material for synthesis $\text{Ba}_{0.6}\text{Sr}_{0.4}\text{TiO}_3$ material

The Particle Size Analyzer (PSA) test results in Table 1 show the BaCO_3 , SrCO_3 , and TiO_2 powders average sizes. Meanwhile, the results of XRD tests on TiO_2 , SrCO_3 , and BaCO_3 powders are shown in Figure 2. The diffraction patterns of TiO_2 , SrCO_3 and BaCO_3 powders are in-line with the diffraction patterns of TiO_2 , SrCO_3 and BaCO_3 in the Inorganic Crystal Structure Database (ICSD), respectively, with numbers 98-009- 6946, 98-016-6088, and 98-016-6090. The Rietveld analysis using High Score Plus software shows that the TiO_2 powder has tetragonal-shaped crystal systems while the SrCO_3 and BaCO_3 powders have orthorhombic crystal systems.

Table 1. Average Particle size (μm) of BaCO_3 , SrCO_3 and TiO_2 Materials

Raw Materials	Average particle size (μm)
BaCO_3	1,979
SrCO_3	3,182
TiO_2	0,795

**Figure 2.** X-ray Diffraction Patterns of TiO_2 , SrCO_3 and BaCO_3 Powders

In this research, BaCO_3 , SrCO_3 and TiO_2 powders were subjected to a wet milling process using a vibratory ball milling machine with a composition of 41.63 grams each, 20.76 grams, and 28.08 grams for 58 hours. The ball to powder ratio (BPR) in the milling process is 10:1. After 58 hours, the mixed BaCO_3 , SrCO_3 and TiO_2 were tested for PSA and XRD. The PSA test results showed that the powder mixture of BaCO_3 , SrCO_3 and TiO_2 had a particle size of $0.4 \mu\text{m}$. Meanwhile, according to the Rietveld analysis using the High Score Plus software, the XRD test results are shown in Figure 3. Figure 3 shows no change in the diffraction pattern of the powder of TiO_2 , SrCO_3 and BaCO_3 . The crystal sizes of BaCO_3 , SrCO_3 and TiO_2 calculated using The Williamson-Hall method [44] are 48 nm, 61 nm, and 71 nm, respectively.

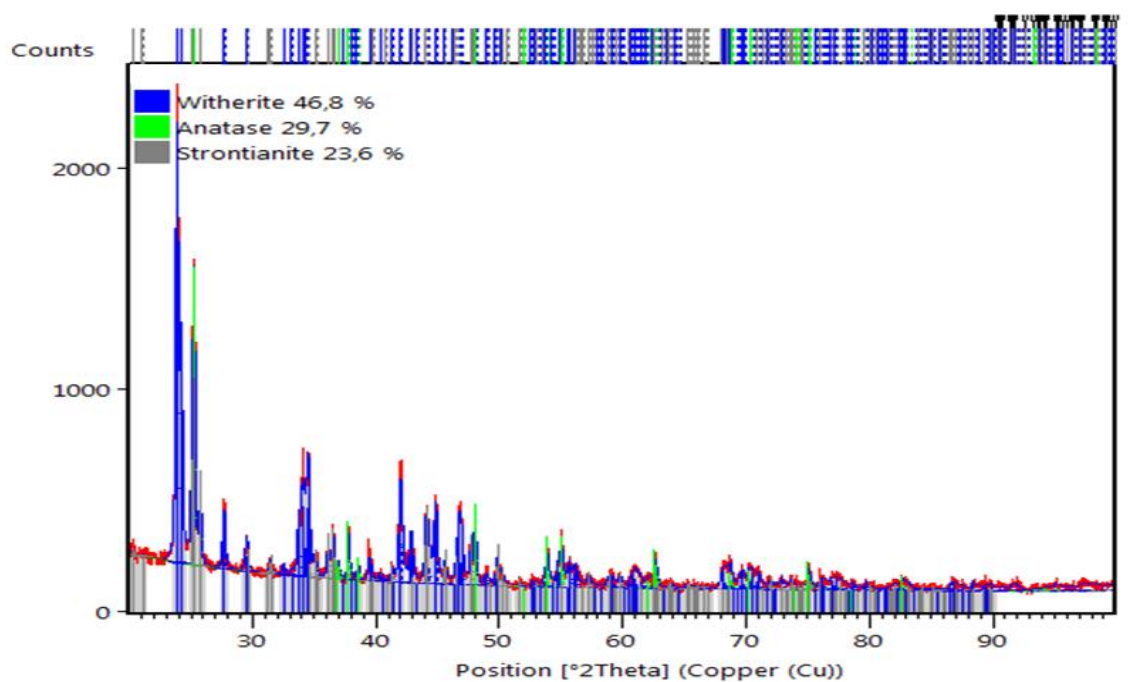


Figure 3. X-ray Diffraction Patterns of TiO_2 , SrCO_3 and BaCO_3 Powders Mixture After 58 Hours of Milling

After characterizing the mixture of milled TiO_2 , SrCO_3 , and BaCO_3 powders, the next step is sintering the powder mixture of TiO_2 , SrCO_3 and BaCO_3 . The sintering process was carried out in the electric chamber furnace (Nabertherm N31/H) with temperature variations of 500°C , 600°C , 700°C , 800°C , 900°C , 1000°C , and 1100°C in the air under atmospheric pressure up to 1 hour. After the sintering process, characterization was carried out using the XRD methods. The Philips XRD was also used to analyze the resulting phase and crystallite size. The "step-scan" method was performed to record the X-ray diffraction patterns. The intensity data during the scanning was taken every 2 seconds for each step on the diffraction angle of 0.005° . The Rietveld analysis was conducted using the High Score Plus software. The description of the diffraction line profiles at Rietveld refinement was achieved using the pseudo-Voigt function.

RESULTS AND DISCUSSION

Figure 4 shows the diffraction pattern of BaCO_3 , SrCO_3 , and TiO_2 powder mixture at each sintering temperature. Figure 4 shows the material sintered at temperatures of 500°C and 600°C , the $\text{Ba}_{0,6}\text{Sr}_{0,4}\text{TiO}_3$ phase was not formed. Meanwhile, while the $\text{Ba}_{0,6}\text{Sr}_{0,4}\text{TiO}_3$ phase was formed at temperatures of 700°C , 800°C and 900°C , other compound phases, BaCO_3 , SrCO_3 , TiO_2 and BaTiO_3 , were observed. Moreover, a single-phase $\text{Ba}_{0,6}\text{Sr}_{0,4}\text{TiO}_3$ was formed at temperatures of 1000°C and 1100°C .

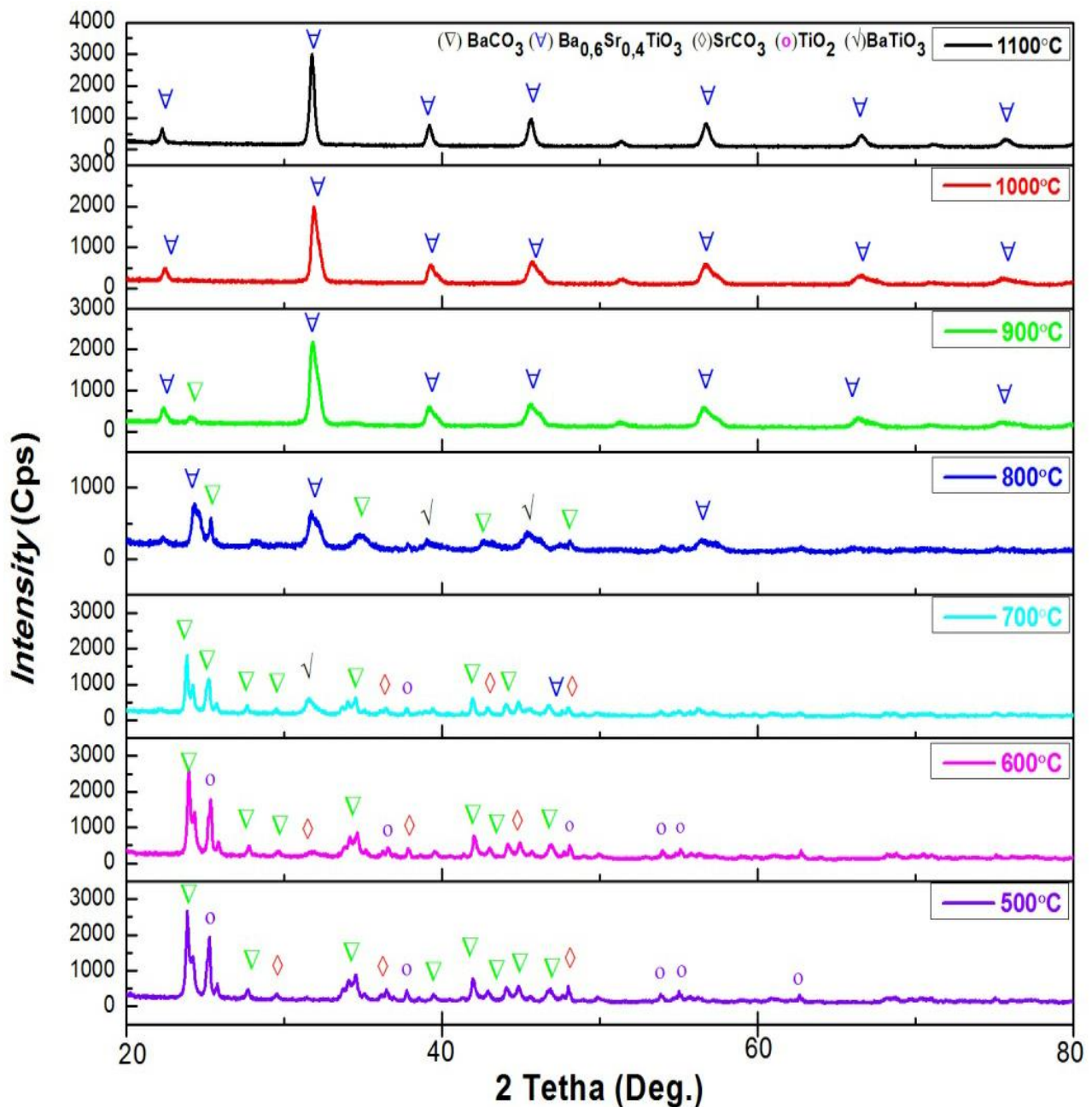


Figure 4. X-ray Diffraction Patterns of The Sintered Samples

Figure 5 to Figure 11 show the Rietveld analysis results using the High Score Plus software based on X-ray diffraction obtained from the test results. Figure 5 shows the X-ray diffraction pattern on a powder that has been sintered at 500°C. The X-ray diffraction pattern shows that the $\text{Ba}_{0.6}\text{Sr}_{0.4}\text{TiO}_3$ phase was not formed. In this light, the phases formed at 500°C sintering temperature variations are BaCO_3 (witherite), TiO_2 (anatase), and SrCO_3 (strontianite), with the respective percentage of 48.3%; 27.2%, and 24.5%. Meanwhile, the crystallite size formed in BaCO_3 , TiO_2 , and SrCO_3 was 54.7 nm, 125.6 nm, and 80.3 nm. The X-ray diffraction pattern of the sintered powder at 600°C is shown in Figure 6. At 600°C, $\text{Ba}_{0.6}\text{Sr}_{0.4}\text{TiO}_3$ was not formed and still in the BaCO_3 , TiO_2 , and SrCO_3 phases, with 51.2%; 24.2% and 24.6%, respectively. The sizes of the crystallites formed after sintering BaCO_3 , TiO_2 , and SrCO_3 at 600°C for are 56.4 nm, 104.3nm, and 122.3 nm, respectively.

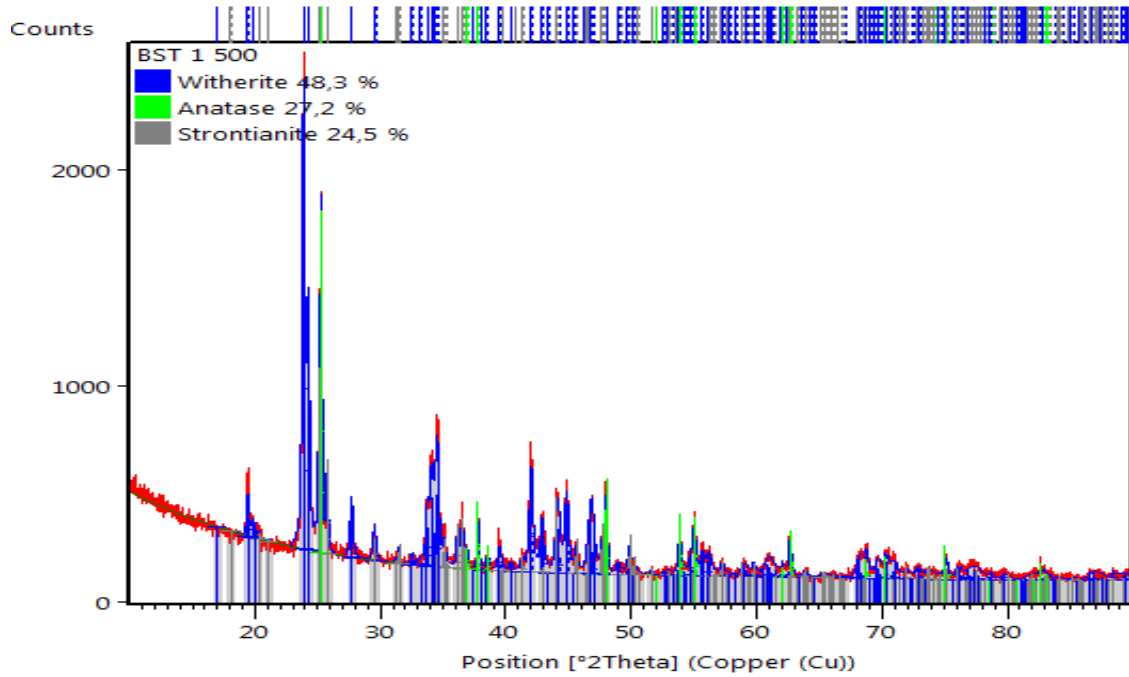


Figure 5. X-ray Diffraction Patterns of The Sintered Samples at 500°C

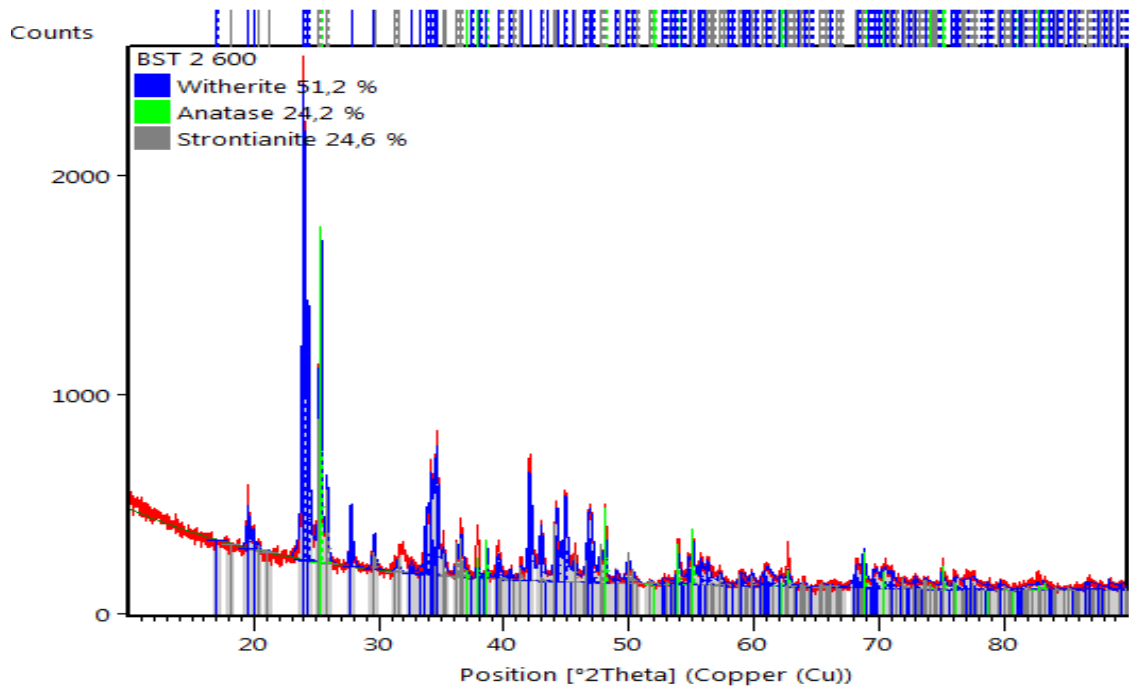


Figure 6. X-ray Diffraction Patterns of The Sintered Samples at 600°C

Figure 7 shows the X-ray diffraction pattern of a mixture of BaCO_3 , SrCO_3 , and TiO_2 powders sintered at 700°C. At a temperature of 700°C, the $\text{Ba}_{0.6}\text{Sr}_{0.4}\text{TiO}_3$ phase was formed with a percentage of 19.4% and a crystallite size of 15.3 nm. However, at 700°C, BaCO_3 , SrCO_3 and TiO_2 phases were still found with the respective percentages of 35.2%, 22.2%, and 19.8% with crystallite sizes of 58.1 nm; 65.6 nm and 66.2 nm, respectively. Apart from the $\text{Ba}_{0.6}\text{Sr}_{0.4}\text{TiO}_3$, BaCO_3 , SrCO_3 and TiO_2 phases, a new phase, BaTiO_3 , with a percentage of 3.4% and a crystallite size of 38 nm, was also formed.

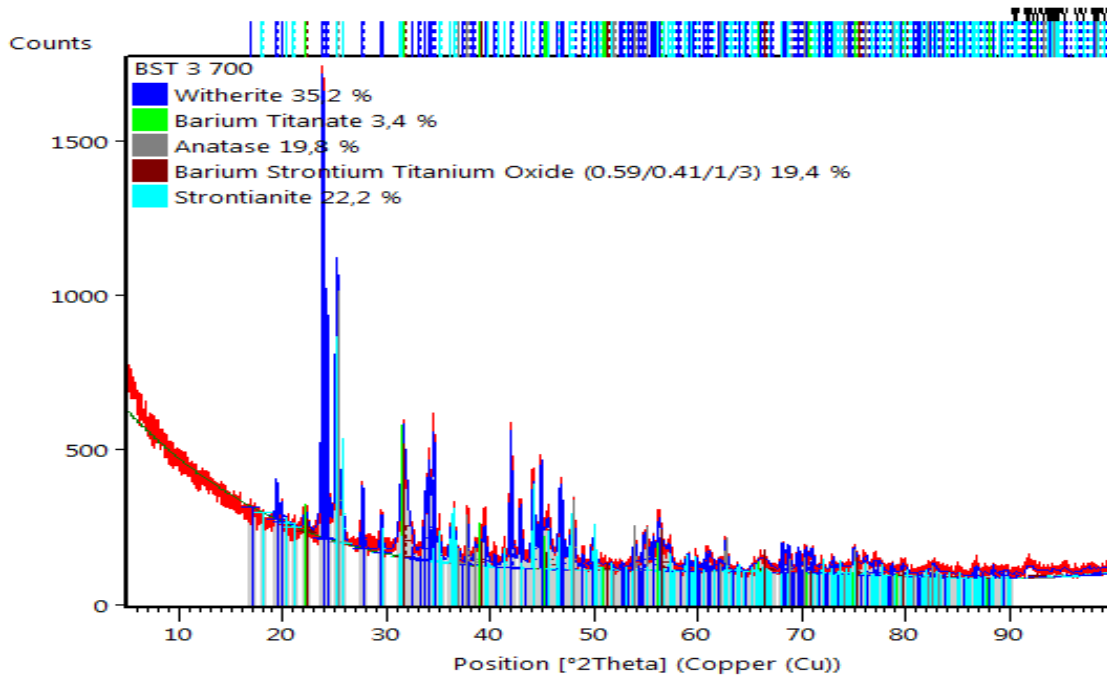


Figure 7. X-ray Diffraction Patterns of The Sintered Samples at 700°C

Figure 8 shows that the crystallite percentage increased to 22.4%, and its size increased to 30.3 nm at the $\text{Ba}_{0.6}\text{Sr}_{0.4}\text{TiO}_3$ phase when sintering at 800°C. In this variation, the crystal size of $\text{Ba}_{0.6}\text{Sr}_{0.4}\text{TiO}_3$ is two times the crystallite size formed at 700°C sintering temperature. Meanwhile, the BaTiO_3 phase percentage decreased to 2.2%, accompanied by a decrease in crystal size to 19.5 nm. BaCO_3 phases were still found with a percentage of 47% with a crystallite size of 40 nm. Apart from the $\text{Ba}_{0.6}\text{Sr}_{0.4}\text{TiO}_3$, BaCO_3 , and BaTiO_3 phases, a new phase, SrTiO_3 , with a percentage of 28.3% and a crystallite size of 32.6 nm, was also formed.

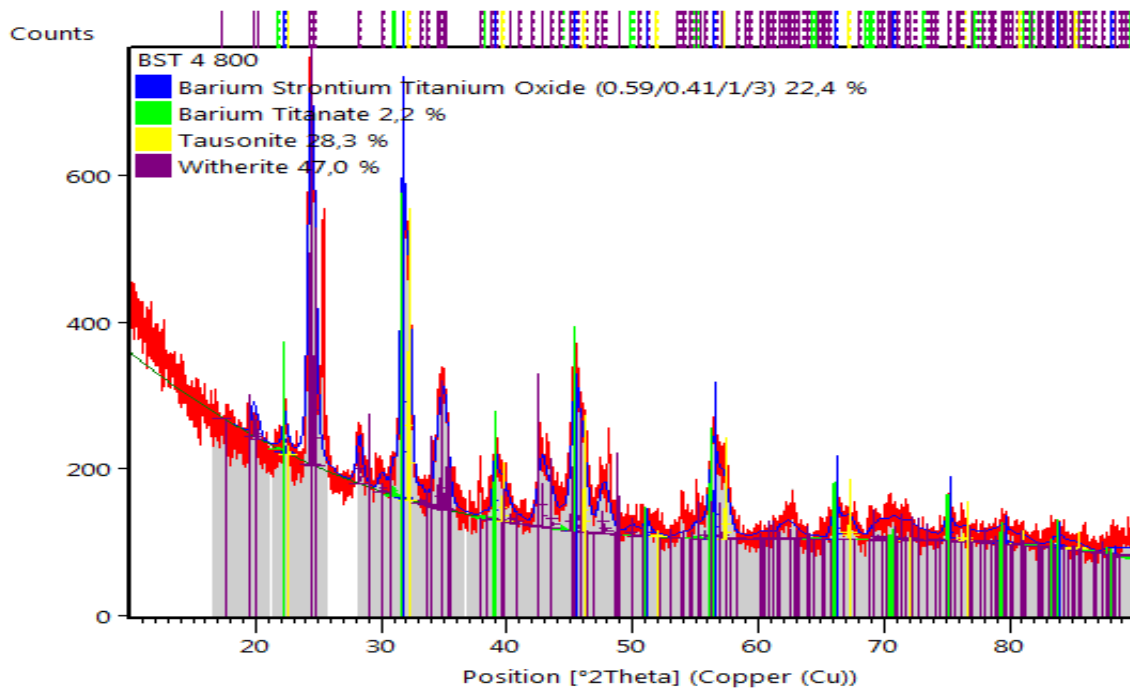


Figure 8. X-ray diffraction patterns of the sintered samples at 800°C

Figure 9 shows the X-ray diffraction pattern at a product sintering temperature of 900°C. The $\text{Ba}_{0.6}\text{Sr}_{0.4}\text{TiO}_3$ phase formed in this variation experienced a significant increase with a percentage of 94.6% and a crystallite size of 40.1 nm. Simultaneously, the other 5.4% is the BaCO_3 phase with a crystallite size of 21.5 nm. The single phase of $\text{Ba}_{0.6}\text{Sr}_{0.4}\text{TiO}_3$ was formed perfectly at various sintering temperatures of 1000°C and 1100°C, as shown in Figure 10 and Figure 11. $\text{Ba}_{0.6}\text{Sr}_{0.4}\text{TiO}_3$ with the crystallites sized 30 nm and 43 nm resulted in sintering temperatures of 1000°C and 1100°C.

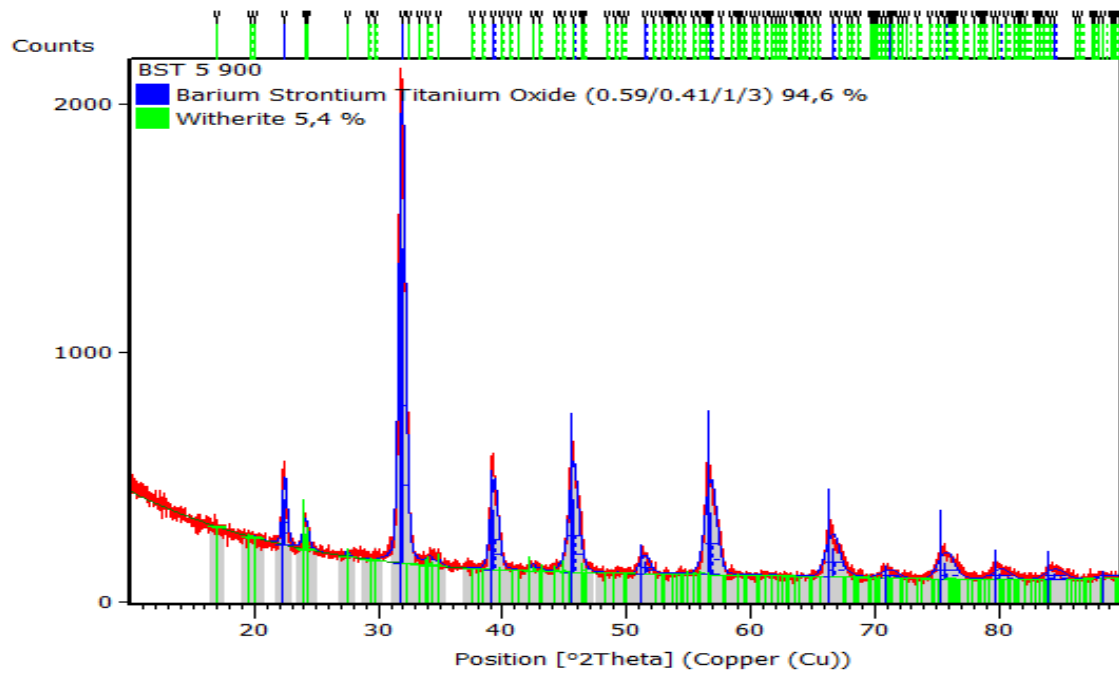


Figure 9. X-ray Diffraction Patterns of The Sintered Samples at 900°C

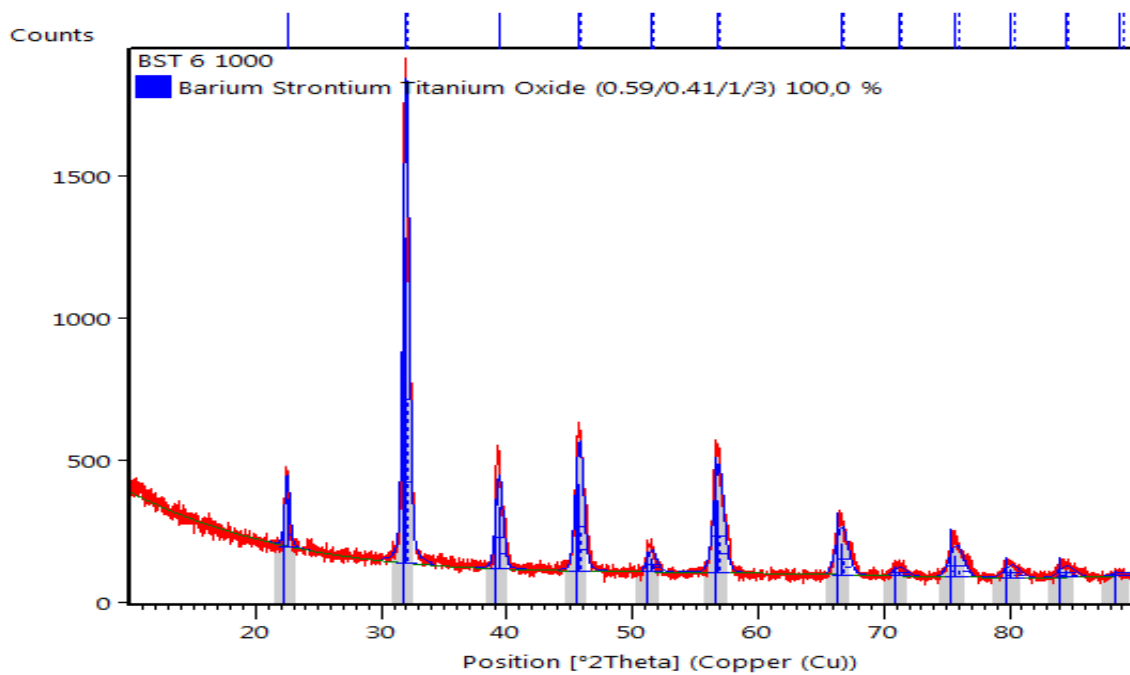


Figure 10. X-ray Diffraction Patterns of The Sintered Samples at 1000°C

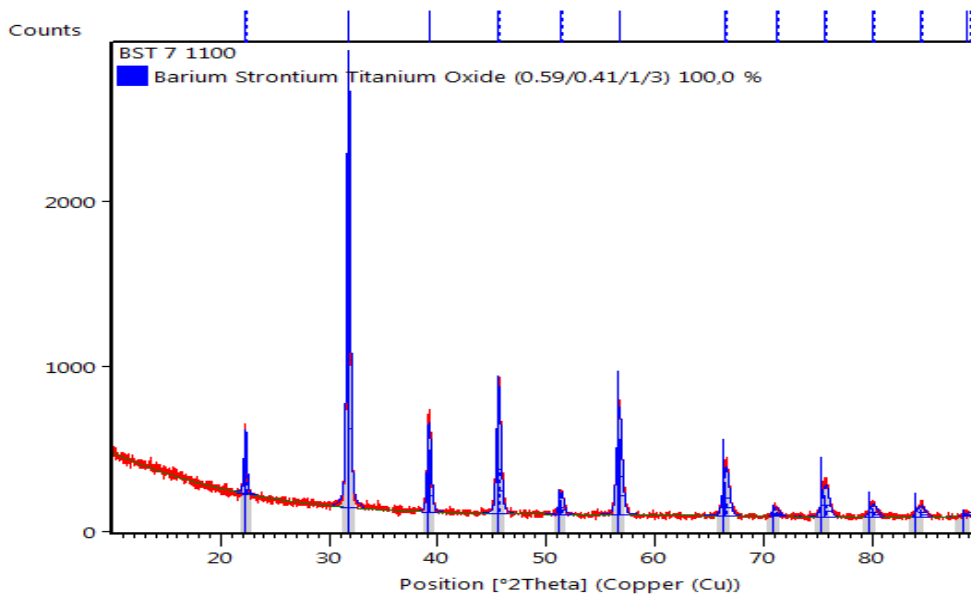


Figure 11. X-ray Diffraction Patterns of The Sintered Samples at 1100°C

The results of this study indicate that the $\text{Ba}_{0.6}\text{Sr}_{0.4}\text{TiO}_3$ material has begun to form at a sintering temperature of 700°C. However, a secondary phase is still formed and completely into single-phase $\text{Ba}_{0.6}\text{Sr}_{0.4}\text{TiO}_3$ at 1000°C and 1100°C. The effect of sintering temperature on the phase composition (%) and crystallite sizes of $\text{Ba}_{0.6}\text{Sr}_{0.4}\text{TiO}_3$ formed is shown in Figure 12. The impurity phase disappears proportionately with the increase in sintering temperature. The kinetic energy in atoms increases due to higher sintering temperatures. The higher temperature makes it easier for the atoms to interact and bond with each other, causing the impurity phase to disappear [36], [38]. Besides, increasing the sintering temperature causes the atomic bonds to become stronger. Thus, sintering carried out at 1000°C and 1100°C resulted in forming a single phase of $\text{Ba}_{0.6}\text{Sr}_{0.4}\text{TiO}_3$ which is more stable. Increasing the sintering temperature will result in a recrystallization process in the raw materials (BaCO_3 , SrCO_3 , and TiO_2) so that a more stable $\text{Ba}_{0.6}\text{Sr}_{0.4}\text{TiO}_3$ phase is formed. An increase in sintering temperature will produce $\text{Ba}_{0.6}\text{Sr}_{0.4}\text{TiO}_3$ with a higher phase composition (%). The crystallite sizes also increased, as reported in previous studies [43], [45]–[47].

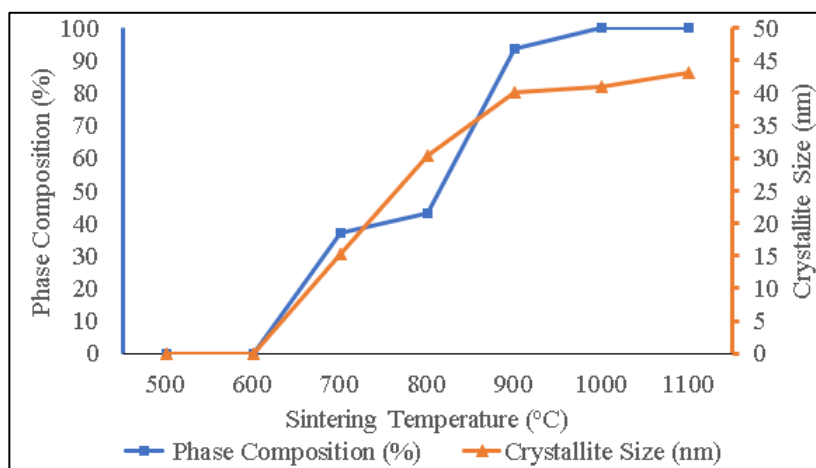


Figure 12. The effect of sintering temperature on the physical properties of $\text{Ba}_{0.6}\text{Sr}_{0.4}\text{TiO}_3$

The use of BaCO_3 , SrCO_3 , and TiO_2 powder mixture, with a particle size of 0.4 μm , has been proven to produce $\text{Ba}_{0.6}\text{Sr}_{0.4}\text{TiO}_3$ material at lower sintering temperatures with a faster duration (1 hour). This is supported by [42] and [43] study which revealed that reducing the particle size of raw materials is another method that can be used to speed up sintering and shorten sintering time. The sintering temperature is reduced with smaller raw material particles. The smaller the raw material particle size, the faster the grain becomes coarse due to the high particle surface energy compared to the large grain size distribution in the batch under the same sintering conditions [42]. Previous research [43] mentioned raw materials with smaller dimensions causes a larger contact surface so that the sinterability increases due to the maximum diffusion process. In this study, sintering carried out at temperatures of 1000°C and 1100°C for 1 hour produced single-phase $\text{Ba}_{0.6}\text{Sr}_{0.4}\text{TiO}_3$. In this study, single-phase $\text{Ba}_{0.6}\text{Sr}_{0.4}\text{TiO}_3$ resulted in lower sintering temperature and shorter sintering duration compared to the results of the study conducted by [34]–[36], [38]. These studies' results showed the single-phase formation of $\text{Ba}_{0.6}\text{Sr}_{0.4}\text{TiO}_3$ was carried out in a sintering temperature range of 1100°C–1350°C with a sintering duration of ≥ 2 hours.

The 1000°C sintering temperature is lower than that of the generally prepared BST powders (1250°C) solid-state method [45]. [45] also found that well-crystallized BST nano-powders are produced at lower calibration temperatures by using raw materials of smaller particle size. BaCO₃, SrCO₃ and TiO₂ conducted high energy ball milling (HEBM) with different milling parameters in their research. The high-energy ball milling (HEBM) process for 5 hours, 400/800 rpm on the raw material, produced a particle size of 0.48 µm (480) nm. The sintering carried out on the material at a temperature of 1000°C for 2 hours were able to produce Well-crystallized BST nano-powders. In addition, [43], [46]–[48] have clearly shown that the decrease in calcination or sintering temperature is due to the reduction in the small particle size of the raw materials ranging from submicrometer or even to the nanoscale. The use of smaller particle size increases the contact area and decreases the reactants' contact distance, thereby increasing the overall reaction kinetics.

The results of this study indicate that the sintering temperature greatly affects the purity, crystal system, and crystallite size of the material Ba_{0.6}Sr_{0.4}TiO₃ produced. The effect of sintering temperature on the physical properties of Ba_{0.6}Sr_{0.4}TiO₃ formed is shown in Table 2. The higher the sintering temperature will result in a sharper peak intensity at Ba_{0.6}Sr_{0.4}TiO₃, which indicates an increase in crystal size. Accordingly, the higher the sintering temperature used, the higher the crystal size of the material Ba_{0.6}Sr_{0.4}TiO₃ formed. This is supported by the studies of [38], [43], [49]. Thus, increasing the sintering temperature will increase the atoms' kinetic energy to diffuse and make the atoms react and bond perfectly. This finding is supported by other studies [43], [49]–[51] that found that the crystallites produced have a larger size and higher crystallinity. In addition, an increase in the sintering temperature in this study will cause changes in the crystal system of the Ba_{0.6}Sr_{0.4}TiO₃ material. At temperatures of 700°C, 800°C, and 900°C, the crystal system in the material Ba_{0.6}Sr_{0.4}TiO₃ is tetragonal. Whereas at temperatures of 1000°C and 1100°C, the crystal system in the Ba_{0.6}Sr_{0.4}TiO₃ is cubic with a higher peak intensity with increasing sintering temperature. The Ba_{0.6}Sr_{0.4}TiO₃ with cubic structure will increase the dielectric properties of the material Ba_{0.6}Sr_{0.4}TiO₃ produced [36], [38], [52]. Besides the crystal structure, the dielectric properties of the Ba_{0.6}Sr_{0.4}TiO₃ material are also influenced by the crystal size. The dielectric property increase with the crystallite size increasing [36]. In this study, the sintering temperature of 1100°C produces Ba_{0.6}Sr_{0.4}TiO₃ material with the best physical properties because it has a cubic-shaped crystal system and the largest crystal size.

Table 2. The Physical Properties in The Formation of (Ba_{0.6}Sr_{0.4})TiO₃.

Sintering Temperature (°C)	Phase	Composition Phase (%)	Crystal system	Crystallite Size (nm)
500	BaCO ₃	48	Orthorhombic	54.7
	TiO ₂	27	Tertragonal	125.6
	SrCO ₃	25	Orthorhombic	80.3
600	BaCO ₃	51.2	Orthorhombic	56.4
	TiO ₂	24.2	Tertragonal	104.3
	SrCO ₃	24.6	Orthorhombic	122.3
700	BaCO ₃	35.2	Orthorhombic	58.1
	TiO ₂	19.8	Tertragonal	19.8
	SrCO ₃	22.2	Orthorhombic	65.6
	BaTiO ₃	3.4	Orthorhombic	38
	(Ba _{0.67} Sr _{0.33}) TiO ₃	19.4	Tertragonal	15.3
800	BaCO ₃	47	Orthorhombic	40
	BaTiO ₃	2.2	Orthorhombic	19.5
	SrTiO ₃	28.3	Orthorhombic	32.6
	(Ba _{0.67} Sr _{0.33}) TiO ₃	22.4	Tertragonal	30.3
900	BaCO ₃	5.4	Orthorhombic	21.5
	(Ba _{0.67} Sr _{0.33}) TiO ₃	94.6	Tertragonal	40.1
1000	(Ba _{0.59} Sr _{0.41}) TiO ₃	100	Cubic	41
1100	(Ba _{0.6} Sr _{0.4}) TiO ₃	100	Cubic	43

CONCLUSION

The effect of sintering temperature on the physical properties of Ba_{0.6}Sr_{0.4}TiO₃ material synthesized with 0.4 µm raw materials (milled up to 58 h) using the solid-state reaction method has been investigated. The use of raw materials, a mixture of BaCO₃, SrCO₃, and TiO₂ with a particle size of 0.4 µm could produce Ba_{0.6}Sr_{0.4}TiO₃ material at a lower sintering temperature of 700°C. Moreover, the single-phase Ba_{0.6}Sr_{0.4}TiO₃ could be produced at temperatures of 1000°C and 1100°C. Increasing the sintering temperature in this study resulted in Ba_{0.6}Sr_{0.4}TiO₃ material with higher purity as marked by the disappearance of the BaTiO₃, BaCO₃, SrCO₃, and TiO₂ phases. Higher sintering temperature will increase the crystal size and change the crystal system from tetragonal to cubic.

The sintering temperature of 1100°C produces $\text{Ba}_{0.6}\text{Sr}_{0.4}\text{TiO}_3$ material with the best physical properties because it has a cubic-shaped crystal system and the largest crystal size.

ACKNOWLEDGEMENT

We would like to express our gratitude to the Ministry of Research and Higher Education for funding this research through Competitive Research Grant with No. 042.06.1.401516/2016.

REFERENCES

- [1] T. Rimmel, R. Gregory, and B. Baumert, *Characterization of barium strontium titanate films using XRD*. Int. Cent. Diffraction Data, 1999.
- [2] G. Akcay, I. B. Misirlioglu, and S. P. Alpay, "Dielectric and pyroelectric properties of barium strontium titanate films on orthorhombic substrates with (110)/(100) epitaxy," *J. Appl. Phys.*, vol. 101, no. 10, p. 104110, 2007.
- [3] M. Enhessari, A. Parviz, K. Ozace, and H. H. Abyaneh, "Synthesis and characterization of barium strontium titanate (BST) micro/nanostructures prepared by improved methods," *Int. J. Nano Dimens.*, vol. 2, no. 2, pp. 85–103, 2011.
- [4] L. Zhou, P. M. Vilarinho, and J. L. Baptista, "Dependence of the structural and dielectric properties of $\text{Ba}_{1-x}\text{Sr}_x\text{TiO}_3$ ceramic solid solutions on raw material processing," *J. Eur. Ceram. Soc.*, vol. 19, no. 11, pp. 2015–2020, 1999.
- [5] B. Su, J. E. Holmes, B. L. Cheng, and T. W. Button, "Processing effects on the microstructure and dielectric properties of barium strontium titanate (BST) ceramics," *J. electroceramics*, vol. 9, no. 2, pp. 111–116, 2002.
- [6] S. Maensiri, W. Nuansing, J. Klinkaewnarong, P. Laokul, and J. Khemprasit, "Nanofibers of barium strontium titanate (BST) by sol-gel processing and electrospinning," *J. Colloid Interface Sci.*, vol. 297, no. 2, pp. 578–583, 2006.
- [7] W. Zhu, D. Peng, J. Cheng, and Z. Meng, "Effect of (Ba+ Sr)/Ti ratio on dielectric and tunable properties of $\text{Ba}_{0.6}\text{Sr}_{0.4}\text{TiO}_3$ thin film prepared by sol-gel method," *Trans. Nonferrous Met. Soc. China*, vol. 16, pp. s261–s265, 2006.
- [8] M. H. Badr, L. M. S. El-Deen, A. H. Khafagy, and D. U. Nassar, "Structural and mechanical properties characterization of barium strontium titanate (BST) ceramics," *J. electroceramics*, vol. 27, no. 3–4, pp. 189–196, 2011.
- [9] D. Y. Lee, K.-H. Lee, M.-H. Lee, N.-I. Cho, and B.-Y. Kim, "Synthesis of electrospun BaSrTiO_3 3/PVP nanofibers," *J. sol-gel Sci. Technol.*, vol. 53, no. 1, pp. 43–49, 2010.
- [10] C. Berbecaru, "Ceramic materials $\text{Ba}_{(1-x)}\text{Sr}_x\text{TiO}_3$ for electronics—Synthesis and characterization," *Thin Solid Films*, vol. 516, no. 22, pp. 8210–8214, 2008.
- [11] A. Ioachim, "Transitions of barium strontium titanate ferroelectric ceramics for different strontium content," *Thin Solid Films*, vol. 515, no. 16, pp. 6289–6293, 2007.
- [12] A. Ioachim, "Barium strontium titanate-based perovskite materials for microwave applications," *Prog. Solid State Chem.*, vol. 35, no. 2–4, pp. 513–520, 2007.
- [13] J. Q. Qi, Y. Wang, W. P. Chen, L. T. Li, and H. L. W. Chan, "Direct large-scale synthesis of perovskite barium strontium titanate nano-particles from solutions," *J. Solid State Chem.*, vol. 178, no. 1, pp. 279–284, 2005, doi: doi.org/10.1016/J.JSSC.2004.12.003.
- [14] H. Yu, M. Li, C. Hui, A. Xu, and W. Shao, "Effect of bottom electrodes on the dielectric properties of barium strontium titanate thin films," *Thin Solid Films*, vol. 493, no. 1, pp. 20–23, 2005.
- [15] Y. Yu, X. Wang, and X. Yao, "Dielectric properties of $\text{Ba}_{1-x}\text{Sr}_x\text{TiO}_3$ ceramics prepared by microwave sintering," *Ceram. Int.*, vol. 39, no. S335–S339, 2013, doi: doi.org/10.1016/j.ceramint.2012.10.089.
- [16] W. Jiang, X. Gong, Z. Chen, Y. Hu, X. Zhang, and X. Gong, "Preparation of barium strontium titanate $\text{Ba}_{1-x}\text{Sr}_x\text{TiO}_3$ ($0 \leq x \leq 0.2$) single-crystal nanorods by a novel combined method," *Ultrason. Sonochem.*, vol. 14, no. 2, pp. 208–212, 2007, doi: doi.org/10.1016/j.ultsonch.2006.02.002.
- [17] D. S. Paik, A. V. P. Rao, and S. Komarneni, "Ba Titanate and Barium/Strontium Titanate Thin Films from Hydroxide Precursors: Preparation and Ferroelectric Behavior," *J. Sol-Gel Sci. Technol.*, vol. 10, no. 2, pp. 213–220, 1997, doi: doi.org/10.1023/A:1018312032470.
- [18] S. Tusseau-Nenez, J.-P. Ganne, M. Maglione, A. Morell, J.-C. Niepce, and M. Paté, "BST ceramics: Effect of attrition milling on dielectric properties," *J. Eur. Ceram. Soc.*, vol. 24, no. 10, pp. 3003–3011, 2004, doi: doi.org/10.1016/j.jeurceramsoc.2003.11.019.
- [19] Y. Xing, H. Liang, X. Li, and L. Si, "High-frequency dielectric properties of BSTO ceramic prepared with hydrothermal synthesized SrTiO_3 and BaTiO_3 powders," *Particuology*, vol. 7, no. 5, pp. 414–418, 2009, doi: doi.org/10.1016/j.partic.2009.03.011.
- [20] et al X. H. Zuo, "A novel method for preparation of barium strontium titanate nanopowders," *Mater. Lett.*, vol. 64, no. 10, pp. 1150–1153, 2010, doi: doi.org/10.1016/j.matlet.2010.02.034.
- [21] C. Liu, P. Liu, X. Lu, C. Gao, G. Zhu, and X. Chen, "A simple method to synthesize $\text{Ba}_{0.6}\text{Sr}_{0.4}\text{TiO}_3$ nano-powders through high-energy ball-milling," *Powder Technol.*, vol. 212, no. 1, pp. 299–302, 2011, doi: doi.org/10.1016/j.powtec.2011.05.010.
- [22] Q. Zhang, J. Zhai, B. Shen, H. Zhang, and X. Yao, "Grain size effects on dielectric properties of barium strontium titanate composite ceramics," *Mater. Res. Bull.*, vol. 48, no. 3, pp. 973–977, 2013, doi: doi.org/10.1016/j.materresbull.2012.11.085.
- [23] L. Yang, Y. Wang, Y. Wang, X. Wang, X. Guo, and G. Han, "Synthesis of single-crystal $\text{Ba}_{1-x}\text{Sr}_x\text{TiO}_3$ ($x=0-1$) dendrites via a simple hydrothermal method," *J. Alloy. Compd.*, vol. 500, no. 1, pp. L1–L5, 2010, doi: doi.org/10.1016/j.jallcom.2010.03.196.
- [24] H. Zhang, L. Zhang, and X. Yao, "Fabrication and electrical properties of barium strontium titanate thick films by modified sol-gel method doi: .," *J. Electroceramics*, vol. 21, no. 1, pp. 503–507, 2008, doi: https://doi.org/10.1007/s10832-007-9229-9.
- [25] J. Li, D. Jin, L. Zhou, and J. Cheng, "Dielectric properties of Barium Strontium Titanate (BST) ceramics synthesized by using mixed-phase powders calcined at varied temperatures," *Mater. Lett.*, vol. 76, pp. 100–102, 2012, doi: https://doi.org/10.1016/j.matlet.2012.02.045.
- [26] T. Sundararajan, S. B. Prabu, and S. M. Vidyavathy, "Combined effects of milling and calcination methods on the characteristics of nanocrystalline barium titanate," *Mater. Res. Bull.*, vol. 47, no. 6, pp. 1448–1454, 2012, doi:

- <https://doi.org/10.1016/j.materresbull.2012.02.044>.
- [27] T. M. K. S. Chowdhury, S. Sen, A. K. Mukhopadhyay, and J. Ghosh, "Influence of crystal structure on dielectric properties of Barium Strontium Titanate during high energy ball milling," *Mater. Today Proc.*, vol. 4, no. 4, pp. 5631–5639, 2017, doi: <https://doi.org/10.1016/j.matpr.2017.06.022>.
 - [28] I. J. Clark, T. Takeuchi, N. Ohtori, and D. C. Sinclair, "Hydrothermal synthesis and characterisation of BaTiO₃ fine powders: precursors, polymorphism and properties," *J. Mater. Chem.*, vol. 9, no. 1, pp. 83–91, 1999, doi: <https://doi.org/10.1039/A805756G>.
 - [29] B. D. Stojanovic, "Mechanochemical synthesis of ceramic powders with perovskite structure," *J. Mater. Process. Technol.*, vol. 143–144, no. 2003, pp. 78–81, 2003, doi: [https://doi.org/10.1016/S0924-0136\(03\)00323-6](https://doi.org/10.1016/S0924-0136(03)00323-6).
 - [30] T. Tsuzuki and P. G. McCormick, "Mechanochemical synthesis of nanoparticles," *J. Mater. Sci.*, vol. 39, no. 16–17, pp. 5143–5146, 2004.
 - [31] M. A. Elqudsy, R. D. Widodo, Rusiyanto, and W. Sumbodo, "The particle and crystallite size analysis of BaTiO₃ produced by conventional solid-state reaction process," *AIP Conf. Proc.*, vol. 1818, no. 1, p. 20012, 2017, doi: <https://doi.org/10.1063/1.4976876>.
 - [32] M. Valant and D. Suvorov, "Low-Temperature Sintering of (Ba_{0.6}Sr_{0.4})TiO₃," *J. Am. Ceram. Soc.*, vol. 87, no. 7, pp. 1222–1226, 2004, doi: <https://doi.org/10.1111/j.1151-2916.2004.tb07716.x>.
 - [33] H. Zhang, L. B. Kong, C.-L. Mak, K.-W. Kwok, Y. Wang, and H. Lai-Wa Chan, "Highly enhanced sinterability of fine-grained Ba_{0.6}Sr_{0.4}TiO₃-MgO bulk ceramics and in-situ nanocomposite thick films", *Ceram. Int.*, vol. 40, no. 7, pp. 10475–10481, 2014, doi: <https://doi.org/10.1016/j.ceramint.2014.03.018>.
 - [34] C. Berbecaru *et al.*, "Ceramic materials Ba(1-x)Sr_xTiO₃ for electronics Synthesis and characterization," *Thin Solid Films*, vol. 516, no. 22, pp. 8210–8214, 2008, doi: <https://doi.org/10.1016/j.tsf.2008.04.031>.
 - [35] E. Yustanti, Hafizah, M. A. E., and A. Manaf, "The effect of milling time and sintering temperature on formation of nanoparticles barium strontium titanate doi:," *AIP Conf. Proc.*, vol. 1788, no. 030099, pp. 1 – 6, 201AD, doi: <https://doi.org/10.1063/1.4968352>.
 - [36] Mudinepalli, L. V.R., Feng, and W. Lin, "Effect of grain size on dielectric and ferroelectric properties of nanostructured Ba_{0.8}Sr_{0.2}TiO₃ ceramics," *J Adv Ceram.*, vol. 4, no. 46–53, 2015.
 - [37] J. Zhu *et al.*, "Influence of sintering temperature on microstructures and energy-storage properties of barium strontium titanate glass-ceramics prepared by sol-gel process," *Phys. Status Solidi*, vol. 212, no. 12, pp. 2822–2829, 2015, doi: <https://doi.org/10.1002/pssa.201532199>.
 - [38] H. A. Gatea and I. S. Naji, "Impact of sintering temperature on structural and dielectric properties of barium strontium titanate prepared by sol-gel method," *J. Ovonic Res.*, vol. 14, no. 6, pp. 467–474, 2018.
 - [39] S. M. Rhim, S. Hong, Bak, H., and O. K. Kim, "Effects of B₂O₃ Addition on the Dielectric and Ferroelectric Properties of Ba_{0.7}Sr_{0.3}TiO₃ Ceramics," *J. Am. Ceram. Soc.*, vol. 83, no. 5, pp. 1145–1148, 2004, doi: <https://doi.org/10.1111/j.1151-2916.2000.tb01345.x>.
 - [40] T. Hu, J. H., A. Uusimäki, and S. Leppävuori, "Ba_{0.7}Sr_{0.3}TiO₃ powders with B₂O₃ additive prepared by the sol-gel method for use as microwave material," *Mater. Sci. Semicond. Process.*, vol. 5, no. 2–3, pp. 215–221, 2002, doi: [https://doi.org/10.1016/S1369-8001\(02\)00076-8](https://doi.org/10.1016/S1369-8001(02)00076-8).
 - [41] J. S. Chappell, T. A. Ring, and J. D. Birchall, "Particle size distribution effects on sintering rates," *Physics, J. Appl.*, vol. 60, no. 1, pp. 383–391, 1986, doi: <https://doi.org/10.1063/1.337659>.
 - [42] J. Hu, "Grain Growth by Ordered Coalescence of Nanocrystals in Ceramics," Stockholm University, Sweden, 2013.
 - [43] L. Nedelcu *et al.*, "Synthesis and dielectric characterization of Ba_{0.6}Sr_{0.4}TiO₃ ferroelectric ceramics doi:," *Thin Solid Films*, vol. 519, no. 17, pp. 5811–5815, 2011, doi: <https://doi.org/10.1016/j.tsf.2010.12.191>.
 - [44] G. K. Williamson and W. H. Hall, "X-ray line broadening from filed aluminium and wolfram," *Acta Met.*, vol. 1, no. 1, pp. 22–31, 1953.
 - [45] C. Liu, P. Liu, X. Lu, C. Gao, G. Zhu, and X. Chen, "A simple method to synthesize Ba_{0.6}Sr_{0.4}TiO₃ nano-powders through high-energy ball-milling," *Powder Technol.*, vol. 212, no. 1, pp. 299–302, 2011, doi: [doi:10.1016/j.powtec.2011.05.010](https://doi.org/10.1016/j.powtec.2011.05.010).
 - [46] T. Kozawa, A. Onda, and K. Yanagisawa, "Accelerated formation of barium titanate by solid-state reaction in water vapour atmosphere-3264," *J. Eur. Ceram. Soc.*, vol. 29, no. 15, p. 3259, 2011, doi: [doi:10.1016/j.jeurceramsoc.2009.05.031](https://doi.org/10.1016/j.jeurceramsoc.2009.05.031).
 - [47] M. T. Buscaglia, M. Bassoli, V. Buscaglia, and R. Vormberg, "Solid-State Synthesis of Nanocrystalline BaTiO₃: Reaction Kinetics and Powder Properties," *J. Am. Ceram. Soc.*, vol. 91, no. 9, pp. 2862–2869, 2008, doi: [10.1111/j.1551-2916.2008.02576.x](https://doi.org/10.1111/j.1551-2916.2008.02576.x).
 - [48] M. T. Buscaglia, M. Bassoli, V. Buscaglia, and R. Alessio, "Solid-State Synthesis of Ultrafine BaTiO₃ Powders from Nanocrystalline BaCO₃ and TiO₂," *J. Am. Ceram. Soc.*, vol. 88, no. 9, pp. 2374–2379, 2005, doi: [doi:10.1111/j.1551-2916.2005.00451.x](https://doi.org/10.1111/j.1551-2916.2005.00451.x).
 - [49] U. Ulfa, K. Kusumandari, and Y. Iriani, "The effect of temperature and holding time sintering process on microstructure and dielectric properties of barium titanate by co-precipitation method," *AIP Conf. Proc.*, vol. 2202, no. 020036, pp. 1–8, 2019, doi: <https://doi.org/10.1063/1.5141649>.
 - [50] D. F. Fitriyana, S. H., Sulardjaka, N. R., and C. W., "Synthesis of Na-P Zeolite from Geothermal Sludge". In: Murakami RI., Koinkar P., Fujii T., Kim TG., Abdullah H. (eds) NAC 2019," *Springer Proc. Phys.*, vol. 242, 2020, doi: https://doi.org/10.1007/978-981-15-2294-9_5.
 - [51] S. D. S. A., J. A., and I. Y., "The effects of sintering temperature on dielectric constant of Barium Titanate (BaTiO₃)," *IOP Conf. Ser. Mater. Sci. Eng.*, vol. 107, no. 012069, pp. 1–6, 2016.
 - [52] R. Maharsi, A. Jamaluddin, A. Supriyanto, and Y. Iriani, "Crystalline Characterization and Dielectric Constant of Barium Strontium Titanates Prepared by Solid State Reaction," *Adv. Mater. Res.*, vol. 1123, no. 123–126, 2015, doi: [doi:10.4028/www.scientific.net/amr.1123.123](https://doi.org/10.4028/www.scientific.net/amr.1123.123).

[IJAME] Editor Decision

2021-05-18 02:07 PM

Dear Dr. R. Rusiyanto, R.D. Widodo, D.H. Al-Janan, K. Rohmah, Januar Parlaungan Siregar, A. Nugroho:

We have reached a decision regarding your submission to International Journal of Automotive and Mechanical Engineering, "Effect of Milling Times and Annealing on The Physical Properties of Ba_{0.6}Sr_{0.4}TiO₃ Prepared by Conventional Solid-State Reaction Process".

Our decision is to: Accept Submission

Please return to us the Copyright Transfer Agreement form.

Salwani Mohd Salleh
ijame2@ump.edu.my

International Journal of Automotive and Mechanical Engineering (IJAME)
<http://journal.ump.edu.my/ijame>

[IJAME] Editor Decision

2021-05-18 02:07 PM

Dear Dr. R. Rusiyanto, R.D. Widodo, D.H. Al-Janan, K. Rohmah, Januar Parlaungan Siregar, A. Nugroho:

We have reached a decision regarding your submission to International Journal of Automotive and Mechanical Engineering, "Effect of Milling Times and Annealing on The Physical Properties of Ba_{0.6}Sr_{0.4}TiO₃ Prepared by Conventional Solid-State Reaction Process".

Our decision is to: Accept Submission

Please return to us the Copyright Transfer Agreement form.

Salwani Mohd Salleh
ijame2@ump.edu.my

International Journal of Automotive and Mechanical Engineering (IJAME)
<http://journal.ump.edu.my/ijame>

III

Copyediting Process

[← Back to Submissions](#)4962 / **Rusiyanto et al.** / Effect of Sintering Temperature on the Physical Properties of Ba...[Library](#)[Workflow](#)[Publication](#)[Submission](#)[Review](#)[Copyediting](#)[Production](#)

Copyediting Discussions

[Add discussion](#)

Name	From	Last Reply	Replies	Closed
Revision required	aqida 2021-05-27 01:12 PM	januar 2021-06-07 03:16 PM	1	<input checked="" type="checkbox"/>
Your Article Proofs in IJAME Volume 18 (Issue 2).June 2021	aqida 2021-06-11 04:41 AM	aqida 2021-06-14 01:05 AM	2	<input checked="" type="checkbox"/>

Copyedited

[Q Search](#)

	23202	4962_PROOF.pdf	June 11, 2021	Article Text
--	-------	--------------------------------	---------------	--------------

Revision required




Participants

S.N. Aqida (aqida)

Salwani Mohd Salleh (salwani)

Januar Parlaungan Siregar (januar)

Messages

Note	From
<p>Dear Dr Januar,</p> <p>We are now re-evaluating the manuscript for publication. The references are too many and not recent. Only 15% of the references are between 2015-2020, which is unfavorable for IJAME to publish. To proceed with publication, please reduce the references to reflect the paper length and include the latest references, at least 60% of them.</p>	<p>aqida 2021-05-27 01:12 PM</p>
<p>▶ Dear Editor-In-Chief,</p> <p>The attached file is the final revision of manuscript No. 4962, Title;</p> <p>The Effect of Sintering Temperature on The Physical Properties of Ba_{0.6}Sr_{0.4}TiO₃ Prepared by Solid-State Reaction.</p> <p>Thank you very much for your attention and corporation.</p> <p>J.P. Siregar</p> <p> 4962-Article Text- The Effect of Sintering Temperature on The Physical Properties of Ba0.6Sr0.4TiO3 Prepared by Solid State-Reaction.docx</p>	<p>januar 2021-06-07 03:16 PM</p>

ORIGINAL ARTICLE

Effect of Sintering Temperature on the Physical Properties of $\text{Ba}_{0.6}\text{Sr}_{0.4}\text{TiO}_3$ Prepared by Solid-State Reaction

Rusiyanto¹, R.D. Widodo¹, D.H. Al-Janan¹, K. Rohmah¹, J.P. Siregar^{2*}, A. Nugroho¹ and D.F. Fitriyana¹

¹Department of Mechanical Engineering, Universitas Negeri Semarang, Kampus Sekaran, Gunungpati, 50229 Semarang, Indonesia

²College of Engineering, Universiti Malaysia Pahang, 26300 Gambang, Kuantan, Malaysia

ABSTRACT – Barium Strontium Titanate (BST) ceramic materials are widely used in electronic devices due to their stable operation at high temperatures, high tunability, low tangent loss, low DC leakage, and alterable curie temperatures. While pure BST materials are usually produced at high sintering temperatures (1250 °C), there are limited studies on the temperature and duration of the sintering process to produce pure BST, synthesised from micro or even nano-sized raw materials. This study aims to determine the effective sintering temperature for producing pure BST material using a mixture of raw materials with a mean particle size of 0.4 µm after milled for 58 hours. The BaCO_3 , SrCO_3 , and TiO_2 materials as raw materials for $\text{Ba}_{0.6}\text{Sr}_{0.4}\text{TiO}_3$ synthesis were milled for 58 hours to produce a homogeneous mixture with a mean particle size of 0.4 µm. Sintering was carried out in a temperature range of 500-1100 °C for 1 hour. This study investigates the impact of sintering temperature on the physical properties and the purity of $\text{Ba}_{0.6}\text{Sr}_{0.4}\text{TiO}_3$ powder using the x-ray diffraction method. The results showed that the $\text{Ba}_{0.6}\text{Sr}_{0.4}\text{TiO}_3$ phase was formed at a sintering temperature of 700 °C. Pure BST material was formed at the sintering temperature of 1000 °C with a crystallite size of 41 nm. Whereas at a higher sintering temperature (1100 °C), the pure BST material formed produced a larger crystallite, sized at 43 nm with cubic structure. The synthesis temperature and duration recorded in this research are lower than recorded in the BST material preparation using the solid-state method. The results of this study indicate that the sintering temperature greatly affects the purity, crystal system and crystallite size of the $\text{Ba}_{0.6}\text{Sr}_{0.4}\text{TiO}_3$ material produced. The sintering temperature of 1100 °C produces $\text{Ba}_{0.6}\text{Sr}_{0.4}\text{TiO}_3$ material with the best physical properties because it has a cubic-shaped crystal system and the largest crystal size.

ARTICLE HISTORY

Received: 18th Aug 2020

Revised: 22nd Mar 2021

Accepted: 11th June 2021

KEYWORDS

Particle-size;

Crystallite-size

Barium-strontium titanate;

Solid-state reaction

INTRODUCTION

Barium Strontium Titanate (BST), $\text{Ba}_{(x)}\text{Sr}_{(1-x)}\text{TiO}_3$, $0 < x < 1$, is a ferroelectric material with a perovskite structure. This material composes of barium titanate (BaTiO_3) and strontium titanate (SrTiO_3). When SrTiO_3 is added to BaTiO_3 , Sr ion replaces Ba ion to form the BST material structure. Barium strontium titanate ceramic material is widely used in electronic devices [1]. As bulk ceramics and thin films, this material has a unique combination of large dielectric constant. It demonstrates a stable operation at high temperature, high tunability, low loss tangent, low DC leakage, and alterable curie temperature [2]. The uniqueness of the BST material is attributed to several factors, such as the Ba / Sr ratio, the synthesis method, and the particle and crystal size [3]. $\text{Ba}_{(x)}\text{Sr}_{(1-x)}\text{TiO}_3$ ceramics with various compositions of x (Ba / Sr ratio) has been widely studied; for example $x = 0.2, 0.3, 0.4, 0.5$, and 0.6 [4]. X-ray diffraction (XRD) results showed BST crystals formation in all variations of x; after the sintering process was carried out at 1000 °C for 3 hours. However, there was still a secondary phase (Sr_2TiO_4 , SrTiO_{10} , and $\text{Sr}_3\text{Ti}_2\text{O}_7$). This can be improved by increasing the sintering temperature. The secondary phase can be removed by increasing the sintering temperature. Increasing the concentration of x causes a transformation of the crystal system from tetragonal to cubic. The grain size and density of the sample decrease with increasing concentration x because Sr is having a smaller radius than Ba. Curie temperatures for samples with $x = 0.2, 0.3, 0.4, 0.5$, and 0.6 were 70 °C, 28.7 °C, -8.4 °C, -45.5 °C, and -82.6 °C, respectively. Curie temperature decreased with increasing x concentration. The highest dielectric constant found in sample with $x = 0.3$ [4]. Furthermore, the high dielectric and pyroelectric properties of the composition $\text{Ba}_{(x)}\text{Sr}_{(1-x)}\text{TiO}_3$ with $0.3 \leq x \leq 0.5$ resulted in the Curie temperature (TC) or ferroelectric-paraelectric phase transformation temperature decrease, near to room temperature (25 °C) [5].

$\text{Ba}_{(x)}\text{Sr}_{(1-x)}\text{TiO}_3$ materials are generally synthesised by hydrothermal method, sol-gel method, and conventional solid-state reaction method [6]. The BST material synthesised by the hydrothermal and sol-gel method produces crystals less than 100 nm. Subsequently, it produces residual hydroxide ions, which resulted in the formation of intergranular pores [7]. The mechanochemical or solid-state method is the most used method for BST nanoparticles large-scale production [8]. The solid-state method has several advantages; it uses low-cost raw materials, simple synthesis processes, and the ability to produce fine particles [8]. During solid-state processes such as high-energy ball milling, the steps that occur during solid-state processes, specifically welding, deformation, and fracture of powder raw materials, are repeated [9].

The mechanical activation during solid-state reaction with mechanical milling increases the raw material specific surface area due to the destruction of agglomerates and particles of the initial precursors [10]. In this regard, the mechanical milling process can produce particles sized $> 1 \mu\text{m}$. In general, the microstructure of the particle and crystallite size of mechanical milling products were influenced by the characteristics of the raw materials used, duration and heating temperature during the mechanical milling process [11].

In recent years, several studies have focused on the effect of sintering temperature on the synthesis of Barium Strontium Titanate (BST). In general, the increase of the temperature and duration time of the sintering process affected the BST material's purity and increased the crystallite size [12]. Pure BST materials are usually produced at high sintering temperatures [4], [12]–[18]. Sandi et al. carried out a sintering process at 1200°C for 2 hours to produce pure BST material by the solid-state reaction method [8]. Yustanti et al. reported that the sintering raw materials measuring an average size of $2.4 \mu\text{m}$ at a temperature of 1200°C produced pure BST material without the presence of impurities [14]. In the meantime, barium strontium titanate ceramic material was synthesised from fine constituent powders produced from high energy ball milling processes at sintering temperatures 1200 – 1350°C , as reported by Mudinepalli et al. [12]. Budkhod et al. performed sintering at temperatures between 1050 – 1350°C to produce $\text{Ba}_{0.7}\text{Sr}_{0.3}\text{TiO}_3$ ceramics using a hybrid method between solid-state reaction and sol-gel combustion methods using urea as a fuel [15]. Meanwhile, Gate et al. conducted a sintering process at a temperature of 1100°C for 3 hours to produce a pure $\text{Ba}_{0.6}\text{Sr}_{0.4}\text{TiO}_3$ material using the sol-gel method [17]. Lastly, Zhu et al. synthesised barium strontium titanate glass and ceramics using the sol-gel method and was sintered at temperatures between 1000 and 1150°C [18].

The high sintering temperature to produce pure BST material has prompted various studies to produce pure BST materials at lower sintering temperatures using glass, polymer and inorganic additives [19]. One way to produce BST material at low sintering temperatures is to add Li_2O material, as reported by Zhang et al. [20]. Zhang et al. investigated the effect of adding Li_2O on the sintering temperature of commercial BST. It was found that by adding $0.5 \text{ wt}\%$, Li_2O could reduce the sintering temperature to 900°C without decreasing the ceramics performance. The sintering temperature of BST materials was reduced from 1350°C to 900°C by adding Li [21]. However, the XRD test showed two secondary phases as impurities caused by the addition of lithium. Besides, this research method has many limitations when applied to commercial production because it requires a very high cost [19], [21].

However, the BST material sintering ability decreased along with the broader particle size distribution [22]. Accordingly, reducing the particle size is another way that can be used to speed up or shorten the sintering time. The sintering temperature is reduced with smaller raw material particles. The smaller the raw material particle size, the faster the grain becomes coarse due to the high particle surface energy compared to the large grain size distribution in the batch under the same sintering conditions [23]. In another reference, the raw material with smaller dimensions causes a larger contact surface so that the sinterability increases due to the maximal diffusion process [24]. Therefore, this study uses a vibratory ball milling for 58 hours to mix BaCO_3 , SrCO_3 , and TiO_2 to obtain a homogeneous mixture with a mean particle size of $0.4 \mu\text{m}$. This research aims to determine the effective sintering temperature to produce pure BST material using a mixture of BaCO_3 , SrCO_3 , and TiO_2 ball-milled for 58 hours.

METHODS AND MATERIALS

$\text{Ba}_{0.6}\text{Sr}_{0.4}\text{TiO}_3$ was synthesised from BaCO_3 , SrCO_3 , and TiO_2 powders using the mechanical alloying method with a purity level of 99%. The powders were obtained from Sigma-Aldrich. The particle size analyser (PSA) test results in Table 1 show the BaCO_3 , SrCO_3 , and TiO_2 powders average sizes. Meanwhile, the results of XRD tests on TiO_2 , SrCO_3 , and BaCO_3 powders are shown in Figure 1(a). The diffraction patterns of TiO_2 , SrCO_3 and BaCO_3 powders are in line with the diffraction patterns of TiO_2 , SrCO_3 and BaCO_3 in the Inorganic Crystal Structure Database (ICSD), respectively, with numbers 98-009- 6946, 98-016-6088, and 98-016-6090. The Rietveld analysis using High Score Plus software shows that the TiO_2 powder has tetragonal-shaped crystal systems while the SrCO_3 and BaCO_3 powders have orthorhombic crystal systems.

Table 1. Average particle size of BaCO_3 , SrCO_3 and TiO_2 .

Raw materials	Average particle size (μm)
BaCO_3	1.979
SrCO_3	3.182
TiO_2	0.795

In this research, BaCO_3 , SrCO_3 and TiO_2 powders were subjected to a wet milling process using a vibratory ball milling machine with a composition of 41.63 grams each, 20.76 grams, and 28.08 grams for 58 hours. The ball to powder ratio (BPR) in the milling process is 10:1. After 58 hours, the mixed BaCO_3 , SrCO_3 and TiO_2 were tested for PSA and XRD. The PSA test results showed that the powder mixture of BaCO_3 , SrCO_3 and TiO_2 had a particle size of $0.4 \mu\text{m}$. Meanwhile, according to the Rietveld analysis using the High Score Plus software, the XRD test results are shown in Figure 1(b). Figure 1(b) shows no change in the diffraction pattern of the powder of TiO_2 , SrCO_3 and BaCO_3 . The crystal sizes of BaCO_3 , SrCO_3 and TiO_2 calculated using The Williamson-Hall method are 48 nm, 61 nm, and 71 nm, respectively.

After characterising the mixture of milled TiO_2 , SrCO_3 , and BaCO_3 powders, the next step is sintering the powder mixture of TiO_2 , SrCO_3 and BaCO_3 . The sintering process was carried out in the electric chamber furnace (Nabertherm

N31/H) with temperature variations of 500 °C, 600 °C, 700 °C, 800 °C, 900 °C, 1000 °C, and 1100 °C in the air under atmospheric pressure up to 1 hour. After the sintering process, characterisation was carried out using the XRD methods. The Philips XRD was also used to analyse the resulting phase and crystallite size. The step-scan method was performed to record the x-ray diffraction patterns. The intensity data during the scanning was taken every 2 seconds for each step on the diffraction angle of 0.005°. The Rietveld analysis was conducted using the High Score Plus software. The description of the diffraction line profiles at Rietveld refinement was achieved using the pseudo-Voigt function.

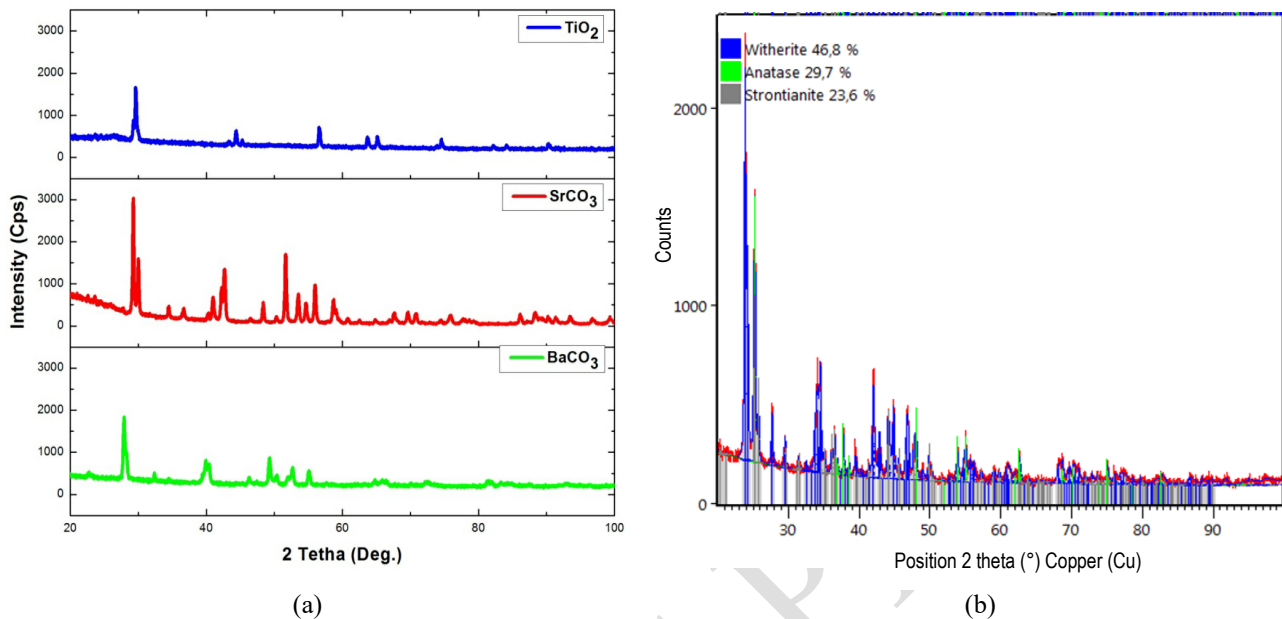


Figure 1. X-ray diffraction patterns of TiO_2 , SrCO_3 and BaCO_3 powders (a) before and (b) after 58 hours of milling.

RESULTS AND DISCUSSION

Figure 2 shows the diffraction pattern of BaCO_3 , SrCO_3 , and TiO_2 powder mixture at each sintering temperature. From the figure, the $\text{Ba}_{0.6}\text{Sr}_{0.4}\text{TiO}_3$ phase was not formed in the material sintered at temperatures of 500 °C and 600 °C. Meanwhile, while the $\text{Ba}_{0.6}\text{Sr}_{0.4}\text{TiO}_3$ phase was formed at temperatures of 700 °C, 800 °C and 900 °C, other compound phases, BaCO_3 , SrCO_3 , TiO_2 and BaTiO_3 , were observed. Moreover, a single-phase $\text{Ba}_{0.6}\text{Sr}_{0.4}\text{TiO}_3$ was formed at temperatures of 1000°C and 1100°C.

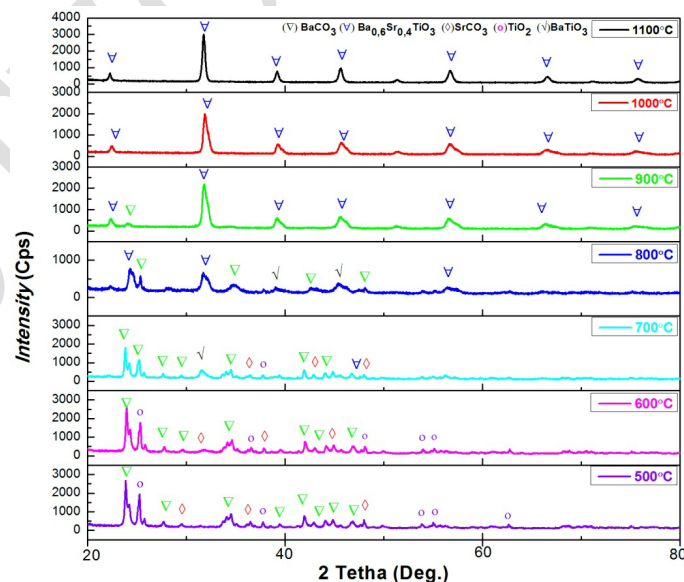


Figure 2. X-ray diffraction patterns of the sintered samples.

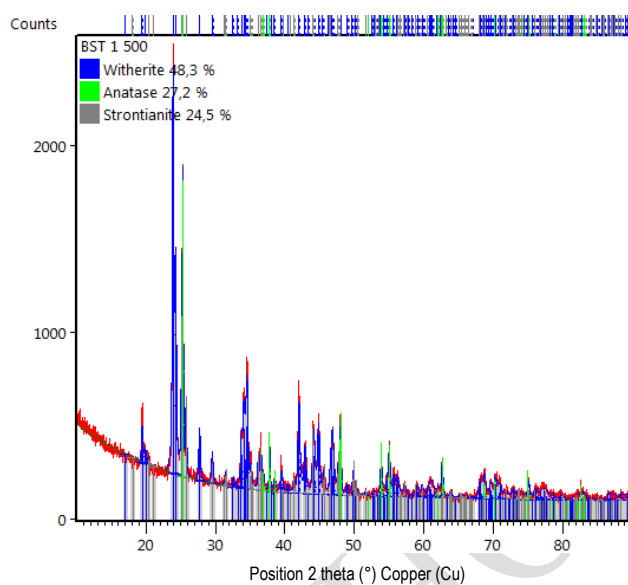
Figure 3 shows the Rietveld analysis results using the High Score Plus software based on X-ray diffraction obtained from the test results. Figure 3(a) shows the x-ray diffraction pattern on a powder that has been sintered at 500 °C. The x-ray diffraction pattern shows that the $\text{Ba}_{0.6}\text{Sr}_{0.4}\text{TiO}_3$ phase was not formed. In this light, the phases formed at 500 °C sintering temperature variations are BaCO_3 (withierite), TiO_2 (anatase), and SrCO_3 (strontianite), with the respective percentage of 48.3%; 27.2%, and 24.5%. Meanwhile, the crystallite size formed in BaCO_3 , TiO_2 , and SrCO_3 was 54.7 nm, 125.6 nm, and 80.3 nm. The x-ray diffraction pattern of the sintered powder at 600 °C is shown in Figure 3(b). At

600 °C, $\text{Ba}_{0.6}\text{Sr}_{0.4}\text{TiO}_3$ was not formed and still in the BaCO_3 , TiO_2 , and SrCO_3 phases, with 51.2%; 24.2% and 24.6%, respectively. The sizes of the crystallites formed after sintering BaCO_3 , TiO_2 , and SrCO_3 at 600 °C for are 56.4 nm, 104.3 nm, and 122.3 nm, respectively.

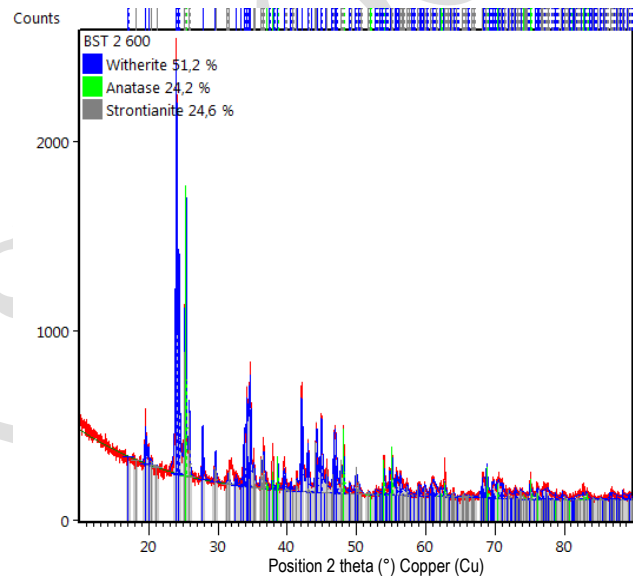
Figure 3(c) shows the x-ray diffraction pattern of a mixture of BaCO_3 , SrCO_3 , and TiO_2 powders sintered at 700 °C. At a temperature of 700 °C, the $\text{Ba}_{0.6}\text{Sr}_{0.4}\text{TiO}_3$ phase was formed with a percentage of 19.4% and a crystallite size of 15.3 nm. However, at 700 °C, the BaCO_3 , SrCO_3 and TiO_2 phases were still found at a respective percentage of 35.2%, 22.2%, and 19.8%, and crystallite sizes of 58.1 nm; 65.6 nm and 66.2 nm, respectively. Apart from $\text{Ba}_{0.6}\text{Sr}_{0.4}\text{TiO}_3$, BaCO_3 , SrCO_3 and TiO_2 phases, a new phase, BaTiO_3 at 3.4% and crystallite size of 38 nm, was also formed.

Figure 3(d) shows that the crystallite percentage increased to 22.4%, and its size increased to 30.3 nm at the $\text{Ba}_{0.6}\text{Sr}_{0.4}\text{TiO}_3$ phase when sintering at 800 °C. In this variation, the crystal size of $\text{Ba}_{0.6}\text{Sr}_{0.4}\text{TiO}_3$ is two times the crystallite size formed at 700 °C sintering temperature. Meanwhile, the BaTiO_3 phase percentage decreased to 2.2%, accompanied by a decrease in crystal size to 19.5 nm. BaCO_3 phases were still found with a composition of 47% with a crystallite size of 40 nm. Apart from $\text{Ba}_{0.6}\text{Sr}_{0.4}\text{TiO}_3$, BaCO_3 , and BaTiO_3 phases, a new phase, SrTiO_3 was also formed at 28.3% and crystallite size of 32.6 nm.

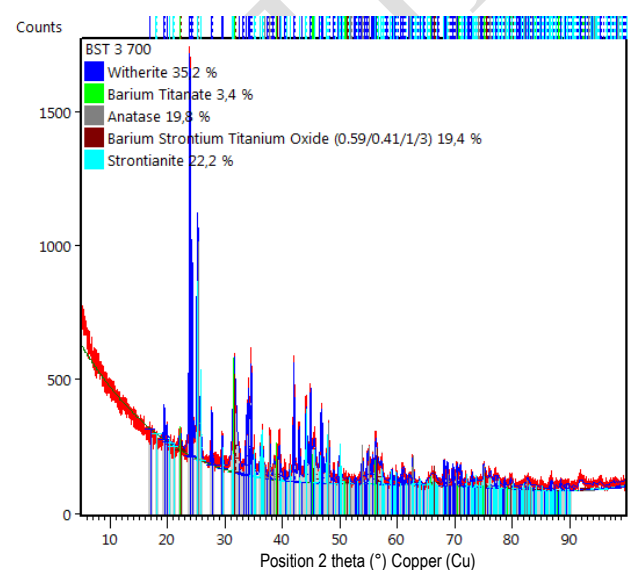
Figure 3(e) shows the x-ray diffraction pattern at a product sintering temperature of 900 °C. The $\text{Ba}_{0.6}\text{Sr}_{0.4}\text{TiO}_3$ phase formed in this variation experienced a significant increase with a percentage of 94.6% and a crystallite size of 40.1 nm. Simultaneously, the other 5.4% is the BaCO_3 phase with a crystallite size of 21.5 nm. The single phase of $\text{Ba}_{0.6}\text{Sr}_{0.4}\text{TiO}_3$ was formed perfectly at various sintering temperatures of 1000 °C and 1100 °C, as shown in Figure 3(f) and 3(g). $\text{Ba}_{0.6}\text{Sr}_{0.4}\text{TiO}_3$ with crystallites size of 30 nm and 43 nm resulted in sintering temperatures of 1000 °C and 1100 °C.



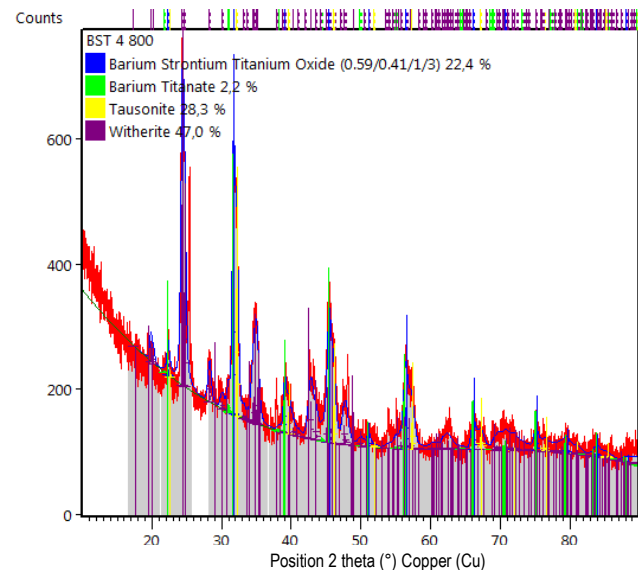
(a)



(b)



(c)



(d)

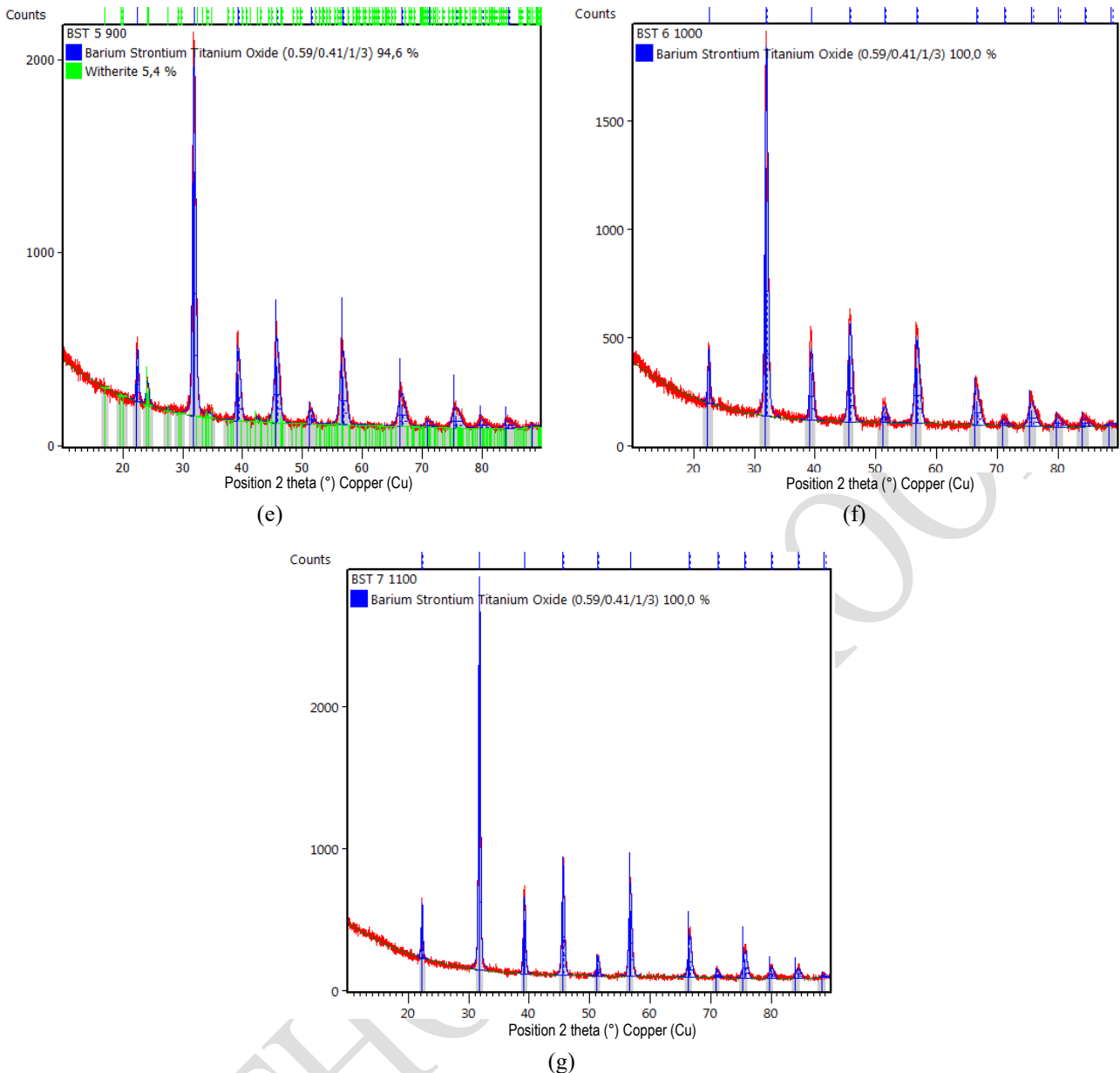


Figure 3. X-ray diffraction patterns of sintered samples at (a) 500 °C, (b) 600 °C, (c) 700 °C (d) 800 °C, (e) 900 °C, (f) 1000 °C and (g) 1100 °C.

The results of this study indicate that the $\text{Ba}_{0.6}\text{Sr}_{0.4}\text{TiO}_3$ material has begun to form at a sintering temperature of 700 °C. However, a secondary phase is still formed and completely into single-phase $\text{Ba}_{0.6}\text{Sr}_{0.4}\text{TiO}_3$ at 1000°C and 1100°C. The effect of sintering temperature on the phase composition (%) and crystallite sizes of $\text{Ba}_{0.6}\text{Sr}_{0.4}\text{TiO}_3$ formed is shown in Figure 4. The impurity phase disappears proportionately with the increase in sintering temperature. The kinetic energy in atoms increases due to higher sintering temperatures. The higher temperature makes it easier for the atoms to interact and bond with each other, causing the impurity phase to disappear [12], [17]. Besides, increasing the sintering temperature causes the atomic bonds to become stronger. Thus, sintering carried out at 1000°C and 1100°C resulted in forming a single phase of $\text{Ba}_{0.6}\text{Sr}_{0.4}\text{TiO}_3$ which is more stable. Increasing the sintering temperature will result in a recrystallisation process in the raw materials (BaCO_3 , SrCO_3 , and TiO_2) so that a more stable $\text{Ba}_{0.6}\text{Sr}_{0.4}\text{TiO}_3$ phase is formed. An increase in sintering temperature will produce $\text{Ba}_{0.6}\text{Sr}_{0.4}\text{TiO}_3$ with a higher phase composition (%). The crystallite sizes also increased, as reported in previous studies [12], [17], [25], [26].

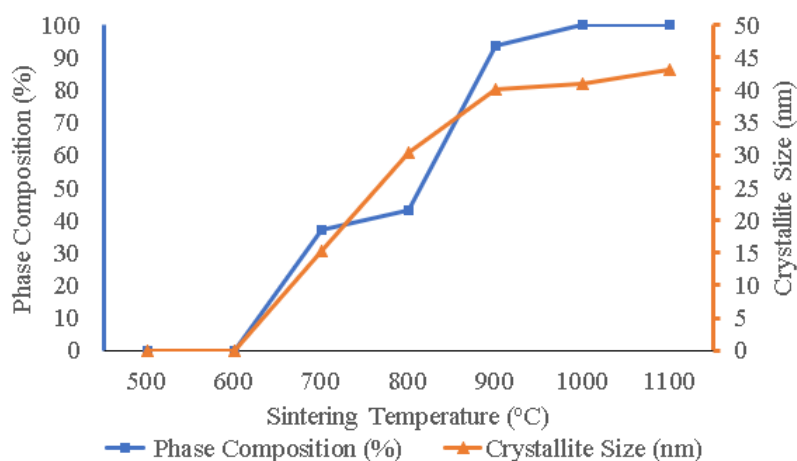


Figure 4. The effect of sintering temperature on the physical properties of $\text{Ba}_{0.6}\text{Sr}_{0.4}\text{TiO}_3$.

The use of BaCO_3 , SrCO_3 , and TiO_2 powder mixture, with a particle size of $0.4\ \mu\text{m}$, has been proven to produce $\text{Ba}_{0.6}\text{Sr}_{0.4}\text{TiO}_3$ material at lower sintering temperatures with a faster duration (1 hour). This is supported by [27] and [24] study, which revealed that reducing the particle size of raw materials is another method that can be used to speed up sintering and shorten sintering time. The sintering temperature is reduced with smaller raw material particles. The smaller the raw material particle size, the faster the grain becomes coarse due to the high particle surface energy compared to the large grain size distribution in the batch under the same sintering conditions [27]. Previous research [24] mentioned raw materials with smaller dimensions causes a larger contact surface so that the sinterability increases due to the maximum diffusion process. In this study, sintering carried out at temperatures of $1000\ ^\circ\text{C}$ and $1100\ ^\circ\text{C}$ for 1 hour produced single-phase $\text{Ba}_{0.6}\text{Sr}_{0.4}\text{TiO}_3$. In this study, single-phase $\text{Ba}_{0.6}\text{Sr}_{0.4}\text{TiO}_3$ resulted in lower sintering temperature and shorter sintering duration compared to the results of the study conducted by [4], [12], [14], [17], [26]. These studies' results showed the single-phase formation of $\text{Ba}_{0.6}\text{Sr}_{0.4}\text{TiO}_3$ was carried out in a sintering temperature range of $1100\ ^\circ\text{C}$ – $1350\ ^\circ\text{C}$ with a sintering duration of ≥ 2 hours.

In addition, [4], [12], [14], [26], [28] have clearly shown that the decrease in calcination or sintering temperature is due to the reduction in the small particle size of the raw materials; ranging from submicrometer or even to the nanoscale. The use of a smaller particle size increases the contact area and decreases the reactants contact distance, thereby increasing the overall reaction kinetics. The results of this study indicate that the sintering temperature greatly affects the purity, crystal system, and crystallite size of the material $\text{Ba}_{0.6}\text{Sr}_{0.4}\text{TiO}_3$ produced. The effect of sintering temperature on the physical properties of $\text{Ba}_{0.6}\text{Sr}_{0.4}\text{TiO}_3$ formed is shown in Table 2. The higher the sintering temperature resulted in a sharper peak intensity at $\text{Ba}_{0.6}\text{Sr}_{0.4}\text{TiO}_3$, which indicates an increase in crystal size. Accordingly, the higher the sintering temperature used, the higher the crystal size of the material $\text{Ba}_{0.6}\text{Sr}_{0.4}\text{TiO}_3$ formed. This is supported by the studies of [4], [17], [26], [29]. Thus, increasing the sintering temperature increased the atoms kinetic energy to diffuse and make the atoms react and bond perfectly. This finding is supported by other studies [29]–[32] that found that the crystallites produced have a larger size and higher crystallinity.

Table 2. The Physical Properties in The Formation of $(\text{Ba}_{0.6}\text{Sr}_{0.4})\text{TiO}_3$.

Sintering temperature ($^\circ\text{C}$)	Phase	Composition phase (%)	Crystal system	Crystallite size (nm)
500	BaCO_3	48	Orthorhombic	54.7
	TiO_2	27	Tertragonal	125.6
	SrCO_3	25	Orthorhombic	80.3
600	BaCO_3	51.2	Orthorhombic	56.4
	TiO_2	24.2	Tertragonal	104.3
	SrCO_3	24.6	Orthorhombic	122.3
700	BaCO_3	35.2	Orthorhombic	58.1
	TiO_2	19.8	Tertragonal	19.8
	SrCO_3	22.2	Orthorhombic	65.6
	BaTiO_3	3.4	Orthorhombic	38
	$(\text{Ba}_{0.67}\text{Sr}_{0.33})\text{TiO}_3$	19.4	Tertragonal	15.3
800	BaCO_3	47	Orthorhombic	40
	BaTiO_3	2.2	Orthorhombic	19.5
	SrTiO_3	28.3	Orthorhombic	32.6
	$(\text{Ba}_{0.67}\text{Sr}_{0.33})\text{TiO}_3$	22.4	Tertragonal	30.3
900	BaCO_3	5.4	Orthorhombic	21.5
	$(\text{Ba}_{0.67}\text{Sr}_{0.33})\text{TiO}_3$	94.6	Tertragonal	40.1
1000	$(\text{Ba}_{0.59}\text{Sr}_{0.41})\text{TiO}_3$	100	Cubic	41
1100	$(\text{Ba}_{0.6}\text{Sr}_{0.4})\text{TiO}_3$	100	Cubic	43

In addition, an increase in the sintering temperature in this study caused changes in the crystal system of the $\text{Ba}_{0.6}\text{Sr}_{0.4}\text{TiO}_3$ material. At temperatures of 700 °C, 800 °C, and 900 °C, the crystal system in the material $\text{Ba}_{0.6}\text{Sr}_{0.4}\text{TiO}_3$ is tetragonal. Whereas at temperatures of 1000 °C and 1100 °C, the crystal system in the $\text{Ba}_{0.6}\text{Sr}_{0.4}\text{TiO}_3$ is cubic with a higher peak intensity with increasing sintering temperature. The $\text{Ba}_{0.6}\text{Sr}_{0.4}\text{TiO}_3$ with cubic structure increased the dielectric properties of the material $\text{Ba}_{0.6}\text{Sr}_{0.4}\text{TiO}_3$ produced [12], [17], [33]. Besides the crystal structure, the dielectric properties of the $\text{Ba}_{0.6}\text{Sr}_{0.4}\text{TiO}_3$ material are also influenced by the crystal size, where the dielectric property increases with the crystallite size [12], [29], [34]. In this study, the sintering temperature of 1100 °C produces $\text{Ba}_{0.6}\text{Sr}_{0.4}\text{TiO}_3$ material with the best physical properties because it has a cubic-shaped crystal system and the largest crystal size.

CONCLUSION

The effect of sintering temperature on the physical properties of $\text{Ba}_{0.6}\text{Sr}_{0.4}\text{TiO}_3$ material synthesised with 0.4 µm raw materials (and milled up to 58 hour) using the solid-state reaction method has been investigated. The use of raw materials, a mixture of BaCO_3 , SrCO_3 , and TiO_2 with a particle size of 0.4 µm could produce $\text{Ba}_{0.6}\text{Sr}_{0.4}\text{TiO}_3$ material at a lower sintering temperature of 700 °C. Moreover, the single-phase $\text{Ba}_{0.6}\text{Sr}_{0.4}\text{TiO}_3$ can be produced at temperatures of 1000 °C and 1100 °C. Increasing the sintering temperature in this study resulted in $\text{Ba}_{0.6}\text{Sr}_{0.4}\text{TiO}_3$ material with higher purity as marked by the disappearance of the BaTiO_3 , BaCO_3 , SrCO_3 , and TiO_2 phases. Higher sintering temperature increased the crystal size and changed the crystal system from tetragonal to cubic. The sintering temperature of 1100 °C produces $\text{Ba}_{0.6}\text{Sr}_{0.4}\text{TiO}_3$ material with the best physical properties because it has a cubic-shaped crystal system and the largest crystal size.

ACKNOWLEDGEMENT

We would like to express our gratitude to the Ministry of Research and Higher Education for funding this research through Competitive Research Grant with No. 042.06.1.401516/2016.

REFERENCES

- [1] Szafraniak B, Fuśnik Ł, Xu J, et al. Semiconducting metal oxides: SrTiO_3 , BaTiO_3 and BaSrTiO_3 in gas-sensing applications: A review. *Coatings* 2021; 11: 1–23.
- [2] Sangle AL, Lee OJ, Kursumovic A, et al. Very high commutation quality factor and dielectric tunability in nanocomposite SrTiO_3 thin films with T(c) enhanced to >300 °C. *Nanoscale* 2018; 10: 3460–3468.
- [3] Vigneshwaran B, Kuppusami P, Ajithkumar S, et al. Study of low temperature-dependent structural, dielectric, and ferroelectric properties of $\text{Ba}_x\text{Sr}_{1-x}\text{TiO}_3$ ($x = 0.5, 0.6, 0.7$) ceramics. *Journal of Materials Science: Materials in Electronics* 2020; 31: 10446–10459.
- [4] Gatea HA, Naji IS. The effect of Ba/Sr ratio on the Curie temperature for ferroelectric barium strontium titanate ceramics. *Journal of Advanced Dielectrics* 2020; 10: 1–11.
- [5] Vu T-H, Phuong NTM, Nguyen T. Lead-free ferroelectric barium titanate -based thin film for tunable microwave device application. *IOP Conference Series: Materials Science and Engineering* 2021; 1091: 012060.
- [6] Alwan H, Jasim S. Preparation and characterization of $\text{Ba}_{1-x}\text{Sr}_x\text{TiO}_3$ by sol-gel method. *Asian Journal of Chemistry* 2019; 31: 186–190.
- [7] Panomsuwan G, Manuspiya H. Morphological and structural properties of barium strontium titanate nanopowders synthesized via a sol-gel method. *Ferroelectrics* 2020; 554: 30–37.
- [8] Sandi DK, Supriyanto A, Jamaluddin A, et al. The influences of mole composition of strontium (x) on properties of barium strontium titanate ($\text{Ba}_{1-x}\text{Sr}_x\text{TiO}_3$) prepared by solid state reaction method. *AIP Conference Proceedings* 2016; 1710: 1–5.
- [9] Dulian P. Solid-state mechanochemical syntheses of perovskites. In: Pan L, Zhu G, editors. *Perovskite Materials - Synthesis, Characterisation, Properties, and Applications*. London: InTech-Open, 2016, p 3–26.
- [10] Zhang L, Huang Z, Liu Y, et al. Effects of mechanical ball milling time on the microstructure and mechanical properties of $\text{Mo}_2\text{NiB}_2\text{-Ni}$ Cermets. *Materials* 2019; 12(12), 1926.
- [11] Widodo RD, Manaf A. Physical characteristics and magnetic properties of $\text{BaFe}_{12}\text{O}_{19}/\text{SrTiO}_3$ based composites derived from mechanical alloying. *AIP Conference Proceedings* 2016; 1725: 125–132.
- [12] Mudinepalli VR, Feng L, Lin WC, et al. Effect of grain size on dielectric and ferroelectric properties of nanostructured $\text{Ba}_{0.8}\text{Sr}_{0.2}\text{TiO}_3$ ceramics. *Journal of Advanced Ceramics* 2015; 4: 46–53.
- [13] Elqudsy MA, Widodo RD, Rusiyanto, et al. The particle and crystallite size analysis of BaTiO_3 produced by conventional solid-state reaction process. *AIP Conference Proceedings* 2017; 1818: 020012.
- [14] Yustanti E, Hafizah M, Manaf A. The effect of milling time and sintering temperature on formation of nanoparticles barium strontium titanate. *AIP Conference Proceedings* 2017; 1788: 30099.
- [15] P Budkhod NS and ST. Synthesis of $\text{Ba}_{0.7}\text{Sr}_{0.3}\text{TiO}_3$ ceramics via hybrid method. *Journal of Physics: Conference Series* 2018; 252: 0–5.
- [16] Trobough ND. Examination of Dielectric Properties of BaTiO_3 - SrTiO_3 Based Systems. BSc Thesis, Oregon State University, USA, 2020.
- [17] Gatea HA, Naji IS. Impact of sintering temperature on structural and dielectric properties of barium strontium titanate prepared

by sol-gel method. *Journal of Ovonic Research* 2018; 14: 467–474.

- [18] Zhu J, Zhang Y, Song X, et al. Influence of sintering temperature on microstructures and energy-storage properties of barium strontium titanate glass-ceramics prepared by sol-gel process. *Physica Status Solidi (A) Applications and Materials Science* 2015; 212: 2822–2829.
- [19] Veerapandiyan V, Benes F, Gindell T, et al. Strategies to improve the energy storage properties of perovskite lead-free relaxor ferroelectrics: A review. *Materials* 2020; 13: 1–47.
- [20] Zhang X, Deng X, Ren Y. Low temperature sintering and nonlinear dielectric properties of Li₂O doped Ba_{0.6}Sr_{0.4}TiO₃ ceramics derived from the citrate method. *IOP Conference Series: Materials Science and Engineering* 2017; 207: 0–5.
- [21] Ma R, Cui B, Hu D, et al. Improving the dielectric properties of the Ba(Zr_{0.1}Ti_{0.9})O₃-based ceramics by adding a Li₂O–SiO₂ sintering agent step by step. *International Journal of Nanoscience and Nanotechnology* 2020; 16: 233–241.
- [22] Amorós JL, Blasco E, Moreno A, et al. Effect of particle size distribution on the sinter-crystallisation kinetics of a SiO₂–Al₂O₃–CaO–MgO–SrO glass-ceramic glaze. *Journal of Non-Crystalline Solids* 2020; 542: 120148.
- [23] Yang L. Effect of particle size on oxygen content and porosity of sintered Ti-6Al-4V. MSc Thesis, University of Utah, USA, 2015.
- [24] Nedelcu L, Ioachim A, Toacsan M, et al. Synthesis and dielectric characterization of Ba_{0.6}Sr_{0.4}TiO₃ ferroelectric ceramics doi: *Thin Solid Films* 2011; 519: 5811–5815.
- [25] Berent K, Komarek S, Lach R, et al. The effect of calcination temperature on the structure and performance of nanocrystalline mayenite powders. *Materials* 2019; 12(21): 3476.
- [26] Gatea HA. Impact of sintering temperature on crystallite size and optical properties of SnO₂ nanoparticles. *Journal of Physics: Conference Series* 2021; 1829: 012030.
- [27] Hu J. Grain Growth by Ordered Coalescence of Nanocrystals in Ceramics. PhD Thesis, Stockholm University, Sweden, 2013.
- [28] Kwon Y Bin, Kang JH, Han CS, et al. The effect of particle size and surface roughness of spray-dried bosentan microparticles on aerodynamic performance for dry powder inhalation. *Pharmaceutics* 2020; 12: 1–15.
- [29] Ulfa U, Kusumandari K, Iriani Y. The effect of temperature and holding time sintering process on microstructure and dielectric properties of barium titanate by co-precipitation method. *AIP Conference Proceedings* 2019; 2202: 020036.
- [30] Zeng L, Sun H, Peng T, et al. The sintering kinetics and properties of sintered glass-ceramics from coal fly ash of different particle size. *Results in Physics* 2019; 15: 102774.
- [31] Sandi D, Supriyanto A, Anif, et al. The effects of sintering temperature on dielectric constant of Barium Titanate (BaTiO₃). *IOP Conference Series: Materials Science and Engineering* 2016; 107: 12069.
- [32] Fitriyana D, Suhaimi H, Sulardjaka S, et al. Synthesis of Na-P Zeolite from geothermal sludge. In: Murakami RI, Koinkar P, Fujii T, Kim TG., Abdullah H, editors. *NAC 2019: Proceedings of the 2nd International Conference on Nanomaterials and Advanced Composites*. Singapore: Springer, 2020, p 51-59.
- [33] Maharsi R, Jamaluddin A, Supriyanto A, et al. Crystalline characterization and dielectric constant of barium strontium titanates prepared by solid state reaction. *Advanced Materials Research* 2015; 1123: 123-126.
- [34] Kurnia, Heriansyah, Suharyadi E. Study on the influence of crystal structure and grain size on dielectric properties of manganese ferrite (MnFe₂O₄) nanoparticles. *IOP Conference Series: Materials Science and Engineering* 2017; 202: 012046.

[IJAME] Editor Decision

2021-06-14 01:07 AM

Dear Dr. R. Rusiyanto, R.D. Widodo, D.H. Al-Janan, K. Rohmah, Januar Parlaungan Siregar, A. Nugroho

The editing of your submission, "Effect of Milling Times and Annealing on The Physical Properties of Ba_{0.6}Sr_{0.4}TiO₃ Prepared by Conventional Solid-State Reaction Process," is complete. We are now sending it to production.

International Journal of Automotive and Mechanical Engineering (IJAME)

<http://journal.ump.edu.my/ijame>

[IJAME] Editor Decision

2021-06-14 01:07 AM

Dear Dr. R. Rusiyanto, R.D. Widodo, D.H. Al-Janan, K. Rohmah, Januar Parlaungan Siregar, A. Nugroho

The editing of your submission, "Effect of Milling Times and Annealing on The Physical Properties of Ba_{0.6}Sr_{0.4}TiO₃ Prepared by Conventional Solid-State Reaction Process," is complete. We are now sending it to production.

International Journal of Automotive and Mechanical Engineering (IJAME)

<http://journal.ump.edu.my/ijame>

IV

Production



← Back to Submissions

4962 / **Rusiyanto et al.** / Effect of Sintering Temperature on the Physical Properties of Ba...

Library

Workflow

Publication

Submission

Review

Copyediting

Production

Production Discussions

Add discussion

Name

From

Last Reply

Replies

Closed

No Items

ORIGINAL ARTICLE

Effect of Sintering Temperature on the Physical Properties of $\text{Ba}_{0.6}\text{Sr}_{0.4}\text{TiO}_3$ Prepared by Solid-State Reaction

Rusiyanto¹, R.D. Widodo¹, D.H. Al-Janan¹, K. Rohmah¹, J.P. Siregar^{2,*}, A. Nugroho¹ and D.F. Fitriyana¹

¹Department of Mechanical Engineering, Universitas Negeri Semarang, Kampus Sekaran, Gunungpati, 50229 Semarang, Indonesia

²College of Engineering, Universiti Malaysia Pahang, 26300 Gambang, Kuantan, Malaysia

ABSTRACT – Barium Strontium Titanate (BST) ceramic materials are widely used in electronic devices due to their stable operation at high temperatures, high tunability, low tangent loss, low DC leakage, and alterable curie temperatures. While pure BST materials are usually produced at high sintering temperatures (1250 °C), there are limited studies on the temperature and duration of the sintering process to produce pure BST, synthesised from micro or even nano-sized raw materials. This study aims to determine the effective sintering temperature for producing pure BST material using a mixture of raw materials with a mean particle size of 0.4 µm after milled for 58 hours. The BaCO_3 , SrCO_3 , and TiO_2 materials as raw materials for $\text{Ba}_{0.6}\text{Sr}_{0.4}\text{TiO}_3$ synthesis were milled for 58 hours to produce a homogeneous mixture with a mean particle size of 0.4 µm. Sintering was carried out in a temperature range of 500-1100 °C for 1 hour. This study investigates the impact of sintering temperature on the physical properties and the purity of $\text{Ba}_{0.6}\text{Sr}_{0.4}\text{TiO}_3$ powder using the x-ray diffraction method. The results showed that the $\text{Ba}_{0.6}\text{Sr}_{0.4}\text{TiO}_3$ phase was formed at a sintering temperature of 700 °C. Pure BST material was formed at the sintering temperature of 1000 °C with a crystallite size of 41 nm. Whereas at a higher sintering temperature (1100 °C), the pure BST material formed produced a larger crystallite, sized at 43 nm with cubic structure. The synthesis temperature and duration recorded in this research are lower than recorded in the BST material preparation using the solid-state method. The results of this study indicate that the sintering temperature greatly affects the purity, crystal system and crystallite size of the $\text{Ba}_{0.6}\text{Sr}_{0.4}\text{TiO}_3$ material produced. The sintering temperature of 1100 °C produces $\text{Ba}_{0.6}\text{Sr}_{0.4}\text{TiO}_3$ material with the best physical properties because it has a cubic-shaped crystal system and the largest crystal size.

ARTICLE HISTORY

Received: 18th Aug 2020

Revised: 22nd Mar 2021

Accepted: 11th June 2021

KEYWORDS

Particle-size;

Crystallite-size

Barium-strontium titanate;

Solid-state reaction

INTRODUCTION

Barium Strontium Titanate (BST), $\text{Ba}_x\text{Sr}_{(1-x)}\text{TiO}_3$, $0 < x < 1$, is a ferroelectric material with a perovskite structure. This material composes of barium titanate (BaTiO_3) and strontium titanate (SrTiO_3). When SrTiO_3 is added to BaTiO_3 , Sr ion replaces Ba ion to form the BST material structure. Barium strontium titanate ceramic material is widely used in electronic devices [1]. As bulk ceramics and thin films, this material has a unique combination of large dielectric constant. It demonstrates a stable operation at high temperature, high tunability, low loss tangent, low DC leakage, and alterable curie temperature [2]. The uniqueness of the BST material is attributed to several factors, such as the Ba / Sr ratio, the synthesis method, and the particle and crystal size [3]. $\text{Ba}_x\text{Sr}_{(1-x)}\text{TiO}_3$ ceramics with various compositions of x (Ba / Sr ratio) has been widely studied; for example x = 0.2, 0.3, 0.4, 0.5, and 0.6 [4]. X-ray diffraction (XRD) results showed BST crystals formation in all variations of x; after the sintering process was carried out at 1000 °C for 3 hours. However, there was still a secondary phase (Sr_2TiO_4 , SrTiO_{10} , and $\text{Sr}_3\text{Ti}_2\text{O}_7$). This can be improved by increasing the sintering temperature. The secondary phase can be removed by increasing the sintering temperature. Increasing the concentration of x causes a transformation of the crystal system from tetragonal to cubic. The grain size and density of the sample decrease with increasing concentration x because Sr is having a smaller radius than Ba. Curie temperatures for samples with x = 0.2, 0.3, 0.4, 0.5, and 0.6 were 70 °C, 28.7 °C, -8.4 °C, -45.5 °C, and -82.6 °C, respectively. Curie temperature decreased with increasing x concentration. The highest dielectric constant found in sample with x = 0.3 [4]. Furthermore, the high dielectric and pyroelectric properties of the composition $\text{Ba}_x\text{Sr}_{(1-x)}\text{TiO}_3$ with $0.3 \leq x \leq 0.5$ resulted in the Curie temperature (TC) or ferroelectric-paraelectric phase transformation temperature decrease, near to room temperature (25 °C) [5].

$\text{Ba}_x\text{Sr}_{(1-x)}\text{TiO}_3$ materials are generally synthesised by hydrothermal method, sol-gel method, and conventional solid-state reaction method [6]. The BST material synthesised by the hydrothermal and sol-gel method produces crystals less than 100 nm. Subsequently, it produces residual hydroxide ions, which resulted in the formation of intergranular pores [7]. The mechanochemical or solid-state method is the most used method for BST nanoparticles large-scale production [8]. The solid-state method has several advantages; it uses low-cost raw materials, simple synthesis processes, and the ability to produce fine particles [8]. During solid-state processes such as high-energy ball milling, the steps that occur during solid-state processes, specifically welding, deformation, and fracture of powder raw materials, are repeated [9].

The mechanical activation during solid-state reaction with mechanical milling increases the raw material specific surface area due to the destruction of agglomerates and particles of the initial precursors [10]. In this regard, the mechanical milling process can produce particles sized $> 1 \mu\text{m}$. In general, the microstructure of the particle and crystallite size of mechanical milling products were influenced by the characteristics of the raw materials used, duration and heating temperature during the mechanical milling process [11].

In recent years, several studies have focused on the effect of sintering temperature on the synthesis of Barium Strontium Titanate (BST). In general, the increase of the temperature and duration time of the sintering process affected the BST material's purity and increased the crystallite size [12]. Pure BST materials are usually produced at high sintering temperatures [4], [12]–[18]. Sandi et al. carried out a sintering process at 1200°C for 2 hours to produce pure BST material by the solid-state reaction method [8]. Yustanti et al. reported that the sintering raw materials measuring an average size of $2.4 \mu\text{m}$ at a temperature of 1200°C produced pure BST material without the presence of impurities [14]. In the meantime, barium strontium titanate ceramic material was synthesised from fine constituent powders produced from high energy ball milling processes at sintering temperatures $1200\text{--}1350^\circ\text{C}$, as reported by Mudinepalli et al. [12]. Budkhod et al. performed sintering at temperatures between $1050\text{--}1350^\circ\text{C}$ to produce $\text{Ba}_{0.7}\text{Sr}_{0.3}\text{TiO}_3$ ceramics using a hybrid method between solid-state reaction and sol-gel combustion methods using urea as a fuel [15]. Meanwhile, Gate et al. conducted a sintering process at a temperature of 1100°C for 3 hours to produce a pure $\text{Ba}_{0.6}\text{Sr}_{0.4}\text{TiO}_3$ material using the sol-gel method [17]. Lastly, Zhu et al. synthesised barium strontium titanate glass and ceramics using the sol-gel method and was sintered at temperatures between 1000 and 1150°C [18].

The high sintering temperature to produce pure BST material has prompted various studies to produce pure BST materials at lower sintering temperatures using glass, polymer and inorganic additives [19]. One way to produce BST material at low sintering temperatures is to add Li_2O material, as reported by Zhang et al. [20]. Zhang et al. investigated the effect of adding Li_2O on the sintering temperature of commercial BST. It was found that by adding $0.5 \text{ wt}\%$, Li_2O could reduce the sintering temperature to 900°C without decreasing the ceramics performance. The sintering temperature of BST materials was reduced from 1350°C to 900°C by adding Li [21]. However, the XRD test showed two secondary phases as impurities caused by the addition of lithium. Besides, this research method has many limitations when applied to commercial production because it requires a very high cost [19], [21].

However, the BST material sintering ability decreased along with the broader particle size distribution [22]. Accordingly, reducing the particle size is another way that can be used to speed up or shorten the sintering time. The sintering temperature is reduced with smaller raw material particles. The smaller the raw material particle size, the faster the grain becomes coarse due to the high particle surface energy compared to the large grain size distribution in the batch under the same sintering conditions [23]. In another reference, the raw material with smaller dimensions causes a larger contact surface so that the sinterability increases due to the maximal diffusion process [24]. Therefore, this study uses a vibratory ball milling for 58 hours to mix BaCO_3 , SrCO_3 , and TiO_2 to obtain a homogeneous mixture with a mean particle size of $0.4 \mu\text{m}$. This research aims to determine the effective sintering temperature to produce pure BST material using a mixture of BaCO_3 , SrCO_3 , and TiO_2 ball-milled for 58 hours.

METHODS AND MATERIALS

$\text{Ba}_{0.6}\text{Sr}_{0.4}\text{TiO}_3$ was synthesised from BaCO_3 , SrCO_3 , and TiO_2 powders using the mechanical alloying method with a purity level of 99%. The powders were obtained from Sigma-Aldrich. The particle size analyser (PSA) test results in Table 1 show the BaCO_3 , SrCO_3 , and TiO_2 powders average sizes. Meanwhile, the results of XRD tests on TiO_2 , SrCO_3 , and BaCO_3 powders are shown in Figure 1(a). The diffraction patterns of TiO_2 , SrCO_3 and BaCO_3 powders are in line with the diffraction patterns of TiO_2 , SrCO_3 and BaCO_3 in the Inorganic Crystal Structure Database (ICSD), respectively, with numbers 98-009- 6946, 98-016-6088, and 98-016-6090. The Rietveld analysis using High Score Plus software shows that the TiO_2 powder has tetragonal-shaped crystal systems while the SrCO_3 and BaCO_3 powders have orthorhombic crystal systems.

Table 1. Average particle size of BaCO_3 , SrCO_3 and TiO_2 .

Raw materials	Average particle size (μm)
BaCO_3	1.979
SrCO_3	3.182
TiO_2	0.795

In this research, BaCO_3 , SrCO_3 and TiO_2 powders were subjected to a wet milling process using a vibratory ball milling machine with a composition of 41.63 grams each, 20.76 grams, and 28.08 grams for 58 hours. The ball to powder ratio (BPR) in the milling process is 10:1. After 58 hours, the mixed BaCO_3 , SrCO_3 and TiO_2 were tested for PSA and XRD. The PSA test results showed that the powder mixture of BaCO_3 , SrCO_3 and TiO_2 had a particle size of $0.4 \mu\text{m}$. Meanwhile, according to the Rietveld analysis using the High Score Plus software, the XRD test results are shown in Figure 1(b). Figure 1(b) shows no change in the diffraction pattern of the powder of TiO_2 , SrCO_3 and BaCO_3 . The crystal sizes of BaCO_3 , SrCO_3 and TiO_2 calculated using The Williamson-Hall method are 48 nm, 61 nm, and 71 nm, respectively.

After characterising the mixture of milled TiO_2 , SrCO_3 , and BaCO_3 powders, the next step is sintering the powder mixture of TiO_2 , SrCO_3 and BaCO_3 . The sintering process was carried out in the electric chamber furnace (Nabertherm

N31/H) with temperature variations of 500 °C, 600 °C, 700 °C, 800 °C, 900 °C, 1000 °C, and 1100 °C in the air under atmospheric pressure up to 1 hour. After the sintering process, characterisation was carried out using the XRD methods. The Philips XRD was also used to analyse the resulting phase and crystallite size. The step-scan method was performed to record the x-ray diffraction patterns. The intensity data during the scanning was taken every 2 seconds for each step on the diffraction angle of 0.005°. The Rietveld analysis was conducted using the High Score Plus software. The description of the diffraction line profiles at Rietveld refinement was achieved using the pseudo-Voigt function.

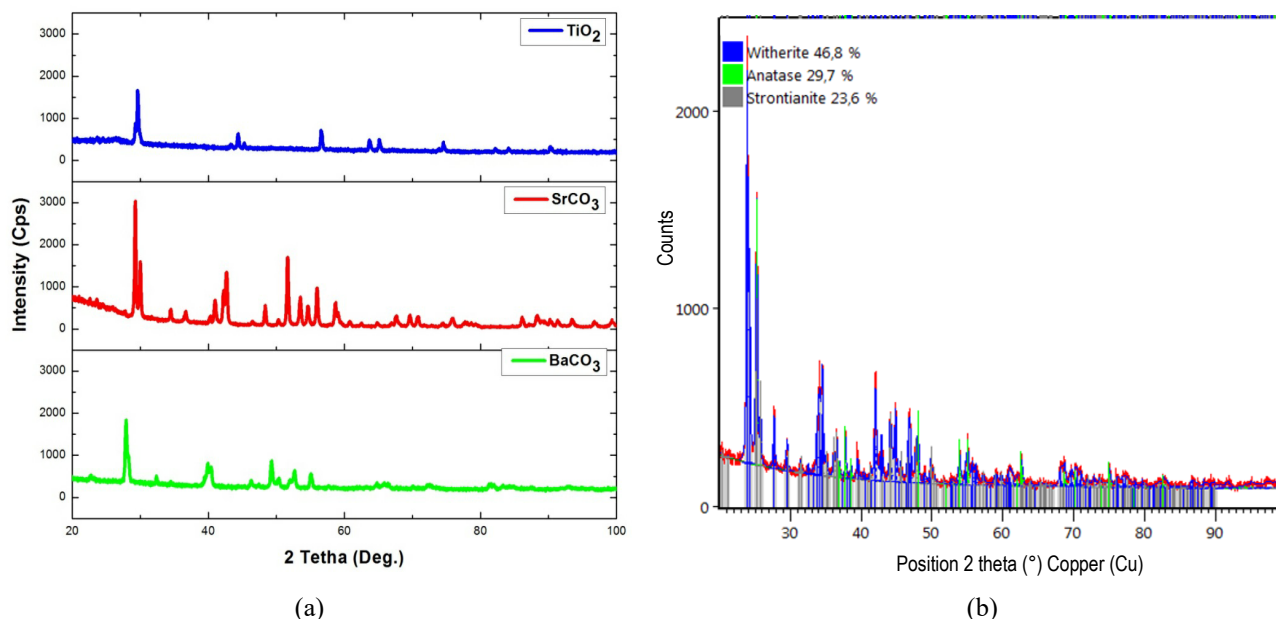


Figure 1. X-ray diffraction patterns of TiO_2 , SrCO_3 and BaCO_3 powders (a) before and (b) after 58 hours of milling.

RESULTS AND DISCUSSION

Figure 2 shows the diffraction pattern of BaCO_3 , SrCO_3 , and TiO_2 powder mixture at each sintering temperature. From the figure, the $\text{Ba}_{0.6}\text{Sr}_{0.4}\text{TiO}_3$ phase was not formed in the material sintered at temperatures of 500 °C and 600 °C. Meanwhile, while the $\text{Ba}_{0.6}\text{Sr}_{0.4}\text{TiO}_3$ phase was formed at temperatures of 700 °C, 800 °C and 900 °C, other compound phases, BaCO_3 , SrCO_3 , TiO_2 and BaTiO_3 , were observed. Moreover, a single-phase $\text{Ba}_{0.6}\text{Sr}_{0.4}\text{TiO}_3$ was formed at temperatures of 1000°C and 1100°C.

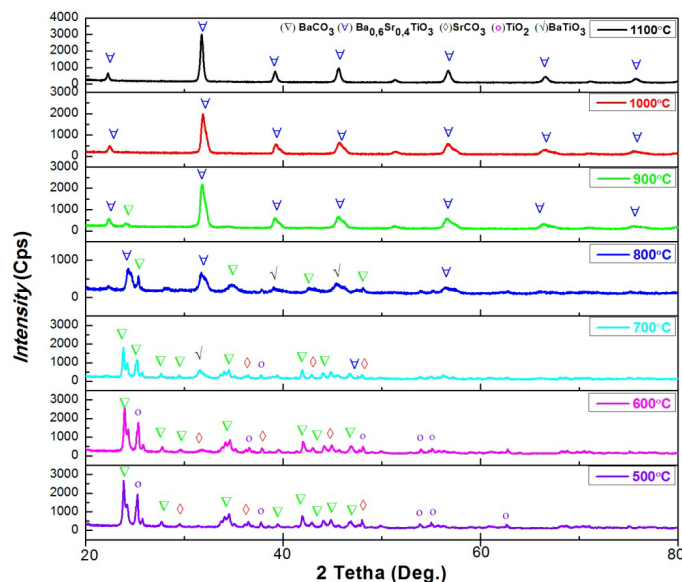


Figure 2. X-ray diffraction patterns of the sintered samples.

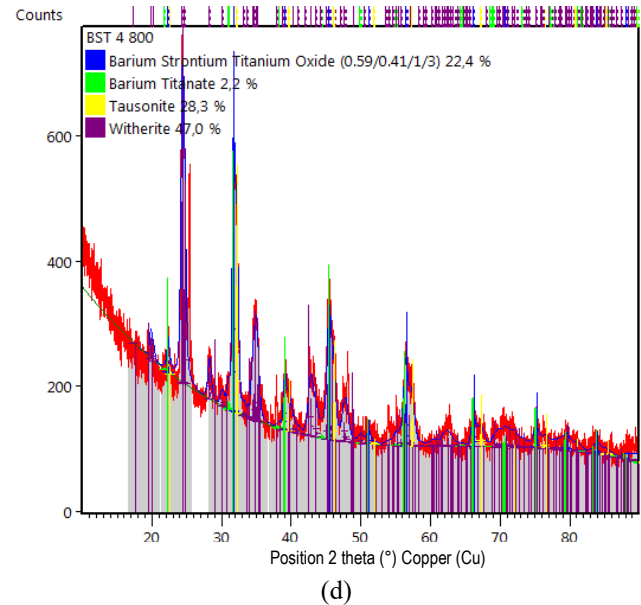
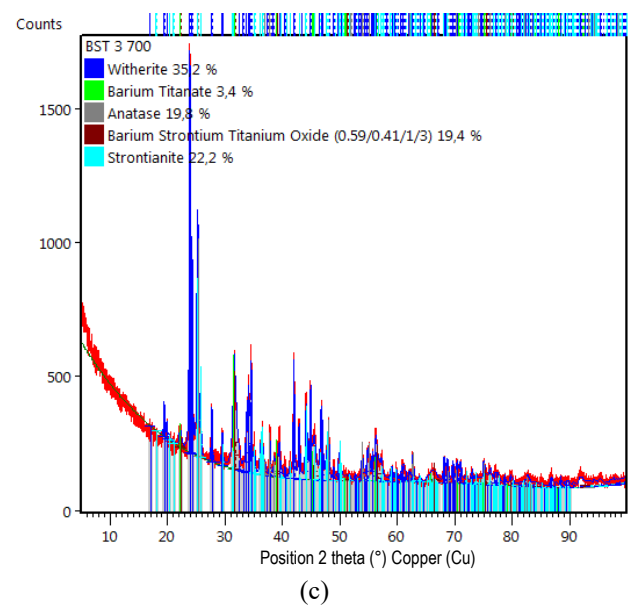
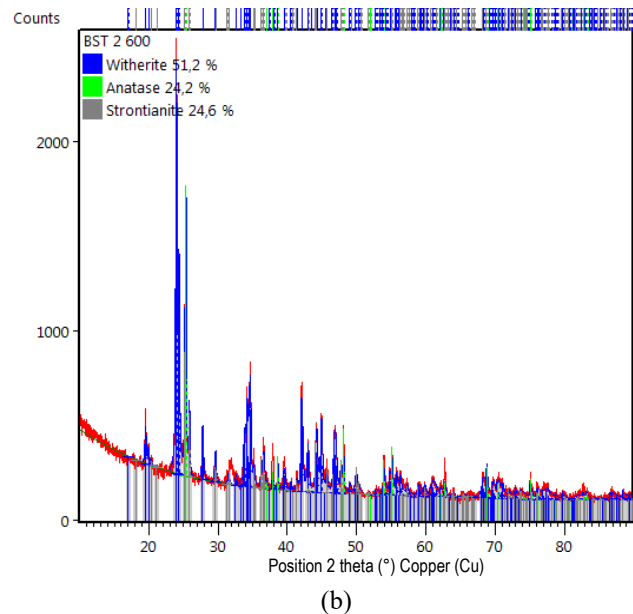
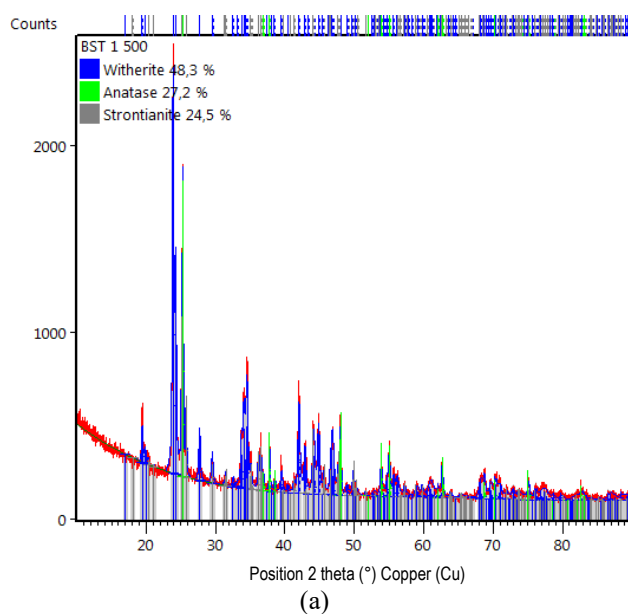
Figure 3 shows the Rietveld analysis results using the High Score Plus software based on X-ray diffraction obtained from the test results. Figure 3(a) shows the x-ray diffraction pattern on a powder that has been sintered at 500 °C. The x-ray diffraction pattern shows that the $\text{Ba}_{0.6}\text{Sr}_{0.4}\text{TiO}_3$ phase was not formed. In this light, the phases formed at 500 °C sintering temperature variations are BaCO_3 (withierite), TiO_2 (anatase), and SrCO_3 (strontianite), with the respective percentage of 48.3%; 27.2%, and 24.5%. Meanwhile, the crystallite size formed in BaCO_3 , TiO_2 , and SrCO_3 was 54.7 nm, 125.6 nm, and 80.3 nm. The x-ray diffraction pattern of the sintered powder at 600 °C is shown in Figure 3(b). At

600 °C, $\text{Ba}_{0.6}\text{Sr}_{0.4}\text{TiO}_3$ was not formed and still in the BaCO_3 , TiO_2 , and SrCO_3 phases, with 51.2%; 24.2% and 24.6%, respectively. The sizes of the crystallites formed after sintering BaCO_3 , TiO_2 , and SrCO_3 at 600 °C for are 56.4 nm, 104.3 nm, and 122.3 nm, respectively.

Figure 3(c) shows the x-ray diffraction pattern of a mixture of BaCO_3 , SrCO_3 , and TiO_2 powders sintered at 700 °C. At a temperature of 700 °C, the $\text{Ba}_{0.6}\text{Sr}_{0.4}\text{TiO}_3$ phase was formed with a percentage of 19.4% and a crystallite size of 15.3 nm. However, at 700 °C, the BaCO_3 , SrCO_3 and TiO_2 phases were still found at a respective percentage of 35.2%, 22.2%, and 19.8%, and crystallite sizes of 58.1 nm; 65.6 nm and 66.2 nm, respectively. Apart from $\text{Ba}_{0.6}\text{Sr}_{0.4}\text{TiO}_3$, BaCO_3 , SrCO_3 and TiO_2 phases, a new phase, BaTiO_3 at 3.4% and crystallite size of 38 nm, was also formed.

Figure 3(d) shows that the crystallite percentage increased to 22.4%, and its size increased to 30.3 nm at the $\text{Ba}_{0.6}\text{Sr}_{0.4}\text{TiO}_3$ phase when sintering at 800 °C. In this variation, the crystal size of $\text{Ba}_{0.6}\text{Sr}_{0.4}\text{TiO}_3$ is two times the crystallite size formed at 700 °C sintering temperature. Meanwhile, the BaTiO_3 phase percentage decreased to 2.2%, accompanied by a decrease in crystal size to 19.5 nm. BaCO_3 phases were still found with a composition of 47% with a crystallite size of 40 nm. Apart from $\text{Ba}_{0.6}\text{Sr}_{0.4}\text{TiO}_3$, BaCO_3 , and BaTiO_3 phases, a new phase, SrTiO_3 was also formed at 28.3% and crystallite size of 32.6 nm.

Figure 3(e) shows the x-ray diffraction pattern at a product sintering temperature of 900 °C. The $\text{Ba}_{0.6}\text{Sr}_{0.4}\text{TiO}_3$ phase formed in this variation experienced a significant increase with a percentage of 94.6% and a crystallite size of 40.1 nm. Simultaneously, the other 5.4% is the BaCO_3 phase with a crystallite size of 21.5 nm. The single phase of $\text{Ba}_{0.6}\text{Sr}_{0.4}\text{TiO}_3$ was formed perfectly at various sintering temperatures of 1000 °C and 1100 °C, as shown in Figure 3(f) and 3(g). $\text{Ba}_{0.6}\text{Sr}_{0.4}\text{TiO}_3$ with crystallites size of 30 nm and 43 nm resulted in sintering temperatures of 1000 °C and 1100 °C.



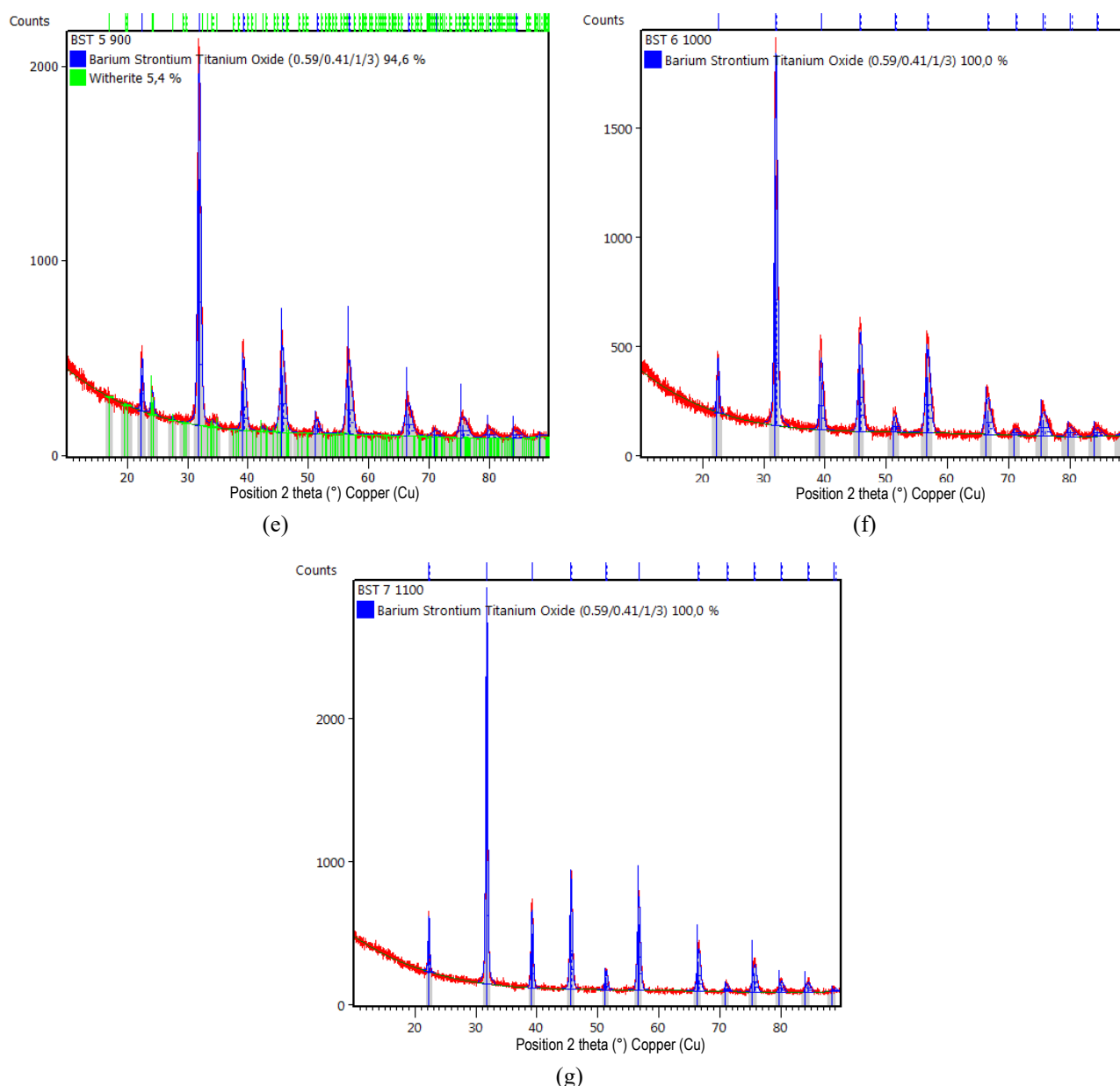


Figure 3. X-ray diffraction patterns of sintered samples at (a) 500 °C, (b) 600 °C, (c) 700 °C (d) 800 °C, (e) 900 °C, (f) 1000 °C and (g) 1100 °C.

The results of this study indicate that the $\text{Ba}_{0.6}\text{Sr}_{0.4}\text{TiO}_3$ material has begun to form at a sintering temperature of 700 °C. However, a secondary phase is still formed and completely into single-phase $\text{Ba}_{0.6}\text{Sr}_{0.4}\text{TiO}_3$ at 1000°C and 1100°C. The effect of sintering temperature on the phase composition (%) and crystallite sizes of $\text{Ba}_{0.6}\text{Sr}_{0.4}\text{TiO}_3$ formed is shown in Figure 4. The impurity phase disappears proportionately with the increase in sintering temperature. The kinetic energy in atoms increases due to higher sintering temperatures. The higher temperature makes it easier for the atoms to interact and bond with each other, causing the impurity phase to disappear [12], [17]. Besides, increasing the sintering temperature causes the atomic bonds to become stronger. Thus, sintering carried out at 1000°C and 1100°C resulted in forming a single phase of $\text{Ba}_{0.6}\text{Sr}_{0.4}\text{TiO}_3$ which is more stable. Increasing the sintering temperature will result in a recrystallisation process in the raw materials (BaCO_3 , SrCO_3 , and TiO_2) so that a more stable $\text{Ba}_{0.6}\text{Sr}_{0.4}\text{TiO}_3$ phase is formed. An increase in sintering temperature will produce $\text{Ba}_{0.6}\text{Sr}_{0.4}\text{TiO}_3$ with a higher phase composition (%). The crystallite sizes also increased, as reported in previous studies [12], [17], [25], [26].

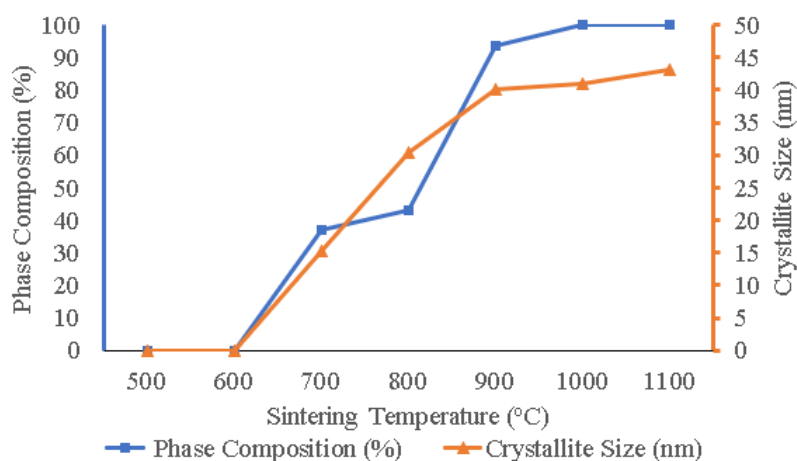


Figure 4. The effect of sintering temperature on the physical properties of $\text{Ba}_{0.6}\text{Sr}_{0.4}\text{TiO}_3$.

The use of BaCO_3 , SrCO_3 , and TiO_2 powder mixture, with a particle size of $0.4\ \mu\text{m}$, has been proven to produce $\text{Ba}_{0.6}\text{Sr}_{0.4}\text{TiO}_3$ material at lower sintering temperatures with a faster duration (1 hour). This is supported by [27] and [24] study, which revealed that reducing the particle size of raw materials is another method that can be used to speed up sintering and shorten sintering time. The sintering temperature is reduced with smaller raw material particles. The smaller the raw material particle size, the faster the grain becomes coarse due to the high particle surface energy compared to the large grain size distribution in the batch under the same sintering conditions [27]. Previous research [24] mentioned raw materials with smaller dimensions causes a larger contact surface so that the sinterability increases due to the maximum diffusion process. In this study, sintering carried out at temperatures of $1000\ ^\circ\text{C}$ and $1100\ ^\circ\text{C}$ for 1 hour produced single-phase $\text{Ba}_{0.6}\text{Sr}_{0.4}\text{TiO}_3$. In this study, single-phase $\text{Ba}_{0.6}\text{Sr}_{0.4}\text{TiO}_3$ resulted in lower sintering temperature and shorter sintering duration compared to the results of the study conducted by [4], [12], [14], [17], [26]. These studies' results showed the single-phase formation of $\text{Ba}_{0.6}\text{Sr}_{0.4}\text{TiO}_3$ was carried out in a sintering temperature range of $1100\ ^\circ\text{C}$ – $1350\ ^\circ\text{C}$ with a sintering duration of ≥ 2 hours.

In addition, [4], [12], [14], [26], [28] have clearly shown that the decrease in calcination or sintering temperature is due to the reduction in the small particle size of the raw materials; ranging from submicrometer or even to the nanoscale. The use of a smaller particle size increases the contact area and decreases the reactants contact distance, thereby increasing the overall reaction kinetics. The results of this study indicate that the sintering temperature greatly affects the purity, crystal system, and crystallite size of the material $\text{Ba}_{0.6}\text{Sr}_{0.4}\text{TiO}_3$ produced. The effect of sintering temperature on the physical properties of $\text{Ba}_{0.6}\text{Sr}_{0.4}\text{TiO}_3$ formed is shown in Table 2. The higher the sintering temperature resulted in a sharper peak intensity at $\text{Ba}_{0.6}\text{Sr}_{0.4}\text{TiO}_3$, which indicates an increase in crystal size. Accordingly, the higher the sintering temperature used, the higher the crystal size of the material $\text{Ba}_{0.6}\text{Sr}_{0.4}\text{TiO}_3$ formed. This is supported by the studies of [4], [17], [26], [29]. Thus, increasing the sintering temperature increased the atoms kinetic energy to diffuse and make the atoms react and bond perfectly. This finding is supported by other studies [29]–[32] that found that the crystallites produced have a larger size and higher crystallinity.

Table 2. The Physical Properties in The Formation of $(\text{Ba}_{0.6}\text{Sr}_{0.4})\text{TiO}_3$.

Sintering temperature ($^\circ\text{C}$)	Phase	Composition phase (%)	Crystal system	Crystallite size (nm)
500	BaCO_3	48	Orthorhombic	54.7
	TiO_2	27	Tertragonal	125.6
	SrCO_3	25	Orthorhombic	80.3
600	BaCO_3	51.2	Orthorhombic	56.4
	TiO_2	24.2	Tertragonal	104.3
	SrCO_3	24.6	Orthorhombic	122.3
700	BaCO_3	35.2	Orthorhombic	58.1
	TiO_2	19.8	Tertragonal	19.8
	SrCO_3	22.2	Orthorhombic	65.6
	BaTiO_3	3.4	Orthorhombic	38
	$(\text{Ba}_{0.67}\text{Sr}_{0.33})\text{TiO}_3$	19.4	Tertragonal	15.3
800	BaCO_3	47	Orthorhombic	40
	BaTiO_3	2.2	Orthorhombic	19.5
	SrTiO_3	28.3	Orthorhombic	32.6
	$(\text{Ba}_{0.67}\text{Sr}_{0.33})\text{TiO}_3$	22.4	Tertragonal	30.3
900	BaCO_3	5.4	Orthorhombic	21.5
	$(\text{Ba}_{0.67}\text{Sr}_{0.33})\text{TiO}_3$	94.6	Tertragonal	40.1
1000	$(\text{Ba}_{0.59}\text{Sr}_{0.41})\text{TiO}_3$	100	Cubic	41
1100	$(\text{Ba}_{0.6}\text{Sr}_{0.4})\text{TiO}_3$	100	Cubic	43

In addition, an increase in the sintering temperature in this study caused changes in the crystal system of the $\text{Ba}_{0.6}\text{Sr}_{0.4}\text{TiO}_3$ material. At temperatures of 700 °C, 800 °C, and 900 °C, the crystal system in the material $\text{Ba}_{0.6}\text{Sr}_{0.4}\text{TiO}_3$ is tetragonal. Whereas at temperatures of 1000 °C and 1100 °C, the crystal system in the $\text{Ba}_{0.6}\text{Sr}_{0.4}\text{TiO}_3$ is cubic with a higher peak intensity with increasing sintering temperature. The $\text{Ba}_{0.6}\text{Sr}_{0.4}\text{TiO}_3$ with cubic structure increased the dielectric properties of the material $\text{Ba}_{0.6}\text{Sr}_{0.4}\text{TiO}_3$ produced [12], [17], [33]. Besides the crystal structure, the dielectric properties of the $\text{Ba}_{0.6}\text{Sr}_{0.4}\text{TiO}_3$ material are also influenced by the crystal size, where the dielectric property increases with the crystallite size [12], [29], [34]. In this study, the sintering temperature of 1100 °C produces $\text{Ba}_{0.6}\text{Sr}_{0.4}\text{TiO}_3$ material with the best physical properties because it has a cubic-shaped crystal system and the largest crystal size.

CONCLUSION

The effect of sintering temperature on the physical properties of $\text{Ba}_{0.6}\text{Sr}_{0.4}\text{TiO}_3$ material synthesised with 0.4 µm raw materials (and milled up to 58 hour) using the solid-state reaction method has been investigated. The use of raw materials, a mixture of BaCO_3 , SrCO_3 , and TiO_2 with a particle size of 0.4 µm could produce $\text{Ba}_{0.6}\text{Sr}_{0.4}\text{TiO}_3$ material at a lower sintering temperature of 700 °C. Moreover, the single-phase $\text{Ba}_{0.6}\text{Sr}_{0.4}\text{TiO}_3$ can be produced at temperatures of 1000 °C and 1100 °C. Increasing the sintering temperature in this study resulted in $\text{Ba}_{0.6}\text{Sr}_{0.4}\text{TiO}_3$ material with higher purity as marked by the disappearance of the BaTiO_3 , BaCO_3 , SrCO_3 , and TiO_2 phases. Higher sintering temperature increased the crystal size and changed the crystal system from tetragonal to cubic. The sintering temperature of 1100 °C produces $\text{Ba}_{0.6}\text{Sr}_{0.4}\text{TiO}_3$ material with the best physical properties because it has a cubic-shaped crystal system and the largest crystal size.

ACKNOWLEDGEMENT

We would like to express our gratitude to the Ministry of Research and Higher Education for funding this research through Competitive Research Grant with No. 042.06.1.401516/2016.

REFERENCES

- [1] Szafraniak B, Fuśnik Ł, Xu J, et al. Semiconducting metal oxides: SrTiO_3 , BaTiO_3 and BaSrTiO_3 in gas-sensing applications: A review. *Coatings* 2021; 11: 1–23.
- [2] Sangle AL, Lee OJ, Kursumovic A, et al. Very high commutation quality factor and dielectric tunability in nanocomposite SrTiO_3 thin films with T(c) enhanced to >300 °C. *Nanoscale* 2018; 10: 3460–3468.
- [3] Vigneshwaran B, Kuppusami P, Ajithkumar S, et al. Study of low temperature-dependent structural, dielectric, and ferroelectric properties of $\text{Ba}_x\text{Sr}_{1-x}\text{TiO}_3$ ($x = 0.5, 0.6, 0.7$) ceramics. *Journal of Materials Science: Materials in Electronics* 2020; 31: 10446–10459.
- [4] Gatea HA, Naji IS. The effect of Ba/Sr ratio on the Curie temperature for ferroelectric barium strontium titanate ceramics. *Journal of Advanced Dielectrics* 2020; 10: 1–11.
- [5] Vu T-H, Phuong NTM, Nguyen T. Lead-free ferroelectric barium titanate -based thin film for tunable microwave device application. *IOP Conference Series: Materials Science and Engineering* 2021; 1091: 012060.
- [6] Alwan H, Jasim S. Preparation and characterization of $\text{Ba}_{1-x}\text{Sr}_x\text{TiO}_3$ by sol-gel method. *Asian Journal of Chemistry* 2019; 31: 186–190.
- [7] Panomsuwan G, Manuspiya H. Morphological and structural properties of barium strontium titanate nanopowders synthesized via a sol-gel method. *Ferroelectrics* 2020; 554: 30–37.
- [8] Sandi DK, Supriyanto A, Jamaluddin A, et al. The influences of mole composition of strontium (x) on properties of barium strontium titanate ($\text{Ba}_{1-x}\text{Sr}_x\text{TiO}_3$) prepared by solid state reaction method. *AIP Conference Proceedings* 2016; 1710: 1–5.
- [9] Dulian P. Solid-state mechanochemical syntheses of perovskites. In: Pan L, Zhu G, editors. *Perovskite Materials - Synthesis, Characterisation, Properties, and Applications*. London: InTech-Open, 2016, p 3–26.
- [10] Zhang L, Huang Z, Liu Y, et al. Effects of mechanical ball milling time on the microstructure and mechanical properties of $\text{Mo}_2\text{NiB}_2\text{-Ni}$ Cermets. *Materials* 2019; 12(12), 1926.
- [11] Widodo RD, Manaf A. Physical characteristics and magnetic properties of $\text{BaFe}_{12}\text{O}_{19}/\text{SrTiO}_3$ based composites derived from mechanical alloying. *AIP Conference Proceedings* 2016; 1725: 125–132.
- [12] Mudinepalli VR, Feng L, Lin WC, et al. Effect of grain size on dielectric and ferroelectric properties of nanostructured $\text{Ba}_{0.8}\text{Sr}_{0.2}\text{TiO}_3$ ceramics. *Journal of Advanced Ceramics* 2015; 4: 46–53.
- [13] Elqudsy MA, Widodo RD, Rusiyanto, et al. The particle and crystallite size analysis of BaTiO_3 produced by conventional solid-state reaction process. *AIP Conference Proceedings* 2017; 1818: 020012.
- [14] Yustanti E, Hafizah M, Manaf A. The effect of milling time and sintering temperature on formation of nanoparticles barium strontium titanate. *AIP Conference Proceedings* 2017; 1788: 30099.
- [15] P Budkhod NS and ST. Synthesis of $\text{Ba}_{0.7}\text{Sr}_{0.3}\text{TiO}_3$ ceramics via hybrid method. *Journal of Physics: Conference Series* 2018; 252: 0–5.
- [16] Trobough ND. Examination of Dielectric Properties of BaTiO_3 - SrTiO_3 Based Systems. BSc Thesis, Oregon State University, USA, 2020.
- [17] Gatea HA, Naji IS. Impact of sintering temperature on structural and dielectric properties of barium strontium titanate prepared

by sol-gel method. *Journal of Ovonic Research* 2018; 14: 467–474.

- [18] Zhu J, Zhang Y, Song X, et al. Influence of sintering temperature on microstructures and energy-storage properties of barium strontium titanate glass-ceramics prepared by sol-gel process. *Physica Status Solidi (A) Applications and Materials Science* 2015; 212: 2822–2829.
- [19] Veerapandiyan V, Benes F, Gindell T, et al. Strategies to improve the energy storage properties of perovskite lead-free relaxor ferroelectrics: A review. *Materials* 2020; 13: 1–47.
- [20] Zhang X, Deng X, Ren Y. Low temperature sintering and nonlinear dielectric properties of Li₂O doped Ba_{0.6}Sr_{0.4}TiO₃ ceramics derived from the citrate method. *IOP Conference Series: Materials Science and Engineering* 2017; 207: 0–5.
- [21] Ma R, Cui B, Hu D, et al. Improving the dielectric properties of the Ba(Zr_{0.1}Ti_{0.9})O₃-based ceramics by adding a Li₂O–SiO₂ sintering agent step by step. *International Journal of Nanoscience and Nanotechnology* 2020; 16: 233–241.
- [22] Amorós JL, Blasco E, Moreno A, et al. Effect of particle size distribution on the sinter-crystallisation kinetics of a SiO₂–Al₂O₃–CaO–MgO–SrO glass-ceramic glaze. *Journal of Non-Crystalline Solids* 2020; 542: 120148.
- [23] Yang L. Effect of particle size on oxygen content and porosity of sintered Ti-6Al-4V. MSc Thesis, University of Utah, USA, 2015.
- [24] Nedelcu L, Ioachim A, Toacsan M, et al. Synthesis and dielectric characterization of Ba_{0.6}Sr_{0.4}TiO₃ ferroelectric ceramics doi: *Thin Solid Films* 2011; 519: 5811–5815.
- [25] Berent K, Komarek S, Lach R, et al. The effect of calcination temperature on the structure and performance of nanocrystalline mayenite powders. *Materials* 2019; 12(21): 3476.
- [26] Gatea HA. Impact of sintering temperature on crystallite size and optical properties of SnO₂ nanoparticles. *Journal of Physics: Conference Series* 2021; 1829: 012030.
- [27] Hu J. Grain Growth by Ordered Coalescence of Nanocrystals in Ceramics. PhD Thesis, Stockholm University, Sweden, 2013.
- [28] Kwon Y Bin, Kang JH, Han CS, et al. The effect of particle size and surface roughness of spray-dried bosentan microparticles on aerodynamic performance for dry powder inhalation. *Pharmaceutics* 2020; 12: 1–15.
- [29] Ulfa U, Kusumandari K, Iriani Y. The effect of temperature and holding time sintering process on microstructure and dielectric properties of barium titanate by co-precipitation method. *AIP Conference Proceedings* 2019; 2202: 020036.
- [30] Zeng L, Sun H, Peng T, et al. The sintering kinetics and properties of sintered glass-ceramics from coal fly ash of different particle size. *Results in Physics* 2019; 15: 102774.
- [31] Sandi D, Supriyanto A, Anif, et al. The effects of sintering temperature on dielectric constant of Barium Titanate (BaTiO₃). *IOP Conference Series: Materials Science and Engineering* 2016; 107: 12069.
- [32] Fitriyana D, Suhaimi H, Sulardjaka S, et al. Synthesis of Na-P Zeolite from geothermal sludge. In: Murakami RI, Koinkar P, Fujii T, Kim TG., Abdullah H, editors. *NAC 2019: Proceedings of the 2nd International Conference on Nanomaterials and Advanced Composites*. Singapore: Springer, 2020, p 51-59.
- [33] Maharsi R, Jamaluddin A, Supriyanto A, et al. Crystalline characterization and dielectric constant of barium strontium titanates prepared by solid state reaction. *Advanced Materials Research* 2015; 1123: 123-126.
- [34] Kurnia, Heriansyah, Suharyadi E. Study on the influence of crystal structure and grain size on dielectric properties of manganese ferrite (MnFe₂O₄) nanoparticles. *IOP Conference Series: Materials Science and Engineering* 2017; 202: 012046.